Chapter 7
Reduction of Reaction Mechanisms

Abstract Increases in both chemical kinetics knowledge and the capacity of computers have led to the availability of very large detailed kinetic mechanisms for many problems. These mechanisms may contain up to several thousand species and several ten thousand reaction steps. For computational reasons, however, large mechanisms still cannot be used in spatially 2D or 3D computational fluid dynamics simulations, where the applied mechanism typically requires less than 100 species. Also, within such large mechanisms, the key processes can be masked by the presence of many reaction steps of only marginal importance. A first step to reducing the size of a kinetic mechanism is to identify species and reaction steps which do not need to be included in order to accurately predict the key target outputs of the model. Such methods lead to so-called "skeletal" schemes. This chapter discusses many different methods for the identification of redundant species and reaction steps within a mechanism, including those based on sensitivity and Jacobian analyses, the comparison of reaction rates, trial and error and calculated entropy production. Another family of methods for the development of skeletal schemes is based on the investigation of reaction graphs. We discuss here the directed relation graph (DRG) method and its derivatives, and the path flux analysis (PFA) method. Mechanism reduction may be also based on optimisation methods which minimise an objective function related to the simulation error between the full and reduced models, subject to a set of constraints (e.g. numbers of species required). Integer programming and genetic algorithm-based methods have been used for such an optimisation and are discussed here. From these skeletal schemes, subsequent reductions can be achieved via either species or reaction lumping. Chemical and mathematical approaches to lumping are discussed with applications in combustion, atmospheric and biological systems. Reduction methods based on timescale separation are then introduced starting with the classic quasi-steady-state approximation (QSSA). Computational singular perturbation (CSP) methods are then described as a means of informing the derivation of analytically reduced models. Further efficiency gains can also be obtained by using a numerical approximation of a function in place of more traditional descriptions of chemical source terms within simulation models. The generation of such numerical reduced models can be based on the original differential equations and the thermodynamics of the problem or deduced from the simulation results. Using any of these methods, the applied function has to meet special requirements, such as the need to be evaluated quickly and to provide an accurate approximation. We discuss a series of

T. Turányi, A.S. Tomlin, *Analysis of Kinetic Reaction Mechanisms*,
DOI 10.1007/978-3-662-44562-4_7

approaches, tabulation methods, artificial neural networks (ANNs) and various types of polynomials, that all have been tested and applied within the context of kinetic modelling.

7.1 Introduction

As discussed in previous chapters, one of the barriers to using complex kinetic mechanisms within larger models of reactive flows is the computational time required to solve the resulting rate equations. If the full comprehensive mechanism is used, then this may lead to compromises being required in modelling other aspects of the flow. Using a coarser model grid resolution is often a compromise that has to be made within computational fluid dynamics (CFD) codes. The more species that are included within the chemical model, the lower the grid resolution that can be afforded on a given hardware architecture. Simplifications of turbulent mixing processes may also have to be made. For example, it is unlikely that highly detailed chemistry could be afforded within a 3D direct numerical simulation of a problem where attempts are made to resolve all important timescales of turbulent mixing. It follows that when trying to couple a chemical kinetic model with a complex physical model, the important dynamics of the chemical system should be represented as efficiently as possible, i.e. with the lowest number of variables possible. Chemical model reduction has therefore become an important area of research as discussed in several review articles (Griffiths 1995; Tomlin et al. 1997; Okino and Mavrovouniotis 1998; Ross and Vlad 1999; Law et al. 2003; Law 2007; Lu and Law 2009; Ross 2008; Pope 2013).

This chapter will introduce various methods for the reduction of kinetic reaction mechanisms. These start with conceptually simple approaches, such as removing unnecessary species and reactions from a scheme for a particular application. In this case, the resulting reduced model is still a kinetic scheme which may be represented by a smaller number of reaction steps and species when compared to the full scheme. Typically such approaches achieve reductions in the number of species of up to one to two thirds of the original number. Several techniques for this *skeletal model reduction* have been developed including sensitivity analysis, graph-based and optimisation-based methods, as discussed in the following sections. For some applications, this may be sufficient, but for CFD calculations, further reductions are often required. Subsequently, other approaches may be used to reduce the number of variables in the system of chemical rate equations. The lumping of species into a smaller number of new variables is one approach, and in this case the new variables may no longer represent individual species but linear or nonlinear combinations of species concentrations as discussed in Sect. 7.7. Timescale-based methods may also be exploited in the context of model reduction so that the dynamics of the reduced model is restricted to the equivalent slow manifold. Finally, tabulation or equivalent

model representation approaches can be taken to find other mathematical representations of the underlying system dynamics using highly reduced numbers of variables (see Sects. 7.12–7.13).

7.2 Reaction Rate and Jacobian-Based Methods for Species Removal

The aim of chemical kinetic modelling is to accurately describe the concentration profiles of *important species* and/or *important feature*s of the model predictions. An important species can be any species that the modeller considers important for any reason and may include, for example, products of the reaction, pollutant concentrations, etc. Important features may include non-local outputs such as the time to ignition for a fuel combustion model, the laminar velocity of a simulated flame or the time period of an oscillating reaction. To simulate these important species and features accurately may also require the presence of coupled intermediates within the reduced mechanism. Such *necessary species* are defined as those which are required in order to simulate the important features to the desired degree of accuracy. All other species can be classified as *redundant* and therefore can be removed from the mechanism. It may also be possible to remove redundant reaction steps which do not affect the prediction of important features. These types of reduction methods can often be local in nature, i.e. they are applied at specific sets of concentrations, pressures, temperatures, etc. In this case, the success of the skeleton scheme when used in a more complex physical model is highly dependent on the reduction being applied over representative composition and temperature conditions compared to the intended final application. Local methods therefore tend to be applied over a range of conditions to give a reduced model of appropriate validity for the representation of selected model outputs. For example, a high degree of generality of the skeleton scheme can be obtained by using ignition simulations to cover low-temperature regions and perfectly stirred reactor (PSR) or 1D flame simulations to represent high-temperature regimes. The reduction to a skeleton scheme usually consists of two stages. The first stage is the identification of species that have a minor effect on selected model outputs and therefore can be eliminated. The second stage involves the removal of reactions that have only a minor influence on the kinetics of the remaining species (and maybe temperature).

7.2.1 Species Removal via the Inspection of Rates

Several methods have been suggested for the identification of *redundant species*. An early approach was introduced by Frenklach et al. (Frenklach et al. 1986; Frenklach 1991) who investigated the elimination of species from a detailed

combustion mechanism where the aim was the accurate simulation of times-to-ignition and temperature profiles. Reactions were eliminated that were much slower than the rate-determining steps and which produced much less heat than the main heat-producing steps. The elimination of these reactions also meant the elimination of some species. This approach was extended to the reduction of mechanisms for the conditions of laminar flame simulations (Wang and Frenklach 1991). Whilst the method was successful for these applications, it was not general, and the list of important species could not be defined.

In Sect. 4.1, element fluxes were used for the characterisation of the features of a chemical mechanism that may change in time and space. Another approach to the application of element fluxes is the calculation of their integral over the whole time domain of the reaction. These integral fluxes can be calculated for each species and element, and then redundant species identified as those which are not connected (directly or indirectly) to the important species considering all fluxes. Several reduction methods, based on similar principles but differing in details, have been developed using this integral flux approach within the literature (Nilsson et al. 1999; Frouzakis and Boulouchos 2000; Németh et al. 2002; Soyhan et al. 2002; Luche et al. 2004; Androulakis et al. 2004; Mauersberger 2005).

Valorani et al. (2006) used the *CSP method* (see Sect. 6.4) for the identification of redundant species. They first define important species and check in which modes they are present. Reaction steps are then identified that have a significant contribution to these modes. These reaction steps may include further species, which will be considered as necessary species. Using an iterative procedure, the number of necessary species is continuously increased until at the end of the process no more important reactions are found.

7.2.2 Species Elimination via Trial and Error

The redundancy of individual species was also investigated by Turányi (1990b) via a trial-and-error approach. A series of reduced mechanisms were created where in each one, all the consuming reactions of the tested species were removed. If the resulting simulation error (i.e. the deviation between the solutions of the full and reduced models) was small, then this species could be eliminated from the mechanism. The disadvantage of this method is that it is not able to identify species that can be eliminated in groups. An extension of this approach to the elimination of groups of species will be discussed in Sect. 7.6.1.

Fischer and Riedel (2013) suggested a "guided" trial-and-error method for the detection of redundant reactions and species. A characteristic value is assigned to each reaction, which is equal to the greatest mole fraction during the simulation of all species participating in this reaction step. The logic behind it is that if a reaction step is related to all high mole fraction species, then it is likely not to be redundant. Small maximum mole fraction may be related to a necessary or a redundant species, which have to be distinguished. Therefore, elimination of reaction groups, formed

from reaction steps having the lowest characteristic values, is tested. A reduced mechanism is accepted, if the simulated concentration profiles of the important species obtained from the reduced mechanism agree within predefined thresholds to those of the original mechanism. A species is redundant if it is not present in an accepted reduced mechanism. Many reduced mechanisms are identified in this way, and the smallest one is considered to be the best.

7.2.3 *Connectivity Method: Connections Between the Species Defined by the Jacobian*

The *connectivity method* (CM) (Turányi 1990c) identifies redundant species via the investigation of the Jacobian. Element $(y_i/f_j)(\partial f_j/\partial y_i)$ of the normalised Jacobian shows the percentage change of the production rate of species j due to a 1 % change in the concentration of species i. If the square of this effect is summed over all important species, then the value B_i shows the effect of a change in the concentration of each species on the concentrations of all important species:

$$B_i = \sum_j \left(\left(y_i/f_j \right) \left(\partial f_j/\partial y_i \right) \right)^2 \tag{7.1}$$

Species characterised by large B_i values are closely connected to the important species and therefore are necessary species. In the next step, these necessary species are also included in the summation, and the B_i values are recalculated. Species characterised by the largest B_i values are again included in the summation, and this iteration is continued until all species that have close connection to the important species, directly or through other species, are identified. The rest of the species are considered to be redundant.

Figure 7.1 shows that starting from the group of important species, in an iterative procedure, all species can be identified that are necessary for the simulation of important species. Groups of species may be identified as redundant and can be eliminated, even if there are strong interactions between the redundant species. This type of approach was subsequently used by several other methods for the identification of redundant species as discussed later.

Since the Jacobian depends on the actual concentration set for nonlinear models, this procedure has to be repeated for several concentration sets, e.g. at several points along a concentration trajectory and at different temperatures and/or pressures. Species that are redundant over all relevant simulation conditions can be removed from a general reduced mechanism. All consuming reactions of the redundant species can also be eliminated from the model at this stage. Further details on the application of this method can be found in Turányi (1990b), Tomlin et al. (1992) and Zsély and Turányi (2003). According to a particular version of the method [encoded in the program KINAL (Turányi 1990a)], at each iteration step, the user

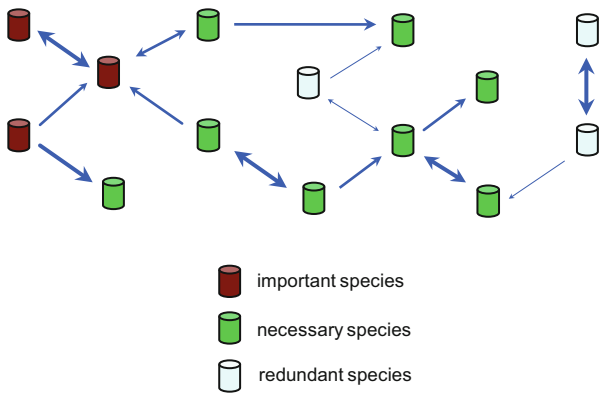

Fig. 7.1 Relationships between species, as handled by several methods for the identification of redundant species. This is common in the connectivity method, the DRG family and the PFA methods. Starting from the important species, all other species are identified that are necessary for the calculation of the concentrations of the important species. The remaining redundant species are only loosely related to the group of important and necessary species

selects the new species to be included in the summation on the basis of the list of B_i values. In the version of the method encoded in option CONNECT of the code KINALC (KINALC)), the list of necessary species is increased by one during each iteration, i.e. that with the highest B_i value.

Experience suggests that if the mechanism contains not too many species (up to about 50), then a gap usually appears in the list of B_i values, and the necessary and redundant species become clearly separated. However, if there are many species in the mechanism, the B_i values often do not show clear gaps. Another potentially negative feature of the connectivity method is that after several iterations, the special role of important species diminishes. Also, the connectivity method does not make a direct connection between the B_i values and the simulation error of important targets, i.e. the deviation of a target prediction obtained with the full and the reduced mechanisms. The latter can only be determined by performing simulations using the reduced mechanism and comparing them to those using the full scheme. The connectivity method in its basic form offers a single reduced mechanism. As discussed below, it is more useful for a method to offer a range of reduced mechanisms having different simulation errors, so that the user may select the one that best suits the required simulation time and predictive accuracy.

7.2.4 Simulation Error Minimization Connectivity Method

Such an approach is taken in the *Simulation Error Minimization Connectivity Method* (SEM-CM) (Nagy and Turányi 2009; Zsély et al. 2011). Using this method, several trial reduced mechanisms are created, and the simulation results obtained

guide the further search for the nearly optimal reduced mechanism. Consequently, the application of the reduction method requires much more computer time than the simple connectivity method but may find a much smaller reduced mechanism. The main advantage of the method is that the required accuracy of the reduced mechanism (the acceptable simulation error) can be defined a priori.

The aim of the SEM-CM method is that all species within the reduced mechanism be living species. A species is called a *living species* if its initial concentration is nonzero, it has an influx (e.g. emission to an atmospheric chemical system) or it is produced by chemical reactions. Vol'pert (1972) has also used the term *reachable species* for such types of species. As the definition indicates, the list of living species is determined by not only the reaction mechanism itself but also the initial and boundary conditions. A reaction mechanism is called *consistent* if all species within it are living. A *complementary set* consists of those species that are not yet selected but would yield at least one additional selected reaction if these were introduced to the current group of selected species.

The algorithm of the SEM-CM method, as detailed in the article of Nagy and Turányi (2009), is rather complex, and only a brief summary is given here. First, the complementary sets of species having the strongest connection to the important species are searched for. If necessary, the mechanisms obtained are made to be consistent. Using these mechanisms, simulations are carried out at all investigated conditions, and the simulation error together with the corresponding mechanism is stored in a database. Starting from the mechanisms associated with the smallest simulation errors, the number of species is gradually increased by adding new complementary sets. In each step, the mechanism obtained is made consistent, simulations are carried out and new entries are added to the database. The number of species is increased until the simulation error decreases below a certain threshold. Whilst other species reduction methods use a top-down approach, always eliminating the species least connected to the important species, the SEM-CM method is a bottom-up approach, and a series of consistent mechanisms are built up using the important species as a core. An advantage of the method is that the generated database contains a wide variety of reduced mechanisms, each belonging to different simulation error. In this way an almost optimal reduced mechanism can be obtained to any requested simulation error. Results obtained in a study of the performance of the SEM-CM method compared with several other methods (CM, DRG restart, DRGASA) are presented later in Fig. 7.5.

7.3 Identification of Redundant Reaction Steps Using Rate-of-Production and Sensitivity Methods

So far we have discussed the removal of redundant species from a mechanism. It may also be useful to reduce the number of reactions for the remaining necessary species since the calculation of their rates at each time step can be computationally

time consuming. Several methods exist for reducing the number of reactions within a mechanism. An early method for the identification of redundant reaction steps is the use of *rate-of-production analysis*. Here the percentage contribution of each reaction step to the production and consumption rate of each species is investigated at several reaction times during a simulation. A reaction step can be eliminated from the mechanism (at least at the simulation conditions under investigation) if the contribution of the reaction step is less than $s\%$ to either the production or the consumption rate of any species at any time. This threshold value is selected by the user, and a typical value may be, for example, 5 %. The size of the reduced mechanism (and the simulation error) can be changed by tuning this threshold.

This method is easy to understand and to apply, but not always very effective. The simulation error depends on the selection of s, but there is no direct relationship between it and the value of s. Moreover, due to the nonlinearity of chemical kinetic systems, it is not guaranteed that the simulation error decreases when s decreases. The method would be made more effective by selecting a different threshold s_i for each species. These methods can be applied for the removal of reaction steps as well as species by basically removing those reaction steps that do not form an important direct or indirect pathway between species which are to be retained in the mechanism.

The method of *principal component analysis of matrix* **S** (PCAS) was discussed in Sect. 5.3. The PCAS method allows the identification of the most important parameters related to selected simulation results. Therefore, if the objective function includes the concentrations of the important and necessary species (see Sect. 7.2) and the investigated parameters are the rate coefficients (or A-factors) of the reaction steps (Vajda et al. 1985; Vajda and Turányi 1986; Turányi 1990b; Xu et al. 1999; Liu et al. 2005), it is also applicable for the generation of a reduced mechanism containing less reaction steps. A further development of the PCAS method is functional principal component analysis (fPCA) (Gokulakrishnan et al. 2006). This method facilitates the investigation of temporal and spatial changes in the importance of reaction steps in reaction−diffusion systems.

Another method for removing redundant reaction steps is the *principal component analysis of matrix* $\boldsymbol{F}$ (*PCAF*), where $\mathbf{F} = \{\partial f_i/\partial x_k\}$ (Turányi et al. 1989; Tomlin et al. 1992; Börger et al. 1992; Heard et al. 1998; Carslaw et al. 1999; Zsély and Turányi 2001; Bahlouli et al. 2014). Here the sensitivity of the net rates of production of species to changes in the input parameters is investigated. Using the *PCAF method*, the objective function has the following form:

$$e' = \sum_{i=1}^{N_R} \left(\frac{\widetilde{f}_i(t) - f_i(t)}{f_i(t)} \right)^2 \tag{7.2}$$

where f_i and $\widetilde{f}_i$ are the right-hand side of the kinetic system of ODEs (2.9), calculated at the original parameter vector $\boldsymbol{\alpha} = \ln \mathbf{x}$ and at the modified values of parameters $\boldsymbol{\alpha} + \Delta\boldsymbol{\alpha}$, respectively. This objective function can be approximated (Turányi et al. 1989) by

$$e'(\boldsymbol{\alpha}) \approx (\Delta\boldsymbol{\alpha})^{\mathrm{T}}\widetilde{\mathbf{F}}^{\mathrm{T}}\widetilde{\mathbf{F}}(\Delta\boldsymbol{\alpha}) \tag{7.3}$$

where $\widetilde{\mathbf{F}} = \{(x_k/f_i)(\partial f_i/\partial x_k)\}$ is the normalised **F**-matrix and its rows correspond to the variables present in the objective function (7.2). The elements of the matrix $\widetilde{\mathbf{F}}$ can be calculated algebraically from the concentration vector and therefore obtained from a single simulation, whilst even the most effective calculation of the sensitivity matrix $\widetilde{\mathbf{S}}$ requires significantly more computer time (see Sect. 5.2). If f_i is the right-hand side of the kinetic system of ODEs for species i (2.9) and parameter k_j is the rate coefficient of the reaction step j, then the elements of matrix $\widetilde{\mathbf{F}}$ can be easily calculated (Turányi et al. 1989) as

$$\widetilde{F}_{i,j} = \frac{\partial \ln f_i}{\partial \ln k_j} = \frac{k_j}{f_i}\frac{\partial f_i}{\partial k_j} = \left(\frac{\nu_{ij} r_j}{f_i}\right) \tag{7.4}$$

If temperature is also considered in the objective function, then the enthalpies of formation of the species and heat capacity of the reaction mixture also have to be taken into account (Zsély and Turányi 2003).

The eigenvalues of matrix $\widetilde{\mathbf{F}}^{\mathrm{T}}\widetilde{\mathbf{F}}$ indicate the effectiveness of a simultaneous change of the values of a group of parameters on the production rates of species. Elements of the eigenvectors show the weight of the individual parameters in the corresponding parameter group. In common with the PCAS method, the PCAF method can determine a list of important reactions, if the parameters investigated are the rate coefficients (or A-factors) of the reaction steps, and the objective function includes the production rates of the important and necessary species.

Although the PCAS and PCAF methods are similar in form, these two methods are fundamentally different. The objective function of PCAF contains the production rates of species, and the matrix **F** can be calculated from the right-hand side of ODE (2.9). The objective function of PCAS contains the concentrations of species [the solution of ODE (2.9)], and the matrix **S** has to be obtained from the solution of the sensitivity differential equations (5.7) and is therefore computationally more time consuming. Put another way, PCAS investigates the effect of parameter changes on the solution of the kinetic system of ODEs, whilst PCAF examines the effect of parameter changes on the right-hand sides of the kinetic system of ODEs (2.9).

When the importance of reactions is investigated using PCAF over an interval of time or distance, the analysis has to be carried out at several independent variable sets. This means that the change in importance of reaction steps over time (or distance) can be monitored with arbitrary resolution. If two different models (e.g. an ignition and a flame model) provide identical concentration and temperature profiles using the same reaction mechanism, then PCAF will provide identical importance measures for the reaction steps (Zsély and Turányi 2003). On the other hand, PCAS investigates the local sensitivity matrices, which indicate the effect of a parameter perturbation on the time-dependent solution, so that very different

sensitivity functions may belong to the same reaction mechanism and concentration—time functions. Moreover, PCAS investigates the integrated deviations in solution (see Eq. 5.15), and therefore, the reaction importance belongs to an interval of time. Another consequence of the differences is that using PCAF, it may be important to apply the analysis over many time or distance points along reaction trajectories in order to ensure that reactions which are only of importance over a subset of the whole domain are picked up by the analysis. Often a simple model scenario can be used (e.g. zero-dimensional reactor simulations or a 1D flame simulation) for the reduction process, and, as long as the concentration, temperature and pressure profiles match those of the final practical model, the reduced models generated can be of use in larger modelling scenarios such as 3D simulations. The use of adaptive reduction where different reduced schemes are utilised over different subsets of the domain is discussed below.

7.4 Identification of Redundant Reaction Steps Based on Entropy Production

All of the previous methods identify redundant reactions via the inspection of the reaction rates or by the study of sensitivity matrices deduced from the kinetic system of differential equations. A very different approach is the application of thermodynamic functions for the identification of redundant reactions. This approach has common features with the derivation of numerical reduced models based on thermodynamics reasoning (see Sect. 7.10.4).

Kooshkbaghi et al. (2014) published a systematic approach based on the relative contribution of each elementary reaction to the total entropy production. In a closed system, the total entropy production per unit volume is a positive semidefinite function that can be calculated in the following way:

$$\frac{\mathrm{d}S}{\mathrm{d}t} = R\sum_{j=1}^{N_R}\left(r_{\mathrm{f},j} - r_{\mathrm{b},j}\right)\ln\left(\frac{r_{\mathrm{f},j}}{r_{\mathrm{b},j}}\right) \tag{7.5}$$

The entropy production vanishes at equilibrium. The relative contribution of each reaction step to the total entropy production is given by

$$q_j = \left[R\sum_{j=1}^{N_R}\left(r_{f,j} - r_{b,j}\right)\ln\left(\frac{r_{f,j}}{r_{b,j}}\right)\right]\left[\frac{\mathrm{d}S}{\mathrm{d}t}\right]^{-1} \tag{7.6}$$

Here R is the gas constant and $r_{f,j}$ and $r_{b,j}$ are the rates of the j-th forward and backward reaction steps, respectively. Kooshkbaghi et al. (2014) investigated the effect of eliminating all reaction steps having q_j relative entropy production less than a threshold ε for an example of an n-heptane ignition mechanism. Their

approach leads to eliminations of both reaction steps and the corresponding species. They found that the simulation error, i.e. the deviation between the simulation results obtained with the reduced and the original mechanisms, is a nonlinear function of the chosen threshold ε. Probing several ε values, an appropriate reduced mechanism with acceptable simulation error could be obtained.

7.5 Graph-Based Methods

7.5.1 Directed Relation Graph Method

Methods for species and reaction removal based on directed relation graphs (DRGs) with specified accuracy requirements have been introduced by Lu and Law (2005, 2006c). In their development of the method, Lu and Law suggest that graph-based methods are highly suited to exploring couplings between species. This means that such methods may be applied to remove groups of species that may be internally coupled, through, for example, fast reactions, but are not strongly coupled to important processes within the mechanism. An example of this type of relationship is shown in the schematic in Fig. 7.2. Each node in the DRG represents a species from the mechanism, and an edge from vertex A to vertex B exists if and only if the removal of species B would directly induce significant error to the production rate of species A. This means that an edge from A to B means that B has to be kept in the mechanism to correctly evaluate the production rate of species A. Note the similarity between Figs. 7.1 and 7.2. Like all other methods for species removal, DRG methods also start from the selection of important species (cf. Sect. 7.2), called "target species" in the DRG terminology. Using a DRG method, all species closely connected to the target species are identified.

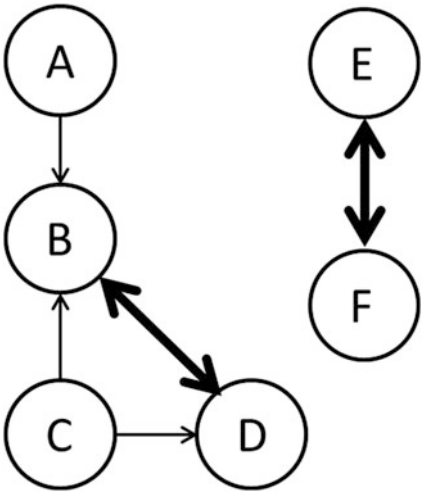

Fig. 7.2 A directed relation graph showing typical relationships between species. Modified from (Lu and Law 2005)

The various DRG-based reduction methods all state a connection weight between pairs of species. These weights define the directed relation graph structure. Starting from the target species, an importance coefficient is calculated for all other species, which quantifies how strongly a given species is connected to the target species. Then, all species are eliminated from the mechanism (with their reactions) whose importance coefficient is below a user-defined threshold. The DRG-based methods differ in their definitions of connection weights and importance coefficients. Tosatto et al. (2013) compared the various DRG-based methods, and we follow their notations in the discussion below.

The original DRG method of Lu and Law (2005) defines the connection weight from species i to species j in the following way:

$$R_{i\to j}^{(\mathrm{Lu})} = \frac{\sum_{\alpha\in C(i,j)} \left|\nu_{i\alpha} r_\alpha\right|}{\sum_{\alpha\in R(i)} \left|\nu_{i\alpha} r_\alpha\right|} \tag{7.7}$$

where $R(i)$ is the set of reactions that are related to species i, $C(i,j)$ is the set of reactions in which both species i and j participate, $\nu_{i\alpha}$ is the stoichiometric coefficient of species i in reaction α and r_α is the net reaction rate (the difference of the forward and backward rates).

A variant of the DGR method was suggested by Luo et al. (2010a) for the reduction of reaction mechanisms containing many isomers. Luo et al. recommended the application of the maximum norm instead of the summation:

$$R_{i\to j}^{(\mathrm{Luo})} = \frac{\max_{\alpha\in C(i,j)} \left|\nu_{i\alpha} r_\alpha\right|}{\max_{\alpha\in R(i)} \left|\nu_{i\alpha} r_\alpha\right|} \tag{7.8}$$

The original DRG method of Lu and Law (2005) defines the importance coefficient of species i as

$$I_i^{(\mathrm{DRG})} = \begin{cases} 1 & \text{if species } i \text{ is a target species} \\ \max\limits_{j\in S} \left(\min\left(R_{j\to i}, I_j^{(DRG)}\right)\right) & \text{otherwise} \end{cases} \tag{7.9}$$

Here S is the full set of chemical species and $R_{j\to i}$ is a connection weight defined in Eqs. 7.7 and 7.8, and it is implicitly assumed that if two species are not connected, then $R_{j\to i} = 0$. This approach defines the importance coefficient for species i as the smallest connection on any path towards a target species. $I_i^{(\mathrm{DRG})}$ is calculated iteratively using a minimum-cost graph search algorithm (Lu and Law 2005). A small threshold value ε can be defined, and if $I_i^{(\mathrm{DRG})} < \varepsilon$, then species i is considered to be redundant for the simulation of the target species. Hence, in Fig. 7.2, if A is an important species, then D must be retained within the scheme since although it is not directly coupled to A, it is part of the dependent set of A by being directly coupled to B, where B is coupled to A. In this example species E and F are

interconnected by a pair of fast reversible reactions, since, although they are strongly coupled to each other, they do not couple to any species in the dependent set of A. The strong two-way coupling between these species indicates that they should be removed as a pair.

In common with the connectivity method (CM, Sect. 7.2.3), the DRG method requires a set of important species ("target species") to be specified which may include the main reactants and important products of the starting reaction mechanism. The method then seeks the dependent sets for each important species, and the skeleton mechanism is formed from the union of these sets. The DRG method is local in the sense that the reaction rates used are specific to a particular set of concentrations and temperature. In common with the CM, the graph has to be computed over a range of conditions relevant to the intended final application. For a generally applicable reduced scheme, the final model must represent the union of mechanisms derived for each operating condition. The success of the final reduced scheme will depend on the relevance of the local conditions chosen for analysis and the selected value of ε. The size of the skeleton mechanism will reduce as larger and larger values of ε are chosen. Several thresholds can be applied and the accuracy of the resulting mechanisms are tested in order to select an appropriate level of reduction. Lu and Law (2005) state that jumps in the number of required species may occur quite abruptly, signifying groups with strong internal coupling but weak intergroup couplings moving out of the skeleton scheme. This is analogous to the large gaps in B_i values that occur in the Jacobian analysis and in a similar manner can help with the selection of threshold values for ε. It should be pointed out that in both the simple connectivity and DRG-based methods, the thresholds only control the local accuracy of the rates of production of necessary species, which does not automatically control the potential growth of errors in a time or spatially dependent model. The impact of *local errors* could be determined via more expensive methods or simulations compared to the full model.

Figure 7.3 shows the result of an investigation where the DRG threshold ε was changed systematically for an example of the reduction of a methane partial oxidation mechanism (Nagy and Turányi 2009). The number of species remaining within the reduced mechanism decreased almost linearly on increasing the logarithm of ε. The most interesting result was that the simulation error did not change monotonically with increasing ε. Also, sudden jumps indicated that sometimes using only a slightly higher ε gave a much worse reduced mechanism, as explained above.

The DRG method was first applied to a model system of ethylene combustion (Lu and Law 2005; Luo et al. 2011) with a full scheme of 70 species. A value of ε of 0.16 gave a skeleton scheme of 33 species, i.e. quite a substantial degree of reduction. In application to *n*-heptane and *iso*-octane combustion using full schemes of 561 and 857 species (Lu and Law 2006c), ε values of 0.19 and 0.17 resulted in reduced schemes of 188 and 233 species, respectively. DRG methods have since been widely applied for the reduction of large combustion schemes including for methane (Sankaran et al. 2007), primary reference fuel (Lu and Law

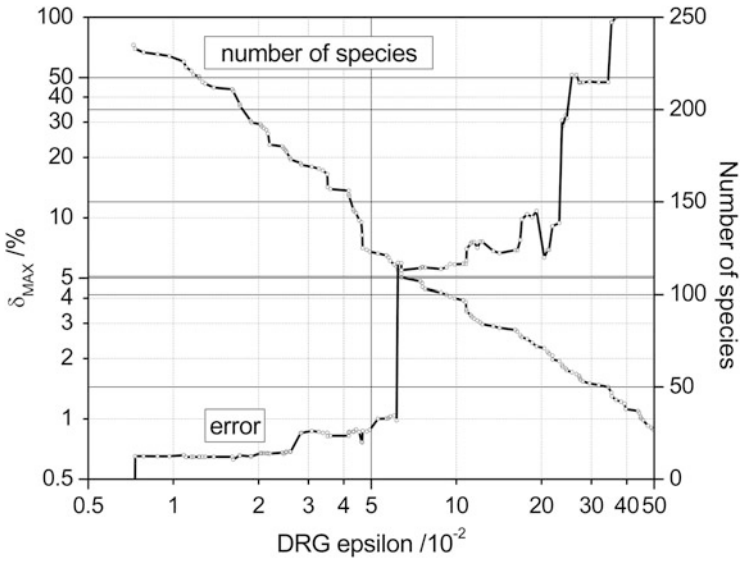

Fig. 7.3 Maximal simulation error and the number of species as a function of ε using the original DRG method. Reprinted from (Nagy and Turányi 2009) with permission from Elsevier

2006c, 2008b; Yoo et al. 2011, 2012; Luong et al. 2013), *n*-dodecane (Luo et al. 2014) and biodiesel mechanisms (Luo et al. 2010a, 2012a, b).

An improved version of the DRG method was developed called "DRG with restart", where the DRG procedure is repeated on the DRG-reduced mechanism (Lu and Law 2006c). Lu and Law found that for examples of large hydrocarbon mechanisms, a two-stage reduction using DRG can lead to smaller skeleton mechanisms than a single-stage reduction with a single value for ε. The reason is that the calculated reaction rates are different at the second stage due to the exclusion of redundant species. This can result in a change of the graph structure, potentially allowing the removal of further species at the second stage. The chosen values for ε are generally larger at the second stage.

Tosatto et al. (2011) introduced the flux-based DRG method. This approach explicitly considers the effect of transport fluxes in flames which leads to the coupling of the governing equations among adjacent grid cells. The resulting numerical scheme operates on a cell-by-cell basis, so that different chemical submodels are applied in different regions of the flame. The flux-based DRG method was employed within two-dimensional simulations of steady and unsteady axisymmetric co-flow flames. Further applications include the work of Ren et al. (2014b) who applied the DRG reduction method within a dynamic adaptive chemistry calculation during the simulation of one-dimensional, unsteady, freely propagating, premixed methane/air laminar flames.

7.5.2 DRG-Aided Sensitivity Analysis

A significant development of the DRG method is *DRG-aided sensitivity analysis* (DRGASA) (Zheng et al. 2007). The name of the method is perhaps a little misleading, because it does not include the calculation of sensitivities, but rather the DRG estimation for the group of redundant species is checked using simulations. First, the redundant species according to the DRG method are selected using a conservative threshold. Then a second group of species is identified using a tighter threshold, and these species are included into the reduced mechanism. A series of simulations are carried out where the consequences of eliminating these species are investigated one by one. The DRGASA method could be more effective than the basic DRG approach, because it investigates the simulation error directly. This simulation error belongs to the group of important species, and therefore, the DRGASA indicates less species to be necessary than the original method for a prescribed error limit. Figure 7.4 shows that combining the DRG method with restart already improves the method compared to DRG. Additional application of DRGASA significantly improves the mechanism reduction procedure.

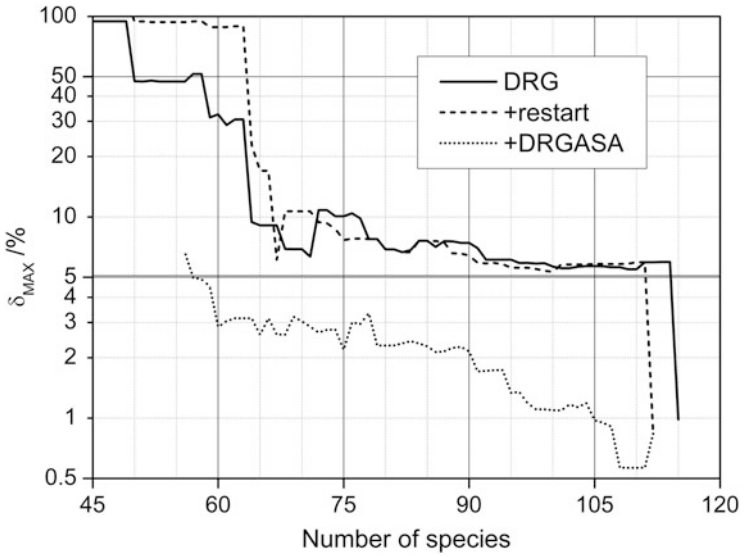

Fig. 7.4 Maximal simulation errors of the mechanisms as function of species number, obtained by applying the original DRG method, and the DRG method with restart and DRGASA extensions. Reprinted from (Nagy and Turányi 2009) with permission from Elsevier

7.5.3 DRG with Error Propagation

Pepiot-Desjardins and Pitsch (2005, 2008) noticed that Eq. (7.7) does not distinguish between reactions that create or destroy species i and suggested an alternative definition:

$$R_{i\to j}^{(\mathrm{Pep})} = \frac{\left|\sum_{\alpha\in C(i,j)} \nu_{i\alpha} r_\alpha\right|}{\max\left(\sum_{\alpha\in R(i)} \left(\nu_{i\alpha} r_\alpha\right)^+, \sum_{\alpha\in R(i)} \left(\nu_{i\alpha} r_\alpha\right)^-\right)} \tag{7.10}$$

The operator $(.)^+$ selects only the positive terms in the summation, and the operator $(.)^-$ selects only the negative terms and makes them positive. Equation (7.10) calculates the ratio of the sum of the rates belonging to the pair of species (i, j) to the total rate of formation or destruction of species i. Note that all forward and backward rates must be considered separately as a single reaction when using the connection weights (7.10), or else partial equilibrium reactions could result in artificially low connection weights.

Pepiot-Desjardins and Pitsch (2008) made further extensions to DRG by incorporating error propagation, called *DRG with error propagation* (DRGEP). In this method the assumption that all coupled species are equally important in the mechanism is lost, and errors are damped as they propagate along the graph from the initially selected important species. The importance index is therefore calculated as

$$I_i^{(\mathrm{DRGEP})} = \begin{cases} 1 & \text{if species } i \text{ is a target species} \\ \max\limits_{j\in S}\left(R_{j\to i}\cdot I_j^{(\mathrm{DRGEP})}\right) & \text{otherwise} \end{cases} \tag{7.11}$$

The aim of error propagation is to try to eliminate more species using the same threshold error by better estimating the induced error, rather than using its upper bound. The approach is combined with an integrity check which aims to avoid truncated chemical paths that may lead to mass accumulation in intermediate species whose consumption paths have been removed. However, for chains of propagating reactions with several fast steps, this may lead to an underestimation of errors since in this case the fast species can be related to the slow ones through algebraic expressions (see Chap. 6) leading to a single rate-determining step within the sequence. According to Lu and Law (2006c), the error propagation method in such cases should be linked to an investigation of the slow and fast subspaces.

The DRGEP approach has been applied adaptively in order to produce *on-the-fly reduced mechanisms* for *n*-heptane (Shi et al. 2010b) and gasoline surrogate mixtures (Liang et al. 2009b; Shi et al. 2010a) in simulations of homogeneous charge compression ignition. In Liang et al. (2009b), computational speed-ups of a factor of 70 were achieved when compared to a detailed starting mechanism containing 1,099 species. The number of species required in the locally reduced models varies throughout the calculations but reaches a maximum of about one third of the number of initial species. The DRG and DRGEP methods were compared for an example of

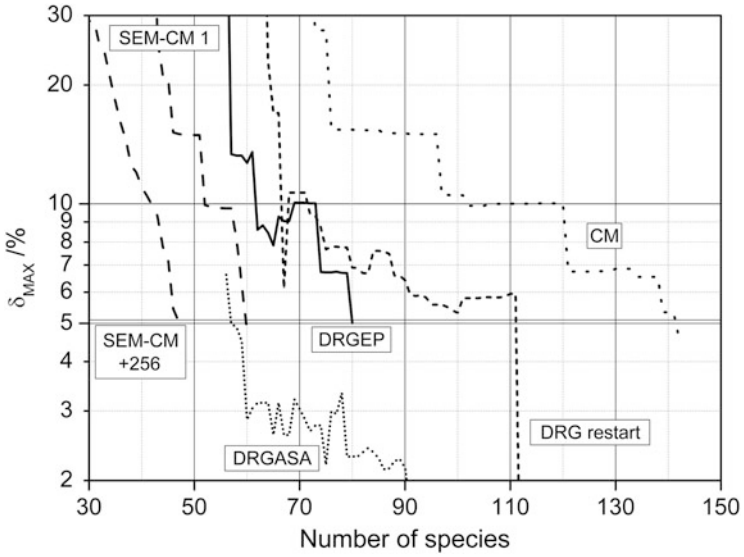

Fig. 7.5 Comparison of the performance of the connectivity method (CM), DRG with restart, DRGEP, DRGASA and SEM-CM for the reduction of a methane partial oxidation mechanism. Maximal simulation errors of the mechanisms are given as function of remaining species numbers within the reduced schemes. Reprinted from (Nagy and Turányi 2009a) with permission from Elsevier

the reduction of *n*-heptane and *iso*-octane mechanisms (An and Jiang 2013). Various graph search algorithms were tested within the DRGEP method by Niemeyer and Sung (2011). DRGEP has also been coupled with sensitivity analysis in Niemeyer et al. (2010), Zsély et al. (2011), Ismail et al. (2013), and Niemeyer and Sung (2014), and the combined method was called DRGEP-ASA.

Other applications of the DRG method and its extensions to skeletal model reduction include modelling the high-temperature combustion of $H_2/CO/C_1-C_4$ hydrocarbons (Wang 2013), methane oxidation (Jiang and Qiu 2009), nitrogen oxide emissions and their control (Lv et al. 2009; Luo et al. 2011), the combustion of *n*-heptane (Liang et al. 2009a; Wang et al. 2013; Bahlouli et al. 2014), surrogate jet fuels (Naik et al. 2010), methyl decanoate (a large methyl ester used as a surrogate for biodiesel, (Seshadri et al. 2009)), surrogate biofuels (Luo et al. 2010a, b; Malik et al. 2013) and the oxidation of *iso*-octane (Kelley et al. 2011). All DRG variants were compared in a recent article of Poon et al. (2013). The DRGEP method has also been applied in atmospheric chemistry to the reduction of a detailed alpha-pinene oxidation mechanism where the aim was to maintain the ability of the reduced mechanism to represent the ozone and organic aerosol-forming properties of the original scheme (Xia et al. 2009). Subsequent application of reaction removal through the principal component analysis of the rate sensitivity matrix followed by QSSA analysis led to an overall reduction of a factor of 2.5 in the number of species and reactions in the scheme.

Figure 7.5 shows a comparison of the performance of the connectivity method (Sect. 7.2.3), DRG with restart (Sect. 7.5.1), DRGEP (Sect. 7.5.3), DRGASA

(Sect. 7.5.2) and SEM-CM (Sect. 7.2.4) for the reduction of a methane partial oxidation mechanism (Nagy and Turányi 2009). Method SEM-CM is presented in two versions, one is faster and less effective ("1"), and the other is slower and more effective ("256"). For each method, the most effective version was used in the comparison. In general, a mechanism reduction method is more effective if the simulation error is smaller for the same number of species or if the same simulation error can be achieved with a mechanism having less species. For this example, the SEM-CM method proved to be the most effective; however, we have to keep in mind that the application of this method requires much more computer time compared to the other methods.

7.5.4 The Path Flux Analysis Method

Path flux analysis (PFA) is a method, similar to DRG, for the generation of skeletal mechanisms (Sun et al. 2010; Gou et al. 2013). In the PFA method, the production and consumption fluxes are used to identify the important reaction pathways. The first-generation production (P_A) and consumption (C_A) fluxes of species A are calculated according to equations

$$P_A = \sum_i \max(\nu_{A,i}\,\omega_i,\ 0) \tag{7.12}$$

$$C_A = \sum_i \max(-\nu_{A,i}\,\omega_i,\ 0) \tag{7.13}$$

where $\nu_{A,i}$ is the stoichiometric coefficient of species A in the i-th reaction and ω_i is the net reaction rate of this reaction. The production (P_{AB}) and consumption (C_{AB}) fluxes of species A via species B are calculated by

$$P_{AB} = \sum_i \max\left(\nu_{A,i}\,\omega_i\,\delta_B^i,\ 0\right) \tag{7.14}$$

$$C_{AB} = \sum_i \max\left(-\nu_{A,i}\,\omega_i\,\delta_B^i,\ 0\right) \tag{7.15}$$

where δ_B^i is unity if species B is involved in the i-th reaction and 0 otherwise. A flux ratio is introduced to represent the share of a particular production and consumption path via species B to the total production and consumption flux of species A. The first-generation flux ratios for the production and consumption of species A via species B are defined as

$$r_{\mathrm{AB}}^{\mathrm{pro-1st}} = \frac{P_{\mathrm{AB}}}{\max(P_{\mathrm{A}}, C_{\mathrm{A}})} \tag{7.16}$$

$$r_{\mathrm{AB}}^{\mathrm{con-1st}} = \frac{C_{\mathrm{AB}}}{\max(P_{\mathrm{A}}, C_{\mathrm{A}})} \tag{7.17}$$

At each time step, production and consumption flux ratios $r_{\mathrm{AB}}^{\mathrm{pro-1st}}$ and $r_{\mathrm{AB}}^{\mathrm{con-1st}}$ are calculated. This process only involves the calculation of the reaction rates, and the CPU time is linearly proportional to the number of species. The reduction starts from the important species and then identifies whether to retain species B in the reduced model by evaluating if the flux ratios of species A via species B satisfy the relation $r_{\mathrm{AB}} > \varepsilon$, where ε is a threshold value and $r_{\mathrm{AB}} = \max(r_{\mathrm{AB}}^{\mathrm{pro-1st}}, r_{\mathrm{AB}}^{\mathrm{con-1st}})$.

An iterative process is used to find the path fluxes of each selected species. Starting from the set of important species, using the relation $r_{\mathrm{AB}} > \varepsilon$, the set of other necessary species are identified. These are added to the investigated set, and the iterative process is continued until no new necessary species are found. Gou et al. (2013) used the PFA method to create a dynamic adaptive chemistry scheme for *n*-heptane and *n*-decane combustion mechanisms.

7.5.5 Comparison of Methods for Species Elimination

A common feature of the connectivity, PFA, DRG and DRGEP methods (with or without ASA) is that the list of important species has to be defined. Then, points on the concentration trajectory are selected, and the analysis is carried out at these points. The set of necessary species are determined at each of the chosen points, and the reaction mechanism that is applicable across the whole domain should contain the union of the species necessary at each point unless adaptive reduction is employed (see later discussion). The list of necessary species is determined by a threshold (the threshold B_i value in the connectivity method and parameter ε in the DRG, DRGEP and PFA methods), which are not linearly related to the simulation error of the resulting reduced mechanism. In general, a smaller threshold leads to a larger mechanism with smaller simulation error, but the decrease of the simulation error is not necessarily monotonic. Using these methods, the efficiency of mechanism reduction has to be judged *a posterior*: a reduction method being more efficient if the reduced mechanism contains less species at the same level of simulation error. We saw that extensions to these methods such as the SEM-CM, DRGASA and DRGEP-ASA methods include the simulation error as part of the necessary species selection and can lead to more effective reduction strategies at the expense of computational cost. Other approaches have also been developed based on methods from optimisation, and these will be discussed in the next section.

7.6 Optimisation Approaches

Although sensitivity analysis, DRG and CSP are perhaps the most common methods for deriving skeletal mechanisms, the application of optimisation methods such as linear and nonlinear integer programming is increasing for reduction analysis. One advantage of such methods is that they preserve the nonlinearity of the reaction system, as opposed to sensitivity analysis, which is in general based on first-order sensitivity coefficients. These methods are based on solving an optimisation problem, i.e. minimising an objective function subject to a set of constraints. In mechanism reduction applications, the objective function is related to the model error between the full and reduced models, which varies between applications, but is usually based on errors in either rates of production of species or species concentrations.

7.6.1 Integer Programming Methods

An early application of this type of approach for reaction removal was carried out by Petzold and Zhu (1999) for several ignition problems. Although this method has its drawbacks, we discuss it in some detail here since it provides a useful illustration of how optimisation approaches are applied in practice. The rate of change of species mass fractions y_i is given by

$$\dot{y}_i = f(\mathbf{y}) = \sum_{j=1}^{N} \upsilon_{ij} R_j(\mathbf{y}) \tag{7.18}$$

which in matrix form can be written as

$$\dot{\mathbf{y}} = \boldsymbol{\upsilon}\mathbf{R}(\mathbf{y}) \tag{7.19}$$

where $\boldsymbol{\upsilon}$ is a matrix whose columns are the stoichiometric vectors and $\mathbf{R}$ is the vector of nonlinear reaction terms. A similar equation set for the reduced model can then be described as

$$\dot{\mathbf{z}} = \boldsymbol{\upsilon}\mathbf{D}\mathbf{R}(\mathbf{z}) \tag{7.20}$$

where $\mathbf{D}$ is an $N \times N$ diagonal matrix whose diagonal elements d_j are either 1 or 0 depending on whether the reaction j is retained in the mechanism or not. Finding the reduced mechanism can then be expressed as a constrained optimisation (Petzold and Zhu 1999):

$$\begin{aligned}
&\min \| \mathbf{y}-\mathbf{z} \| \\
&\text{subject to} \\
&\dot{\mathbf{y}} = \boldsymbol{\upsilon}\mathbf{R}(\mathbf{y}), \qquad \mathbf{y}(\mathbf{0}) = \mathbf{y_o} \\
&\dot{\mathbf{z}} = \boldsymbol{\upsilon}\mathbf{DR}(\mathbf{z}), \qquad \mathbf{z}(\mathbf{0}) = \mathbf{z_o} \quad 0 \leq t \leq b \\
&\sum_{j=1}^{N} d_j = k, \qquad d_j = 0 \text{ or } 1
\end{aligned} \tag{7.21}$$

where the minimum is over $d_1, \ldots, d_N$ and $k < N$. Here k is the number of reactions in the reduced scheme and is chosen by the user. The norm is weighted according to user supplied relative and absolute tolerances. If one was interested in the overall error during a simulation time, then the local term $\min \|\mathbf{y} - \mathbf{z}\|$ could be extended to an integral between initial time t_i and final time t_f, thus calculating $\min \left\| \int_{t_i}^{t_f} \mathbf{y}(\mathbf{t}) - \mathbf{z}(\mathbf{t}) \right\|$. The resulting optimisation becomes an integer nonlinear programming problem as discussed by Edwards et al. (2000). It is also a combinatorial problem. For example, for a 5-reaction starting mechanism, there are 2^5–1 possible reduced mechanisms. Since the number of possible reduced mechanisms grows exponentially with reaction size, there is clearly a need to restrict the optimisation problem where possible. Several variations on the methodology were proposed by Petzold and Zhu to reduce the computational cost of the method. The first is based on the fact that it may not be necessary to find the absolute minimum of $\|\mathbf{y} - \mathbf{z}\|$, and any reduced mechanism with a small enough value may be good enough. A modified version of Eq. (7.21) is proposed as

$$\begin{aligned}
&\min \| \mathbf{y} - \mathbf{z} \| \\
&\text{subject to} \\
&\dot{\mathbf{y}} = \boldsymbol{\upsilon}\mathbf{R}(\mathbf{y}), \qquad \mathbf{y}(\mathbf{0}) = \mathbf{y_o} \\
&\dot{\mathbf{z}} = \boldsymbol{\upsilon}\mathbf{DR}(\mathbf{z}), \qquad \mathbf{z}(\mathbf{0}) = \mathbf{z_o} \quad 0 \leq t \leq b \\
&k_1 \leq \sum_{j=1}^{N} d_j \leq k_2, \qquad 0 \leq d_j \leq 1 \\
&g(d_1, \ldots, d_N) \leq r
\end{aligned} \tag{7.22}$$

where k_1 and k_2 are upper and lower bounds, respectively, on the number of reactions in the reduced model, g is a nonlinear function which when equal to 0 forces the d_j to take integer values and r is a small positive number that relaxes to the nonlinear constraint. The restrictions on the possible number of reactions in the reduced mechanism lower the overall number of combinations within the optimisation. Petzold and Zhu use the following function to describe g:

$$g = \sum_{j=1}^{N} \left(d_j - {d_j}^2\right)^2 = 0 \tag{7.23}$$

The optimisation problem described by (7.22) is then solved using sequential quadratic programming, and in order to obtain the reduced model, the values of d_j are rounded to 0 or 1.

The method can also be applied to the removal of species, and a two-tier approach is suggested by Petzold and Zhu (1999) and by Mitsos et al. (2008), where the search for redundant species is performed prior to reaction removal in common with several other skeletal reduction approaches as outlined above. Since the number of species is usually much lower than the number of reactions, a significant cost saving in the application of the method can be made since all reactions of redundant species are removed at the first stage, thus reducing the cost of the reaction removal procedure. In addition, the method proposed by Petzold and Zhu first applies the so-called "greedy" algorithm for both species and reaction removal prior to the solution of the full optimisation problem. In the greedy method, the reactions are removed from the model one by one with those causing the smallest error under the given norm being dropped first (a trial-and-error approach as discussed in Sect. 7.2.2). The approach scales as N^2, however, which makes it computationally costly for large reaction mechanisms. In addition, care must be taken for mechanisms containing fast reversible reactions since, as indicated in Sects. 7.2 and 7.5, sometimes reactions/species can be more successfully removed in groups rather than individually.

A slightly different approach to the use of optimisation methods is presented by Androulakis (2000) based on the minimisation of the number of reactions in the reduced mechanism subject to constraints on the error of the reduced mechanism with respect to the full scheme. In this example, a weighted error norm containing terms involving species mass fractions, temperature and induction time for the reaction is developed. In common with the approach of Petzold and Zhu (1999), a pre-processing step is applied in this work to identify a subset of important reactions with high ranking based on removing the reactions one at a time. This subset is then excluded from the constraints in the full optimisation problem in order to improve computational efficiency. Problems with fast reversible reactions may also be encountered using this approach, and hence, the use of this pre-processing step will lead to an upper bound on the numbers of reactions within the final reduced scheme. The application of species removal prior to reaction removal may help to alleviate this problem.

The integer programming technique applied by Androulakis is a branch-and-bound algorithm which splits the feasible region of input values into smaller subregions (branching) with the subregions forming a search tree. Upper and lower bounds on the optimal solution in each subregion can then be determined (bounding), and if the *lower* bound for a subregion A from the search tree is greater than the *upper* bound for any other (previously examined) subregion, then A may be safely discarded from the search (pruning). If an optimal solution is found to a subregion (e.g. if the upper bound matches the lower bound), it is a feasible solution to the full problem, but not necessarily globally optimal. It can be used for pruning, however, since if the lower bound for a node exceeds the best known feasible solution, no globally optimal solution can exist in the subspace of the feasible region represented by the node. The procedure stops when all nodes of the search tree are either pruned or solved. Within the subregions, the relaxation of the integer problem is solved by successive quadratic programming. The methods are

illustrated for a hydrogen combustion model in a stirred reactor where the use of different objective functions is compared. Androulakis shows that the use of errors at only the final time point leads to a smaller reaction mechanism when compared to using a range of reaction times, but does not give a good representation of the intermediate dynamics. The approach was also applied to species removal by Androulakis (2000) and Banerjee and Ierapetritou (2003).

Anderson et al. (2011) transformed the original chemical kinetic model of a mitogen-activated protein kinase (MAPK) signalling pathway to a linear parameter-varying (LPV) model. This LPV model was then used to identify loosely connected blocks of the original model, taking into account the uncertainty ranges of the important parameters. Hannemann-Tamás et al. (2014) considered mechanism reduction as a convex mixed-integer quadratic problem, for which efficient solvers exist. They discussed the relationship of this approach with the sensitivity analysis-based mechanism reduction methods (Sect. 7.3). The rate coefficients of the reduced mechanisms were optimised to give a better reproduction of solutions of the full mechanisms.

One advantage of integer programming methods is that they can be formulated in a general way, and the constraints can therefore include any required measure of the simulation error between the reduced and full models. This means that the actual simulation error in important species or target outputs can be taken into account, in contrast to the standard DRG and connectivity methods discussed above which were based on local approaches. However, for large mechanisms, the number of possible reduced mechanisms could be huge, and if each were to be tested, then the methods become very computationally costly. Screening type algorithms have therefore been included using the so-called greedy approach, but these are really trial-and-error-based algorithms, and as discussed in Sect. 7.2.1, they ignore the couplings between species. In order to make reduction algorithms more efficient, it is sensible to utilise the information on species couplings contained either in the Jacobian matrix or the DRG, and hence, the combination of the connectivity approach with error minimisation as used in the Simulation Error Minimization Connectivity Method (SEM-CM, Sect. 7.2.4) is likely to be more computationally effective.

A further extension of integer programming methods was also developed in the work of Bhattacharjee et al. (2003) based on earlier ideas developed in Schwer et al. (2003). Here the reduction is based on a linear integer programming method providing computational savings over nonlinear methods. The linearity is achieved by applying constraints to local rates of production rather than to concentration and temperature profiles, forcing the error constraints to be linear in the rates of production. Therefore, similarly to the results of reduction methods based on DRG or rate sensitivity matrices, the reduced mechanisms are only strictly applicable for the local points at which they were generated. The global error is now also related to the locally controlled error in a more complex way, since small local errors in rates of production may grow and propagate during time-dependent simulations. The derivation of a rigorous quantitative relationship between the

tolerances used within the optimisation procedure and the resulting simulation errors in concentration profiles is a significant challenge for all local methods.

7.6.2 *Genetic Algorithm-Based Methods*

Gradient-based and "branch-and-bound" methods are not guaranteed to find the global minimum of a function for non-convex problems. Other approaches to solving optimisation problems in mechanism reduction include binary encoded genetic algorithms (GAs) as discussed in Edwards et al. (1998), Banerjee and Ierapetritou (2003), Elliott et al. (2004, 2005, 2006), Montgomery et al. (2006), Hernández et al. (2010) and Sikalo et al. (2014). Note that several authors also used genetic algorithms for the optimisation of parameters of reaction mechanisms (Polifke et al. 1998; Katare et al. 2004; Elliott et al. 2004; Perini et al. 2012).

GAs are a subset of evolutionary algorithms in which a population of abstract representations (called *chromosomes*) of candidate solutions (called *individuals*) to an optimisation problem evolves towards better solutions. The basic steps of the process are outlined in Fig. 7.6. Solutions are generally represented as binary vectors of 0s and 1s. At each step of an iterative process, the behaviour of each individual solution is evaluated using a fitness function, and the search process stops when the specified fitness criterion is reached.

In the context of mechanism reduction, a 1 or 0 represents a particular species or reaction (Hernández et al. 2010) being present or not within the final reduced

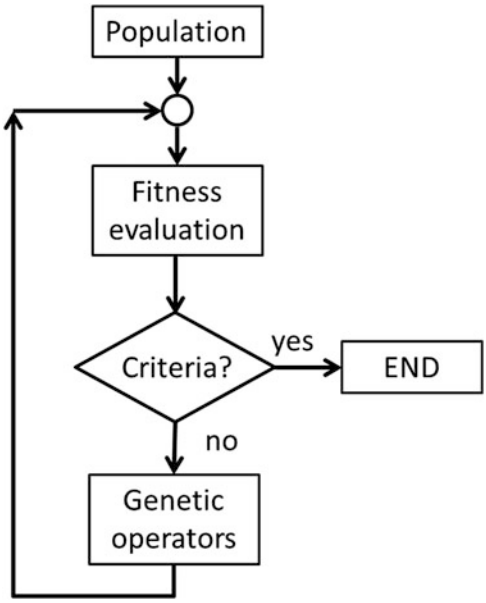

Fig. 7.6 Schematic of steps in GA methodology. Reproduced from (Hernández et al. 2010) with permission from Elsevier

model. For example, an initial population of four individuals for a final reduced model specified to have five species from a full model with ten species may be written as follows:

Individual 1 1100101010
Individual 2 1100111000
Individual 3 1100100011
Individual 4 1110001010

Important species may also be defined such as fuel, oxidiser or important products. Species 1 and 2 in the above example are always fixed at 1, i.e. always present in the mechanism, thus reducing the search space by 2. A reaction is chosen to be present in the reduced model only if all reactant and product species exist within the reduced species set. The fitness criterion is then used to determine which individuals to propagate to the next generation. For example, Elliot et al. (2005) use a criterion based on a weighted sum of errors in species molar concentrations using an L_2 norm. The fittest individuals are then selected probabilistically using a k-tournament selection in order to be parents for the next generation. Cross-over and mutation (genetic operators) are then used to exchange information between parents in order to develop the next generation of individuals as described in Harris et al. (2000). The approach involves selecting two parents and identifying those species common to both parents. A child is formed by keeping common species and randomly selecting new ones from unused positions in the chromosome. Mutation is used to avoid local minima. The fitness criterion is then used again, and the fittest parents and children are selected to form a new generation. After a certain number of generations, where there is no further improvement, the best chromosome represents an optimal solution. The method was successfully applied in Elliott et al. (2005) to the reduction of the GRI methane oxidation mechanism to a 16-species skeleton mechanism, although even when using a fairly large set of important species, the optimisation process took 2 days of CPU on a 3.2 GHz Pentium 4 processor. The method was further extended to optimisation of the rate parameters in the reduced scheme based on an experimental set of 1D laminar flame profiles. The combined approach of model reduction and parameter selection using GA-based optimisation methods has also been applied to biochemical networks in Mauryaa et al. (2006, 2009) and to reduced models for the combustion of aviation fuels in Elliott et al. (2006).

A slightly different approach was applied in the earlier work of Edwards et al. (1998) where the search was for the minimum number of reactions/species needed to satisfy specified error bounds rather than for the best reduced mechanism for a fixed number of species and a given error tolerance. A heuristic comparison was made in this work between the computational expense of the GA approach and global sensitivity-based methods. The number of functional evaluations for the GA approach was stated to be lower than for global sensitivity analysis, although the same would not be true for the local rate sensitivity and DRG-based methods described above. The potential user therefore has the choice between applying global methods such as optimisation with the associated computational expense

of acquiring a truly global solution or the use of much more computationally efficient local methods, with the proviso that they are highly dependent on the conditions chosen for analysis and the nominal values of the rate parameters. The application of these types of methods is to a certain extent user driven. The user may wish to specify a tolerated error in the prediction of a target output. On the other hand, it may also be useful to use such methods to identify the optimal scheme for a given number of variables. For example, in complex flow models such as 3-dimensional turbulence problems, a limited number of scalars can usually be tolerated within the code due to computational costs. In such cases it may be better to define the allowed number of variables and to use an optimisation approach.

Sikalo et al. (2014) compared several options for the application of genetic algorithms to mechanism reduction, exploring the trade-off between the size and accuracy of the resulting mechanisms. Information on the speed of solution was also taken into account, so that, for example, the least stiff system (Sect. 6.7) could be selected. An automatic method for the reduction of chemical kinetic mechanisms was suggested and tested for the performance of reduced mechanisms used within homogeneous constant pressure reactor and burner-stabilised flame simulations. The flexibility of this type of approach has clear utility when restrictions are placed on the number of variables that can be tolerated within a scheme in the computational sense. However, the development of skeletal mechanisms is rarely the end point of any reduction procedure since the application of lumping or timescale-based methods can be applied subsequently. These methods will be discussed in later sections.

7.6.3 Optimisation of Reduced Models to Experimental Data

Usually, the aim of a reduction algorithm is to produce a skeletal scheme with minimal error compared to the full scheme over a wide range of conditions. However, if a large degree of reduction is required, e.g. for use in a spatially 3D calculation, then simulation errors may creep in. In some circumstances it may therefore be necessary to make adjustments to the model within the bounds of uncertainty of its parameters, in order to improve agreement with target experimental data. Apri et al. (2012, 2014) developed such an approach based on optimisation, where mechanism reduction and parameter estimation were coupled via comparison to experimental data. In their method they optimise the full model to experimental data and then try to remove species and reactions from the model, in order of increasing normalised local sensitivity coefficients. The trial reduced model is re-optimised to the experimental data, and the mechanism reduction is considered successful, if the given set of experimental data cannot discriminate between the full and the reduced mechanisms. If the reduced model generates the same predictions as that of the full model for any feasible experimental conditions, then full model can be replaced by the reduced model. The agreement is defined by

a user-controlled tolerance. The method was successfully applied to biochemical kinetic systems.

Gokulakrishnan et al. (2013) developed a similar approach for use in combustion which was tested for several models describing ethylene, Jet-A and methane oxidation. Their method estimated the Arrhenius parameters and reaction orders of several-step reduced models by optimising against target data generated either from a detailed model or by experiment. The procedure uses the simulated annealing (Kirkpatrick 1983; Ingber and Rosen 1992) optimisation algorithm. Several types of target data were used, including ignition delay times, blow-out times, laminar flame speeds, species time-history profiles and species reactivity profiles. Such types of approaches are clearly useful when large reductions in species numbers and reactions are required. However, in order for the resulting mechanism to be used in a predictive way, the optimisation must have been carried out over as wide a range of conditions as would be encountered in the final model application, which might, for example, be a spatially 3D reactive flow simulation. Hence, as wide as possible, a target data set should be used. In Gokulakrishnan et al. (2013), a simultaneous optimisation was carried out against multiple target data sets over a wide range of temperatures, pressures and equivalence ratios.

7.6.4 Application to Oscillatory Systems

Oscillatory models pose interesting challenges for model reduction since complex dynamic behaviour needs to be captured by the reduced model in such cases. The local variable concentrations may not be an appropriate basis for error criteria since small shifts in oscillatory period may lead to large local concentration errors. Instead, the success of a reduced model may be judged on features such as oscillatory period or phase-shift behaviour. For example, the mammalian circadian clock controls the timing of many physiological processes, including sleep patterns, and responds to changes in external conditions such as temperature and light fluctuations. The ability to model the phase response of such a system to external signals is therefore critical to the success of a reduced model attempting to describe its dynamics. The *phase response curve* (PRC) is commonly used to describe such behaviour, i.e. depending upon the phase of a signal's arrival, an oscillator may advance, delay or maintain its phase (Taylor et al. 2008). Taylor et al. developed a model reduction strategy based on a nonlinear integer programming optimisation method to reduce a 61-state model of the mammalian circadian clock to a reduced model with only 13 states. A nonlinear constraint was imposed on the problem since the solution was required to show oscillations. Taylor et al. (2008) state that the landscape of the resulting cost function is therefore likely to lack differentiability and convexity making the problem less amenable to deterministic optimisation methods such the branch-and-bound methods introduced above. The cost function is not defined when the system does not oscillate and such regions are not known a priori. GA-based methods are therefore used in this study. The reduced model was

seen to preserve the phase response of the full model, and when coupled with sensitivity, analysis revealed that four of the feedback loops in the original model were redundant with respect to the appropriate PRC and the phase relationships between the reduced model components.

7.7 Species Lumping

The development of skeletal mechanisms as discussed in Sects. 7.2–7.6 may often provide a significant reduction in the number of species required for modelling a given application, but for incorporation into complex CFD codes, the number of variables may still be prohibitive. This is especially true for models involving the combustion of complex hydrocarbons where comprehensive mechanisms may contain many isomers with complex multistep pathways, and therefore large numbers of intermediate species and reactions. In such cases, other methods are required for reduction that may involve some reformulation of the chemical model from its original form of elementary chemical reactions. Species lumping is one available method, which at the simplest level may involve the use of lumped components that represent the sum of several isomers of a particular hydrocarbon species. In this case the different isomers are not distinguished if they have the same chemical formula and functional groups (Bounaceur et al. 1996; Battin-Leclerc et al. 2000), and therefore, the resulting reactions are global rather than elementary. Several approaches for chemical kinetic and thermodynamic lumping are discussed in Astarita and Sandler (1991).

The crucial issues involved in the application of lumping are (1) to determine which species are to be lumped; (2) to classify how the selected species should contribute to the lumped species, i.e. define the lumping transformation; and (3) to estimate kinetic parameters for the reactions of the lumped species. Developments in lumping methods can be loosely classified into two categories. In "chemical lumping", the chemical structure of species is used to determine appropriate lumping groups, and rules for combining species and reactions. Such methods utilise the fact that detailed kinetic mechanisms are often built in a hierarchical manner, particularly where automatic methods of mechanism generation are used (Ranzi et al. 1995; Warth et al. 2000). A detailed review of chemical lumping methods and applications was given in Ranzi et al. (2001) and Stagni et al. (2014), and these methods will be discussed in Sect. 7.7.1 below.

Algorithmic approaches have also been developed that attempt to define mathematical rules for the selection of lumped groups as well as methods for the determination of reaction rates for the new reactions of the lumped species. Such methods have the advantage that they are based on formal principles and therefore do not rely on chemical knowledge or a priori assumptions about the chemical reactivity of the original species. They may, however, require the application of quite stringent mathematical restrictions that make wide application difficult and may result in a reduced model form that cannot easily be cast in terms of a set of

kinetic reactions. Approximate methods for algorithmic lumping have been developed in order to overcome these restrictions and will be discussed in Sect. 7.7.4.

7.7.1 Chemical Lumping

The approach used in chemical lumping is based on the fact that for complex hydrocarbons with several isomers, the main propagation reactions can be split into relatively few reaction classes (see discussion in Sect. 3.1). For example, for *n*-heptane, the classes of propagation routes are defined in Ranzi et al. (1995) as:

- Decomposition and isomerisation of alkyl radicals R•
- H abstraction with O_2 to form HO_2 and conjugate olefins
- Direct and reverse O_2 addition to R• to form peroxy radicals ROO•
- Internal isomerisation between ROO• and hydroperoxyalkyl radicals •QOOH
- Decomposition of •QOOH radicals to form olefins
- Decomposition of •QOOH radicals to form HO_2 and conjugate olefins
- Decomposition of •QOOH to form heterocomponents (cyclic ethers, aldehydes and ketones) and OH•
- Direct and reverse O_2 addition on •QOOH to form hydroperoxyalkyl peroxy radicals •OOQOOH
- Decomposition of •OOQOOH radicals to form keto-hydroperoxides

A discussion of reaction classes and their potential use in mechanism generation is given in Sect. 3.1 and the references cited therein. Reference rate parameters can be defined for each reaction class based on literature data or similarity rules. For example, values can be defined for the abstraction of a hydrogen radical from a peroxy radical based on its location at a primary, secondary or tertiary site or for isomerisation reactions for hydrogen transfer from different sites (Ranzi et al. 1995). The pathways for each isomer and the resulting intermediate radicals can then be lumped to give a simplified scheme with only a single pathway representing degradation to the average products of all the isomers. The rate parameters for the lumped scheme can be obtained using fitting with respect to experimental data, by weighted averages for the different component isomers depending on the relative weights within the initial fuel, or based on the system of algebraic equations derived from the long chain approximation, i.e. the QSSA approximation applied only to the propagation steps (Battin-Leclerc et al. 2000; Fournet et al. 2000).

For example, within the *n*-heptane scheme described in Battin-Leclerc et al. (2000) and Fournet et al. (2000), there are 4 alkyl radicals noted by $R^{\bullet}_1$, $R^{\bullet}_2$, $R^{\bullet}_3$, $R^{\bullet}_4$ giving rise to 4 reactions involving the addition of O_2:

$$\begin{aligned} R^{\bullet}_1 + O_2 &\rightarrow R_1OO^{\bullet} \\ R^{\bullet}_2 + O_2 &\rightarrow R_2OO^{\bullet} \\ R^{\bullet}_3 + O_2 &\rightarrow R_3OO^{\bullet} \\ R^{\bullet}_4 + O_2 &\rightarrow R_4OO^{\bullet} \end{aligned}$$

The lumped alkyl radical is then defined by

$$[R^{\bullet}] = [R^{\bullet}_1] + [R^{\bullet}_2] + [R^{\bullet}_3] + [R^{\bullet}_4],$$

with the corresponding lumped reaction given by

$$R^{\bullet} + O_2 \rightarrow ROO^{\bullet}.$$

The rate coefficient is calculated using the weighted mean of the elementary rate coefficients for the individual isomers:

$$k_5 = \frac{k_1[R^{\bullet}_1] + k_2[R^{\bullet}_2] + k_3[R^{\bullet}_3] + k_4[R^{\bullet}_4]}{[R^{\bullet}]}$$

A full description of the methodology is given in Fournet et al. (2000). Battin-Leclerc et al. (2000) showed that using such techniques, the primary mechanism for *n*-heptane combustion could be reduced from 410 free radicals and 70 molecules in 1,654 reactions to a lumped scheme with only 25 free radicals and 70 molecules in 189 reactions. The lumped mechanism was shown to give a good representation of the prediction of *n*-heptane conversion compared to the full scheme in the negative temperature coefficient regime. The lumping process developed in Battin-Leclerc et al. (2000) and Fournet et al. (2000) has been included as an integral part of the automatic reaction generation software EXGAS in order to allow the user to limit the size and improve the computational efficiency of the generated schemes where required. A similar methodology was used by Ahmed et al. (2007) for the creation of a compact *n*-heptane oxidation model.

A lumped *n*-heptane scheme was also developed in Ranzi et al. (1995) containing only four lumped radicals as shown in Fig. 7.7. Here the rate coefficients for the lumped scheme were obtained by fitting against predictions from the full scheme. This high degree of lumping leads to reactions with non-integer stoichiometries which represent the relative weights of the different product channels. For example, in the lumped *n*-heptane scheme represented in Fig. 7.7, one of the decomposition steps for •Q7OOH is represented by

$$\begin{aligned} \bullet Q7OOH \rightarrow\ & OH^{\bullet} + 0.3HCHO + 0.32C_5H_{10} + 0.3C_4H_8 + 0.35CH_3CHO \\ & + 0.31C_3H_6 + 0.35C_2H_5CHO + 0.4C_2H_4 + 0.06C_7H_{14} \end{aligned}$$

Other examples of reduced hydrocarbon mechanisms developed via chemical lumping include a primary oxidation mechanism for *iso*-octane containing only five intermediate lumped radicals (Ranzi et al. 1997), lumped schemes for higher

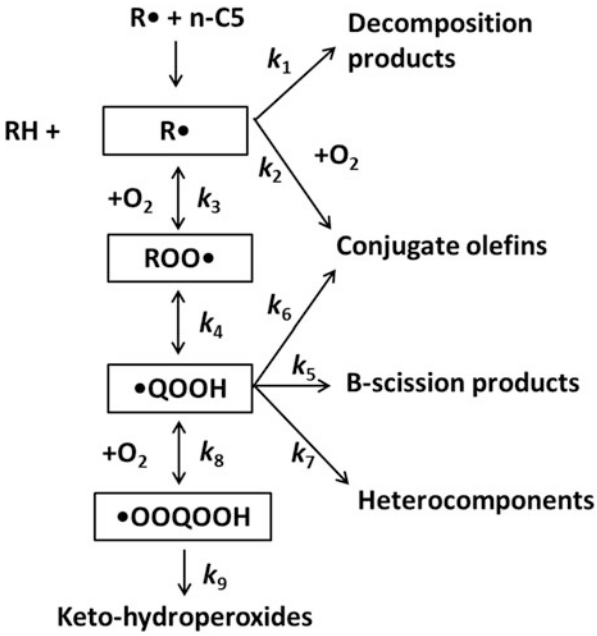

Fig. 7.7 Schematic of the lumped scheme developed in Ranzi et al. (1995) for the primary oxidation of *n*-alkanes. Reproduced from Ranzi et al. (1995) with permission from Elsevier

n-alkanes up to *n*-hexadecane (Ranzi et al. 2005) and naphthenes (Granata et al. 2003).

A second example of chemical lumping has been developed to describe soot formation in combustion systems. Frenklach (1991) presents a polymer system where the chemical reactions describing polymer growth are of the same type, whilst the rate parameters and thermodynamic data vary only slightly between polymer sizes. For soot formation, the reaction is described by a distribution function for the degree of polymerisation and a repeating reaction cycle for particle growth (Frenklach 1985; Warnatz 1992). The structure and rate coefficients for each repeated cycle are treated as being the same. To illustrate the approach, we now discuss an example describing the production of polycyclic aromatic hydrocarbons (PAHs) in flames. A suggested mechanism of PAH growth proceeds by a replication process involving hydrogen abstraction and the addition of acetylene (HACA mechanism), so that lumping can be guided by similarities in structure of the hydrocarbon species in the repeating sequence. Using Frenklach's example, we start with the following reaction sequence:

$$
\begin{array}{ll}
(i,1) & \mathrm{A}_i + \mathrm{H} \leftrightarrow \mathrm{A}_i^{\cdot} + \mathrm{H}_2 \\
(i,2) & \mathrm{A}_i^{\cdot} + \mathrm{C_2H_2} \leftrightarrow \mathrm{A}_i\mathrm{CHCH}^{\cdot} \\
(i,3) & \mathrm{A}_i\mathrm{CHCH}^{\cdot} + \mathrm{C_2H_2} \rightarrow \mathrm{A}_{i+1} + \mathrm{H} \\
(i+1,1) & \mathrm{A}_{i+1} + \mathrm{H} \leftrightarrow \mathrm{A}_{i+1}^{\cdot} + \mathrm{H}_2 \\
(i+1,2) & \mathrm{A}_{i+1}^{\cdot} + \mathrm{C_2H_2} \leftrightarrow \mathrm{A}_{i+1}\mathrm{CHCH}^{\cdot} \\
(i+1,3) & \mathrm{A}_{i+1}\mathrm{CHCH}^{\cdot} + \mathrm{C_2H_2} \rightarrow \mathrm{A}_{i+2} + \mathrm{H} \\
(i+2, i+3, \ldots, n) & \ldots \text{ etc}
\end{array}
$$

where A_i is an aromatic molecule containing i fused aromatic rings, $\mathrm{A}_i^{\cdot}$ is an aromatic radical formed by H abstraction and $\mathrm{A}_i\mathrm{CHCH}^{\cdot}$ is a radical formed by adding $\mathrm{C_2H_2}$ to $\mathrm{A}_i^{\cdot}$. Each replication of the reaction sequence represents completing the building cycle of one ring continuing in principle to infinity. The building process is limited by the emergence of solid soot particles. Obviously in this case the number of species can build up to be very large, leading to a large set of rate equations which would need to be solved.

In non-lumped form, the reaction system is described by the following set of rate equations:

$$
\begin{aligned}
&\frac{\mathrm{d}[\mathrm{A}_i]}{\mathrm{d}t} = r_o - k_1[\mathrm{A}_i][\mathrm{H}] + k_{-1}\left[\mathrm{A}_i^{\cdot}\right][\mathrm{H_2}] \\
&\frac{\mathrm{d}\left[\mathrm{A}_i^{\cdot}\right]}{\mathrm{d}t} = k_1[\mathrm{A}_i][\mathrm{H}] - k_{-1}\left[\mathrm{A}_i^{\cdot}\right][\mathrm{H_2}] - k_2\left[\mathrm{A}_i^{\cdot}\right][\mathrm{C_2H_2}] + k_{-2}[\mathrm{A}_i\mathrm{CHCH}^{\cdot}] \\
&\frac{\mathrm{d}[\mathrm{A}_i\mathrm{CHCH}^{\cdot}]}{\mathrm{d}t} = k_2\left[\mathrm{A}_i^{\cdot}\right][\mathrm{C_2H_2}] - k_{-2}[\mathrm{A}_i\mathrm{CHCH}^{\cdot}] - k_3[\mathrm{A}_i\mathrm{CHCH}^{\cdot}][\mathrm{C_2H_2}] \\
&\frac{\mathrm{d}[\mathrm{A}_{i+1}]}{\mathrm{d}t} = k_3[\mathrm{A}_i\mathrm{CHCH}^{\cdot}][\mathrm{C_2H_2}] - k_1[\mathrm{A}_{i+1}][\mathrm{H}] + k_{-1}\left[\mathrm{A}_{i+1}^{\cdot}\right][\mathrm{H_2}] \\
&\frac{\mathrm{d}\left[\mathrm{A}_{i+1}^{\cdot}\right]}{\mathrm{d}t} = k_1[\mathrm{A}_{i+1}][\mathrm{H}] - k_{-1}\left[\mathrm{A}_{i+1}^{\cdot}\right][\mathrm{H_2}] - k_2\left[\mathrm{A}_{i+1}^{\cdot}\right][\mathrm{C_2H_2}] + k_{-2}[\mathrm{A}_{i+1}\mathrm{CHCH}^{\cdot}] \\
&\frac{\mathrm{d}[\mathrm{A}_{i+1}\mathrm{CHCH}^{\cdot}]}{\mathrm{d}t} = k_2\left[\mathrm{A}_{i+1}^{\cdot}\right][\mathrm{C_2H_2}] - k_{-2}[\mathrm{A}_{i+1}\mathrm{CHCH}^{\cdot}] - k_3[\mathrm{A}_{i+1}\mathrm{CHCH}^{\cdot}][\mathrm{C_2H_2}] \\
&\ldots \text{etc.}
\end{aligned}
\tag{7.24}
$$

where r_o is the rate of formation of A_i by initiation reactions. The rate coefficients k_j are assumed to have the same value for each cycle due to chemical similarities between the species. This allows chemical lumping to be applied in order to reduce the number of variables.

If we sum Eq. (7.24), then we get

$$
\frac{\mathrm{d}M_o}{\mathrm{d}t} = r_o \tag{7.25}
$$

where $M_o = [\mathrm{A}_i] + [\mathrm{A}_i^{\cdot}] + [\mathrm{A}_i\mathrm{CHCH}^{\cdot}] + [\mathrm{A}_{i+1}] + \ldots$, i.e. the sum of all species. This one-dimensional system describes the evolution of the total PAH concentration M_o. The details of the dynamics of the system are lost however if such a severe lumping

is used. Another approach is to multiply each of the equations in (7.24) by an integer which roughly corresponds to the molecular mass of the species, i.e. the number of carbon atoms, before summing the terms. Hence, we multiply the first equation by m_o (the number of carbon atoms in A_i), the second by m_o and the third by (m_o+2), etc., giving a lumped equation system

$$\frac{dM_1}{dt} = \left(m_o \frac{d[A_i]}{dt} + m_o \frac{d[A_i^{\cdot}]}{dt} + (m_o+2) \frac{d[A_iCHCH^{\cdot}]}{dt} + (m_o+4) \frac{d[A_{i+1}]}{dt} + \ldots \right)$$
$$= m_o r_o + 2k_2[C_2H_2] \sum_i [A_i^{\cdot}] - 2k_{-2} \sum_i [A_iCHCH^{\cdot}] + 2k_3[C_2H_2] \sum_i [A_iCHCH^{\cdot}]$$

where $M_1 = m_o[A_i] + m_o[A_i^{\cdot}] + (m_o+2)[A_iCHCH^{\cdot}] + (m_o+4)[A_{(i+1)}] + (m_o+4)[A_{(i+1)}^{\cdot}] + \cdots$, is the total number of carbon atoms accumulated in the PAHs, i.e. the first moment of the PAH distribution.

In terms of species lumping, we can now see that it is possible to define a new set of variables which define the lumped species

$$\hat{c}_1 = \sum_i [A_i]$$
$$\hat{c}_2 = \sum_i [A_i^{\cdot}]$$
$$\hat{c}_3 = \sum_i [A_iCHCH^{\cdot}]$$

The corresponding lumped equation system is then given by

$$\frac{d\hat{c}_1}{dt} = r_o - k_1[H]\hat{c}_1 + k_{-1}[H_2]\hat{c}_2 + k_3[C_2H_2]\hat{c}_3$$
$$\frac{d\hat{c}_2}{dt} = k_1[H]\hat{c}_1 - k_{-1}[H_2]\hat{c}_2 - k_{-2}\hat{c}_3$$
$$\frac{d\hat{c}_3}{dt} = k_2[C_2H_2]\hat{c}_2 - k_{-2}\hat{c}_3 - k_3[C_2H_2]\hat{c}_3$$

The example shows that in this case, lumping based on chemical similarities results in new variables which are simply linear sums of the original species concentrations. It is therefore just a special case of linear lumping which will be discussed further in the following section. One point of caution is that the ability to specify a new system of lumped equations in exact form relies on the fact that identical rate coefficients have been used for the same reaction type for PAHs with different numbers of carbon atoms. Hence, whilst the lumping may be exact, errors may result from the use of this assumption. The sensitivity of the predictions of soot volume fraction in ethylene/air flames at high pressure using the above approach was investigated by Hu et al. (1999). Their work indicated the highest sensitivity to the acetylene addition step. Moment-based methods were also extended to

modelling the dynamics of particle systems including coagulation/agglomeration in Frenklach and Harris (1987), and Kazakov and Frenklach (1998).

Chemical lumping has also been applied within atmospheric mechanisms based on a number of slightly different approaches. For example, within the tropospheric, Master Chemical Mechanism (MCM), lumping is used in the case of peroxy radicals to define the generic species ROO• (Saunders et al. 2003). The full MCM, however, remains for the most part an explicit, detailed mechanism. Reduced forms of the MCM were developed in the Common Representative Intermediates (CRI) mechanism using lumping methods (Jenkin et al. 2008; Watson et al. 2008). At the first stage, a version of structural chemical lumping is applied based on the assumption that the ozone-forming potential of a volatile organic compound (VOC) is related to the number of reactive bonds (i.e. C–C and C–H) it contains. Based on structural similarities, a set of generic intermediates or "common representatives" is then defined, each containing a large set of species from the full MCM possessing the same ozone-forming index as the common representative. At the second stage of reduction, the CRI mechanism uses a surrogate approach, where the masses of minor VOCs are redistributed into a much lower number of surrogate compounds. These surrogates are selected in order to maintain the chemical class of the redistributed VOCs with the aim of preserving the tropospheric ozone-forming ability of each category. Several different levels of reduction were offered in Watson et al. (2008). When coupled with the first reduction stage, over an order of magnitude reduction was achievable when compared to the equivalent explicit MCM mechanism.

Lumping based on functional groups was also developed in Whitten et al. (1980), Gery et al. (1989), Fish (2000), Yarwood et al. (2005) and Kirchner (2005) as discussed in Sect. 3.1. In these approaches, each carbon atom is given a type depending on the number of carbon atoms to which it is bonded and a status depending on its functional group. Structural activity relationships are then used to generate rate coefficients for the lumped groups, and the fraction of the original VOCs within the lumped quantities is tracked.

Lumping is also associated with the so-called *family method* in atmospheric chemistry (Crutzen 1971; Turco and Whitten 1974; Austin 1991; Jacobson 2005). Here, the families of chemical species are defined not only on the basis of structural similarity but also on other chemical reasoning such as reactivity. The approach has tended to be used mostly in the context of fast numerical methods for solving ODEs related to atmospheric chemical systems. It is based on the principle that for some groups or "families" of species, atoms transfer quickly among species within the family but are lost slowly from it (Jacobson 2005). For example, within the family *odd oxygen* $[O_X] = [O] + [O(^1D)] + [O_3]$, the O atoms cycle rapidly between the species atomic oxygen, excited atomic oxygen (O^1D) and ozone but are slowly lost from within this group. Similar groups exist for odd nitrogen (NOy), hydrogen (HOx), bromine (Bry) and chlorine (Cly) species.

Using families within the solution to ODEs requires several steps. First, the rates of production and loss of individual species are calculated from the initial concentrations, and then summed across a family. The family concentration is then

advanced to the next time step using something like a forward Euler approximation (Elliott et al. 1993). In the final stage, individual species concentrations have to be repartitioned within the family ready for the next time step. Several methods for this repartitioning (a version of inverse lumping as discussed in the next section) can be used, and the reader is referred to Jacobson (2005) for detailed examples. It is important to note, however, that these usually have to invoke some kind of approximation, such as the use of the QSSA, or a linearisation of the equations, and hence, the family method can lead to numerical errors if family groupings are not appropriately chosen. Austin, for example, discovered errors of order 20 % to be induced in OH radical concentrations within photochemical stratospheric models when too small a number of families were used (Austin 1991).

The errors induced within methods based on timescale separations will be discussed in more detail in Sect. 7.8 below. On the other hand, since equilibrations will exist within the groups, the introduction of such families is likely to lead to the elimination of fast timescales, thus reducing the stiffness of the reduced system of differential equations with resultant increases in simulation speed. O^1D, for example, has an atmospheric lifetime of the order of 10^{-8} s (see Sect. 6.3), and therefore, its presence within a scheme can lead to large stiffness ratios when treated as an individual species. Within reactive flow models, further computational gains may also be made by advecting these families within the transport step rather than individual species, thereby reducing the number of transported variables.

The family method was applied within an atmospheric chemistry box model to NOy, HOx, Cly, Ox and Bry families in order to study the effect of increases in ground level bromine emissions on stratospheric ozone by Ramaroson et al. (1992), and for simulations of lower stratospheric HCl in Douglass and Kawa (1999). The nonlinear features of tropospheric ozone production from nitrogen oxides and VOCs were reproduced using a numerical method based on family methods in Elliott et al. (1996).

Approaches to lumping in biochemical and systems biology applications tend to be based on mathematical algorithms and will therefore be discussed after such algorithms are introduced within the next section.

7.7.2 Linear Lumping

We saw in the previous section that chemical lumping is often based on defining new species whose concentrations are linear combinations of those of the starting species within a mechanism. This approach can be generalised within a mathematical framework. The formal definition of lumping is the transformation of the original vector of variables $\mathbf{Y}$ to a new transformed variable vector $\hat{\mathbf{Y}}$ using the transformation function $\mathbf{h}$:

$$\hat{\mathbf{Y}} = \mathbf{h}(\mathbf{Y}) \tag{7.26}$$

The dimension $\hat{n}$ of the new variable vector $\hat{\mathbf{Y}}$ is smaller than that of the original concentration vector ($\hat{n} < N_S$). Due to the transformation above, a new kinetic system of ODEs is formed:

$$\frac{\mathrm{d}\hat{\mathbf{Y}}}{\mathrm{d}t} = \hat{\mathbf{f}}\left(\hat{\mathbf{Y}}, \hat{\mathbf{k}}\right), \quad \hat{\mathbf{Y}}(t_0) = \hat{\mathbf{Y}}_0. \tag{7.27}$$

An important feature is the ability to recover the original vector of concentrations from the transformed variables $\hat{\mathbf{Y}}$ using the inverse transformation function $\overline{\mathbf{h}}$:

$$\mathbf{Y} = \overline{\mathbf{h}}\left(\hat{\mathbf{Y}}\right) \tag{7.28}$$

Function $\overline{\mathbf{h}}$ is not unique, since several different functions $\overline{\mathbf{h}}$ may belong to the same transformation function $\mathbf{h}$. This inverse mapping is as important as the forward mapping not only because it provides the link between the lumped variables and the original species concentrations, but because its existence is a necessary condition of exact lumping.

If the function $\mathbf{h}$ is linear, then in chemical kinetics, this approach would be termed *linear species lumping* and is essentially a formalisation of the chemical lumping approach described in the previous section. In the linear case the transformation is simply a matrix multiplication operation:

$$\hat{\mathbf{Y}} = \mathbf{M}\mathbf{Y} \tag{7.29}$$

where $\mathbf{M}$ is a matrix of size $\hat{n} \times N_S$. Consider, for example, the following matrix:

$$\mathbf{M} = \begin{pmatrix} 1 & 0 & 0 & 0 \\ 0 & 1 & 1 & 1 \end{pmatrix}. \tag{7.30}$$

This lumping matrix transforms an original concentration vector (Y_1, Y_2, Y_3, Y_4) to the concentration vector $\left(\hat{Y}_1, \hat{Y}_2\right)$ of lumped species, where $\hat{Y}_1 = Y_1$ and $\hat{Y}_2 = Y_2 + Y_3 + Y_4$.

Linear species lumping is called *proper species lumping* (Okino and Mavrovouniotis 1998), if the concentration of each original species appears in the transformation function of only one lumped species. If there are lumped species present in a kinetic reaction mechanism, such a mechanism is called a *lumped reaction mechanism*. In some cases, it is possible to regain the exact original concentration vector after using the transformation in Eq. (7.26), solving the differential Eq. (7.27) and then using the inverse transformation in Eq. (7.28). This is the case when the lumping is based on conserved properties, and therefore,

no information is lost during lumping. This type of lumping is called *exact species lumping* (Wei and Kuo 1969; Li and Rabitz 1989; Farkas 1999).

If we assume that the original kinetic system of differential equations contains first-order reaction steps only, and therefore the concentration changes can be described by the following initial value problem:

$$\frac{\mathrm{d}\mathbf{Y}}{\mathrm{d}t} = -\mathbf{K}\mathbf{Y}, \quad \mathbf{Y}(t_0) = \mathbf{Y}_0 \tag{7.31}$$

then linear species lumping results in the following different initial value problem:

$$\frac{\mathrm{d}\hat{\mathbf{Y}}}{\mathrm{d}t} = -\hat{\mathbf{K}}\hat{\mathbf{Y}}, \quad \hat{\mathbf{Y}}(t_0) = \hat{\mathbf{Y}}_0 \tag{7.32}$$

Wei and Kuo (1969) have shown that the necessary and sufficient condition of exact linear lumping is the following equation:

$$\mathbf{M}\mathbf{K} = \hat{\mathbf{K}}\,\mathbf{M} \tag{7.33}$$

It is always possible to find matrices $\hat{\mathbf{K}}$ and $\mathbf{M}$ that fulfil Eq. (7.33), but the solution is not unique. The equivalent problem is finding invariant subspaces of the original equations, i.e. invariant subspaces of the transpose of the Jacobian $\mathbf{J}^{\mathrm{T}}(\mathbf{Y})$ so that the eigenvalues of $\mathbf{J}^{\mathrm{T}}(\mathbf{Y})$ and $\mathbf{J}^{\mathrm{T}}(\mathbf{M}^{-1}\mathbf{M}\mathbf{Y})$ are identical, which is fairly straightforward for this linear example where the Jacobian is a constant matrix. However, this is often a difficult task for more general nonlinear ODEs where applying the restrictions imposed by exact lumping may limit the level of reduction possible for the reduced scheme.

We include here a short example of linear lumping taken from Li and Rabitz (1989) in order to illustrate the approach. Consider the first-order reaction system involving reversible reactions between three species as follows:

$$\begin{aligned} &\mathrm{C}_1 \leftrightarrows \mathrm{C}_2, \quad k_{1f} = 3, k_{1b} = 2 \\ &\mathrm{C}_2 \leftrightarrows \mathrm{C}_3, \quad k_{2f} = 10, k_{2b} = 6 \\ &\mathrm{C}_1 \leftrightarrows \mathrm{C}_3, \quad k_{3f} = 10, k_{3b} = 4 \end{aligned}$$

The corresponding kinetic equations are

$$\frac{\mathrm{d}c_1}{\mathrm{d}t} = -13c_1 + 2c_2 + 4c_3 \tag{7.34}$$

$$\frac{\mathrm{d}c_2}{\mathrm{d}t} = 3c_1 - 12c_2 + 6c_3 \tag{7.35}$$

$$\frac{\mathrm{d}c_3}{\mathrm{d}t} = 10c_1 + 10c_2 - 10c_3 \tag{7.36}$$

where the rate constants are essentially arbitrary numbers.

In vector form we can write this system as

$$\frac{\mathrm{d}\mathbf{c}}{\mathrm{d}t} = \mathbf{K}\mathbf{c} \tag{7.37}$$

Where $\mathbf{K}$ is the matrix of rate constants and

$$\mathbf{J}^{\mathrm{T}}(\mathbf{c}) = \begin{pmatrix} -13 & 2 & 4 \\ 3 & -12 & 6 \\ 10 & 10 & -10 \end{pmatrix} \tag{7.38}$$

The eigenvector matrix $\mathbf{X}$ of $\mathbf{J}^{\mathrm{T}}(\mathbf{c})$ is given by

$$\mathbf{X} = \begin{pmatrix} 1 & 1 & 0.6 \\ 1 & 1 & -0.4 \\ 1 & -1 & 0 \end{pmatrix} \tag{7.39}$$

Any subspace spanned by a subset of these eigenvectors will be $\mathbf{J}^{\mathrm{T}}(\mathbf{c})$ invariant and could therefore form a suitable lumping matrix. For example, span $(\mathbf{x}_1, \mathbf{x}_2)$ gives the two-dimensional lumping matrix:

$$\mathbf{M} = \begin{pmatrix} 1 & 1 & 1 \\ 1 & 1 & -1 \end{pmatrix} \tag{7.40}$$

The lumped form of the equations is given by

$$\frac{\mathrm{d}\hat{\mathbf{c}}}{\mathrm{d}t} = \mathbf{M}\mathbf{K}\mathbf{c} \tag{7.41}$$

However, in order to express the right-hand side in terms of the new lumped variables $\hat{\mathbf{c}}$, then the generalised inverse $\mathbf{M}^{-1}$ needs to be found. The inverse will not be unique, but its form does not affect the form of the lumped equations. We can arbitrarily choose

$$\mathbf{M}^{-1} = \begin{pmatrix} 0.5 & 0 \\ 0.5 & 0 \\ 0 & 1 \end{pmatrix} \tag{7.42}$$

and the lumped equations become

$$\frac{\mathrm{d}\hat{\mathbf{c}}}{\mathrm{d}t} = \mathbf{M}\mathbf{K}\mathbf{M}^{-1}\hat{\mathbf{c}} = \begin{pmatrix} -10 & 10 \\ 10 & 10 \end{pmatrix}\hat{\mathbf{c}} \tag{7.43}$$

In this simple case, it is possible to interpret this as a lumped kinetic scheme

$$\hat{C}_1 \leftrightarrows \hat{C}_2$$

where $\hat{C}_1 = c_1 + c_2 + c_3$ and $\hat{C}_2 = c_1 + c_2 - c_3$. Of course the above example is for a simple first-order system where an exact linear lumping approach can be applied.

Several developments of the lumping method have been proposed to help to overcome the restrictions placed by exact linear lumping. The first is *constrained species lumping* (Li and Rabitz 1991). Usually we are not interested in predicting the concentrations of all species in the original kinetic system of ODEs, but only in important ones such as key products or pollutants. In constrained lumping the original vector of concentrations is rearranged so that the first n elements consist of the concentrations of the n important species. Then, transformation $\mathbf{h}$ is selected so that it does not change the first n elements of vector $\mathbf{Y}$. Chu et al. (2011) suggested a new algorithm for approximate, linear constrained lumping. Some variables of the original model are selected to be retained in the lumped model, whilst the other variables are lumped by linear combination. The technique is based on the Petrov–Galerkin projection, and the projection matrix is computed from simulation data obtained from the original model. The projection matrix is calculated in a computationally inexpensive way using a sequential algorithm based on a modified Gram–Schmidt orthogonalisation procedure.

Other recent advances in the application of algorithmic methods for linear lumping have attempted to develop methods that are based on formal mathematical principles but do not lead to the stringent restrictions on the numbers of lumped species achievable caused by the application of exact linear lumping methods. Huang et al. (2005) defined a formal lumping procedure for intermediate species where the fraction of each component within the lump α_i (equivalent to the inverse lumping matrix $\overline{\mathbf{M}}$) is defined in terms of the fractional formation rate of the components of the lump. The intention of the procedure is to suggest suitable lumped groups whilst maintaining the flexibility required to model the consequences of chemistry arising from reactions of the individual species within each lump. The selection of suitable lumping groups is determined via the calculation of the ratio of the normalised formation rates between candidate species i and j denoted by $\gamma_{i,j}$. If the ratio is approximately constant over the course of the simulation, then the two species can be lumped. The method was extended to larger lumped groups. For example, for a lumped group containing three species A, B and C, then $\boldsymbol{\alpha}$ is calculated as follows:

$$\begin{aligned} \alpha_A &= \frac{R_A}{R_A + m_1 R_B + m_2 R_C} \\ \alpha_B &= \frac{m_1 R_B}{R_A + m_1 R_B + m_2 R_C} \\ \alpha_C &= \frac{m_2 R_C}{R_A + m_1 R_B + m_2 R_C} \end{aligned} \tag{7.44}$$

where R_i is the formation rate of species i, $m_1 = \gamma_{\mathrm{A,B}}$, $m_2 = \gamma_{\mathrm{A,C}}$ and $\alpha_1 + \alpha_2 + \alpha_3 = 1$.

The method was illustrated with respect to the simulation of higher hydrocarbon generation during the isothermal oxidation of fuel-rich methane–oxygen mixtures, where 31 species were lumped into nine groups giving a reduction in the number of species of 22. In this application, the selection of groups is achieved by first ordering the maximum gradients of the ratio $\gamma_{i,j}$ over the simulation, given by $\varphi_{i,j}$. The first group is then formed by selecting two species that have the lowest $\varphi_{i,j}$. Other candidates are then tested for inclusion in this group by comparing $\varphi_{i,j}$ values with current members compared to a user-defined tolerance. When no further candidates can be added, then two new starting candidates are selected from the remaining ordered list, and the operation is continued until no further groups are achievable. Integer programming methods could potentially be used to extend this method to defining fully optimal lumped groups.

7.7.3 Linear Lumping in Systems with Timescale Separation

Other algorithmic methods for linear lumping have been developed for atmospheric chemistry applications (Sportisse and Djouad 2000; Djouad and Sportisse 2002; Djouad et al. 2003; Whitehouse et al. 2004c) but could potentially be relevant to other types of chemical kinetic simulations. These methods have exploited a timescale analysis in order to define lumped groups. For example, in Whitehouse et al. (2004c), species are grouped according to their chemical lifetimes and reactivity structures. This work applied the methods to the comprehensive tropospheric Master Chemical Mechanism (MCM). Several large lumped groups were achievable which were composed of peroxyacyl nitrates, nitrates, carbonates, oxepins, substituted phenols, oxyacids and peracids with similar lifetimes and reaction rates with OH. This approach could be considered as a formalisation of chemical lumping where chemical similarities are not judged by expert opinion but are calculated on the basis of reaction rates.

Djouad and Sportisse (Sportisse and Djouad 2000; Djouad and Sportisse 2002) use lumping techniques based on the stoichiometric matrix of the fast subspace of the system to define the partitioning between slow and fast species. The method is equivalent to searching for slow species as linear combinations of fast ones and is therefore aimed at reducing the stiffness of the modelling problem for use with efficient numerical solvers. The approach also provides information on the dynamic behaviour of the model and was successfully demonstrated for tropospheric reaction systems including multi-phase applications (Djouad et al. 2003). It should be pointed out that the wide applicability of simple linear algorithms for lumping in atmospheric chemistry is in part due to the low-temperature dependence of reaction rates for these schemes. Extension to non-isothermal systems would provide an interesting area for further work.

We now briefly provide a formalised framework for linear lumping in systems with timescale separation which is based on a similar approach to that presented in Sect. 6.3. We start with the initial value problem

$$\frac{\mathrm{d}\mathbf{Y}}{\mathrm{d}t} = \mathbf{f}(\mathbf{Y}, \mathbf{k}), \quad \mathbf{Y}(t_0) = \mathbf{Y}_0 \tag{7.45}$$

with the linear approximation to 7.45 given by

$$\frac{\mathrm{d}\mathbf{Y}}{\mathrm{d}t} = \mathbf{J}\mathbf{Y} \tag{7.46}$$

where $\mathbf{J}$ is the Jacobian matrix. We can define new variables $\mathbf{Z}$ by choosing an $n \times n$-dimensional lumping matrix $\mathbf{Q}^{\mathrm{T}}$ such that

$$\mathbf{Z} = \mathbf{Q}^{\mathrm{T}}\mathbf{Y} \tag{7.47}$$

The Schur decomposition is defined by $\mathbf{Q}^{\mathrm{T}}\mathbf{J}\mathbf{Q} = \mathbf{T}$ where $\mathbf{T}$ is an upper triangular matrix, $\mathbf{Q}\mathbf{Q}^{\mathrm{T}} = \mathbf{Q}^{\mathrm{T}}\mathbf{Q} = \mathbf{I}$, and

$$\mathbf{Q} = (\,\mathbf{q}_1 \quad \mathbf{q}_2 \cdots \mathbf{q}_n) \tag{7.48}$$

where $\mathbf{q}_i$ are the Schur basis vectors. The Schur decomposition (Golub and Van Loan 1983) is used instead of applying the eigenvectors as a basis since it has more general application to ill-conditioned matrices where degenerate eigenvalues may exist (Maas and Pope 1992). $\mathbf{Q}$ can be chosen such that the eigenvalues of $\mathbf{J}$ appear in any order along the diagonal of $\mathbf{T}$ and hence could be ordered according to fast and slow timescales. If we choose $\mathbf{Q}^{\mathrm{T}}$ such that the eigenvalues appear in descending order on the diagonal, then

$$\mathbf{Q}^{\mathrm{T}}\mathbf{J}\mathbf{Q} = \begin{pmatrix} \mathbf{J}'^{(11)} & \mathbf{J}'^{(12)} \\ 0 & \mathbf{J}'^{(22)} \end{pmatrix} \tag{7.49}$$

where $\mathbf{J}'^{(11)}$ corresponds to the $n - \hat{n}$ most negative eigenvalues (i.e. the fastest relaxing timescales) and $\mathbf{J}'^{(22)}$ corresponds to the $\hat{n}$ positive or small negative eigenvalues. Therefore, the local linear system for $\mathbf{Z}$ is given by

$$\frac{\mathrm{d}\mathbf{Z}}{\mathrm{d}t} = \begin{pmatrix} \mathbf{J}'^{(11)} & \mathbf{J}'^{(12)} \\ 0 & \mathbf{J}'^{(22)} \end{pmatrix} \mathbf{Z} \tag{7.50}$$

If a gap in timescales exists as discussed in Sect. 6.3, then the lumping matrix can be partitioned as

$$\mathbf{Q}^{\mathrm{T}} = \begin{pmatrix} \mathbf{Q}_f^{\mathrm{T}} \\ \mathbf{Q}_s^{\mathrm{T}} \end{pmatrix} \tag{7.51}$$

where $\mathbf{Q}_f^{\mathrm{T}}$ is of dimension $(n - \hat{n}) \times n$ and spans the space of the fast timescales. $\mathbf{Q}_s^{\mathrm{T}}$ is of dimension $\hat{n} \times n$ and defines an $\hat{n} \times n$ lumping matrix which spans the slow subspace and determines the lumped variables. $\mathbf{Z}$ can therefore be partitioned as

$$\mathbf{Z} = \begin{pmatrix} \mathbf{F} \\ \mathbf{S} \end{pmatrix} \tag{7.52}$$

and the equations describing the linear system become

$$\frac{\mathrm{d}\mathbf{F}}{\mathrm{d}t} = \mathbf{J}'^{(11)}\mathbf{F} + \mathbf{J}'^{(12)}\mathbf{S} \tag{7.53}$$

$$\frac{\mathrm{d}\mathbf{S}}{\mathrm{d}t} = \mathbf{J}'^{(22)}\mathbf{S}$$

The variables in the slow subspace **S** are therefore decoupled from those in the fast subspace, and therefore, the lumping allows the definition of a reduced set of variables **S** describing the longer timescale dynamics. The connections with the slow manifold methods described in Sect. 6.5 also become clear since the calculation of the points on the manifold involves solving the following algebraic set of equations:

$$\mathbf{Q}_f^{\mathrm{T}}\mathbf{f}(\mathbf{Y}, \mathbf{k}) = 0 \tag{7.54}$$

We return to a discussion of numerical methods for solving such relationships in Sect. 7.10.

7.7.4 General Nonlinear Methods

The methods of chemical and linear lumping outlined above can be extremely effective for large systems where similarities in rate coefficients exist for chemically similar groups. However, they are difficult to extend in a general sense where nonlinear couplings exist between groups of species. One solution may be to consider the system as locally linear so that different lumping schemes are developed for different regions of composition space. However, one can imagine that for highly nonlinear problems such as ignition or oscillatory systems, the lumping transformations may vary rapidly, and the overhead in switching between different lumped variables may outweigh any benefits gained from reducing the number of variables. Methods for approximate nonlinear lumping have therefore been developed as discussed in the earlier review of Tomlin et al. (1997). Development of a general nonlinear approach to lumping is, however, a non-trivial task. Instead of simple matrix calculations, global canonical forms are now sought for the chemical rate equations which separate the variables in a general way for many sets of conditions. Nonlinear methods therefore may provide a more general approach which is applicable over wider ranges of external conditions such as temperatures and pressures, but this may be at the expense of algebraic complexity, since the transformation from original to lumped variables is now of a nonlinear form.

The theory of nonlinear lumping has been developed by Li and co-workers who started first by establishing necessary and sufficient conditions for exact nonlinear lumping (Li et al. 1994a). Starting with the equation system (7.45), we can define new lumped variables using a general $\hat{n}$-dimensional nonlinear transformation to new variables $\hat{\mathbf{Y}} = \mathbf{h}(\mathbf{Y})$ with a new $\hat{n}$-dimensional equation system given by

$$\frac{\mathrm{d}\hat{\mathbf{Y}}}{\mathrm{d}t} = \hat{\mathbf{f}}\left(\hat{\mathbf{Y}}(t)\right) \tag{7.55}$$

If we define the Jacobian of the transformation $\mathbf{h}(\mathbf{Y})$ as $D_{\mathbf{h},\mathbf{c}}(\mathbf{Y}) = \partial\mathbf{h}/\partial\mathbf{Y}$, then

$$D_{\mathbf{h},\mathbf{c}}(\mathbf{Y})\mathbf{f}(\mathbf{Y}) = \mathbf{D}_{\mathbf{h},\mathbf{c}}\overline{\mathbf{h}}(\mathbf{h}(\mathbf{Y}))\mathbf{f}\left(\overline{\mathbf{h}}(\mathbf{h}(\mathbf{Y}))\right) \tag{7.56}$$

is a necessary and sufficient condition for exact lumping. In parallel to the linear case, exact lumping depends on the existence of the generalised inverse transformation $\overline{\mathbf{h}}$. Since $\mathbf{h}$ is now a nonlinear function, the calculation of $\overline{\mathbf{h}}$ becomes challenging for high-dimensional or highly coupled systems.

For easier comparison with the linear case, we can redefine the system using a linear partial differential operator A, which, using index notation, is given by

$$A = \sum_{i=1}^{n} f_i(\mathbf{Y}(t))\frac{\partial}{\partial Y_i} \tag{7.57}$$

giving the original system of equations in the form

$$\frac{\mathrm{d}\mathbf{Y}}{\mathrm{d}t} = A(\mathbf{Y}) \tag{7.58}$$

Therefore, finding the nonlinear transformation $\mathbf{h}$ depends on finding canonical forms for the original operator A or on finding invariant manifolds of the original system, i.e. the nonlinear equivalent of searching for canonical forms of the Jacobian $\mathbf{J}$ (e.g. diagonal or upper triangular form) and its invariant subspaces. The intention is that in the new canonical form, the corresponding differential equations will be partially or completely decoupled. For example, the diagonal form of a nonlinear operator with a basis of eigenfunctions $\varphi_i(\mathbf{Y})$ and invariants $\omega_j(\mathbf{Y})$ would be as follows:

$$A\sum_{i=1}^{k}\lambda_i(\omega)\varphi_i(\mathbf{Y})\frac{\partial}{\partial\varphi_i(\boldsymbol{Y})} \tag{7.59}$$

where the eigenvalues $\lambda_i(\omega)$ are the equivalent of the diagonal elements in the linear case. Hence, one approach is to search for the eigenfunctions of A which relate to eigenvalues which are no longer constant but are functions of $\mathbf{Y}(t)$ (Li et al. 1994a). Li et al. (1994a) have demonstrated that finding a full space of eigenfunctions for a general nonlinear system is a difficult task. They therefore developed a nonlinear

lumping approach based on finding approximate canonical forms for A (Li et al. 1994b, c). Again, if we think about the corresponding linear case, one way of finding approximate invariant manifolds was to exploit the timescale separation within the system. Similar approaches can be taken in the nonlinear case (Li et al. 1993, 1994b) as will be discussed in the following section on timescale-based reduction methods.

7.7.5 *Approximate Nonlinear Lumping in Systems with Timescale Separation*

It was noted in the previous section that the approach taken for lumping based on timescale separation is to seek a canonical form for the Jacobian which separates the slow and fast subspaces for the variables. This type of approach can also be pursued for nonlinear approximate lumping where approximate canonical forms are now sought for the operator A (see Eq. (7.57)) which separate the slow and fast variables. The approach is based on the application of algebraic methods in nonlinear perturbation theory (Bogaevski and Povzner 1991; Li et al. 1993, 1994b, c). The aim is to find a suitable canonical form that separates the nonlinear right-hand sides of the lumped kinetic equations into slow and fast components. Therefore, the operator A is defined in the form

$$A = A_0 + \varepsilon A_1 + \varepsilon^2 A_2 + \cdots, \tag{7.60}$$

where ε is a small parameter. Then, a special form is sought for the operator which allows the separation of groups of slow and fast variables as in the case of ILDM (see Sect. 6.5). If A_o is dominant in magnitude compared to other $A_i s$ and the leading operator A_o is already in a canonical form such as diagonal, triangular or a quasi-linear one, then finding canonical forms for each of the A_i is an easier task than finding a general canonical form. The approach developed by Li et al. was based on algebraic methods in nonlinear perturbation theory (Bogaevski and Povzner 1991; Li et al. 1993).

Using the algebraic method in nonlinear perturbation theory, it is possible to find a transformation operator S such that the resultant operator

$$\hat{A} = e^{-S} A e^{S} \tag{7.61}$$

has a canonical form similar to A_o, and S is similarly expanded

$$S = \varepsilon S_1 + \varepsilon^2 S_2 + \ldots, \tag{7.62}$$

where all the S_i operators are linear partial differential operators. The dependent variables in the corresponding differential equation system for $\hat{A}$ will be partially or

completely decoupled, and hence, the differential equations for the new decoupled variables form lower-dimensional lumped differential equation systems (Li and Rabitz 1996b).

The use of nonlinear canonical forms provides advantages over linear lumping methods since the lumped groups may be valid over large regions of composition/temperature space. The methods essentially provide higher-order accuracy than methods such as the QSSA albeit at the cost of potentially complex algebraic manipulations in order to find the terms of the perturbation expansion. For constrained nonlinear lumping, the dependent variables of the lumped model are the same as the original ones. Thus, the solutions of the original variables of interest can be obtained directly by solving a lower-dimensional lumped differential equation system. This approach has been successfully demonstrated for H_2/O_2 combustion system including ignition (Tomlin et al. 1994) and oscillatory behaviour (Li and Rabitz 1995). The method was further extended for H_2/O_2 and CO/H_2/air combustion cases in Li and Rabitz (1996a, 1997) to the "special perturbation method" in an attempt to improve the accuracy of higher-order terms generated by constrained approximate nonlinear lumping methods, which were shown to be divergent in some cases. A correction term was added to the first-order term, and a Shanks transformation (Shanks 1949) was then applied to improve the convergence of the corrected first-order perturbation series. The method was shown to give very good accuracy for both the isothermal and non-isothermal case studies in H_2/O_2 and CO/H_2/air combustion with the advantage of avoiding the derivation of higher-order terms. The approximation is shown in both examples to be significantly more accurate than lower-order expressions based on QSSA and pre-equilibrium approximations, particularly during the initial phase of the reaction trajectories. One of the disadvantages of these methods is the complex algebraic manipulations that result from couplings between the variables. In Li and Rabitz (1996b), the approach was combined with numerical methods for solving the resulting complex algebraic relationships making the method more applicable for complex, non-isothermal reaction systems.

7.7.6 Continuous Lumping

Besides the lumping of species using discrete weighted sums, another method for decreasing the number of species in a model is the introduction of *continuous species* (Aris and Gavalas 1966; Bailey 1972; Aris 1989; Astarita and Ocone 1992; Laxminarasimhan et al. 1996; Zhao et al. 2002). Such techniques are useful in models of processes involving highly complex hydrocarbon mixtures such as petroleum feedstocks, for example. Here, extremely large numbers of species may be present, many of which can be ordered according to one of their chemical or physical features. This feature then becomes a relatively simple function of the ordering variable. For example, in a polymerisation system, the melting point and the reactivity of the oligomers are a smooth function of the number of monomer

units in the oligomer species. If the kinetic system contains several ten thousands of oligomers of different sizes, then it is not useful to calculate the concentrations and properties of each of the oligomers separately. Another example is mixtures of hydrocarbons containing many similar hydrocarbon molecules. In such systems the discrete species can be represented by a continuum, and the lumping procedure becomes a process of integration rather than summation. This approach of continuous species has found application in models of catalytic cracking (Weekman 1979; Cicarelli et al. 1992; Laxminarasimhan et al. 1996) and modelling the liquefaction of coal (Prasad et al. 1986).

The reactivity and physical properties of continuous species are defined as a function of a dimensionless variable $x \in [0, \infty)$. This variable is usually related to a measurable physical quantity, such as molecular weight or boiling point. The fraction of a continuous species belonging to an interval of variable x can be calculated by integrating the time-dependent probability density function $\rho(x, t)$ over this interval. According to its definition, the integral of this *pdf* is unit over the whole domain of definition of x at any time.

The rate equations for lumped mixtures will now be discussed. If we consider an isothermal reaction system containing m different reactant types which react irreversibly with an n-th order rate, then the resulting rate equations become

$$\frac{\mathrm{d}c_i}{\mathrm{d}t} = -k_i c_i^n \tag{7.63}$$

If the reaction order is assumed to be constant for all species, then the only species-dependent parameter is k_i, and hence, a species can be defined by its concentration c_i and its reactivity k_i.

For m discrete species, a reactant lump can be expressed as

$$\hat{C}(t) = \sum_i^m c_i(k_i, t) \tag{7.64}$$

If m becomes sufficiently large, then k can be treated as a continuous function, and the lump can be expressed in integral form

$$\hat{C}(t) \approx \int_{k\_}^{\overline{k}} g(k, t)\,\mathrm{d}k \tag{7.65}$$

Here $k\_$ and $\overline{k}$ are the lower and upper limits for the particular mixture. The product $g(k,t)\mathrm{d}k$ is the total concentration of a species with rate constants between k and $k + \mathrm{d}k$, and should be interpreted as a concentration distribution function. As the number of species within the mixture grows and approaches infinity, then the separation between $k\_$ and $\overline{k}$ becomes larger, and for convenience, it is assumed that $k\_ \to 0$ and $\overline{k} \to \infty$. This leads to the conventional form of the lumping equation for continuous mixtures:

$$\hat{C}(t) \approx \int_0^{\infty} g(k,t)\mathrm{d}k \tag{7.66}$$

Chou and Ho (1988) modified this approach slightly so that Eq. (7.66) is expressed as an integral over reactivity k by taking into account the fact that the number of reactant types per unit range of k can vary along the k axis. This leads to a modified expression for the lumped concentration:

$$\hat{C}(t) \approx \int_0^{\infty} c(k,t)D(k)\mathrm{d}k \tag{7.67}$$

with time dependence

$$\frac{\mathrm{d}\hat{C}}{\mathrm{d}t} \approx -\int_0^{\infty} D(k)kc(k,t)^n\mathrm{d}k \tag{7.68}$$

Here, $D(k)$ acts as a weighting factor which takes into account that in the discrete system the k_i's may not be equally spaced along the k axis but will depend on the type of feedstock to the reactor. An advantage of this approach is that rate coefficients and physical properties can be measured at fixed points, and then the appropriate function for k can be determined by fitting to these measured values.

If the continuous species participates in first-order reactions only, then it is easy to calculate (Okino and Mavrovouniotis 1998) the total concentration of the continuous species at each time point, as well as the *pdf* belonging to this time and the mean values of physical properties. If the continuous species participates in reactions other than first order, then general solutions do not exist, but solutions can be derived for several special cases (Astarita and Ocone 1986; Ho and Aris 1987; Astarita 1989; Astarita and Nigam 1989; Ocone and Astarita 1993).

7.7.7 *The Application of Lumping to Biological and Biochemical Systems*

Lumping methods have found a number of applications within biological and biochemical systems although the methods are sometimes referred to as the "zooming" of states. An overview of the suitability of lumping methods for such types of models is provided within the review of Maria (2004). Both symbolic and numerical methods for unconstrained and constrained lumping were developed in Brochot et al. (2005) and were demonstrated for 2- and 6-compartment physiologically based pharmacokinetic (PBPK) models for 1,3-butadiene. Whilst symbolic approaches were deemed to be useful for starting models with a low number of variables, numerical methods were required for more complex models.

Sunnaker et al. (2010) developed a linear lumping approach with application to a model predicting the observed behaviour of fluorescence emission in photosynthesis. Their approach was based on timescale separations within the system. It has strong similarities with the "family" approach developed in atmospheric systems (see Sect. 7.7.1), since the criteria used for lumping a group of states include the reactions between them occurring on a much faster timescale than the overall system timescale. Graph-based methods were used to identify components within each lump. The approach was generalised for nonlinear systems in Sunnaker et al. (2011) and includes methods to determine the inverse transformation, i.e. the functional relationship between the lumped states and the original ones. The authors claim that this makes the lumped model more easily interpreted from the biological point of view. The definition of inverse transformations is based on assumptions regarding the system dynamics that result in a sufficient number of equations being linear so that an inverse transform can be defined. These assumptions are based on the QSSA and on conservation relations that typically occur in models based on mass action kinetics (as discussed in 2.3) and are common in models involving transporters and enzymes. The method was demonstrated for a model describing glucose transport across the cell membrane in baker's yeast.

The exploitation of timescale separation was also performed by Liao and Lightfoot (1988) within a formal linear lumping approach similar to that outlined in Sect. 7.7.3. They demonstrated the approach for the red cell glycolysis model for which the original system has 15 variables. They show that with different degrees of lumping or "zooming", the reduced model is able to represent the system dynamics on different timescales. For example, the lumped 2 variable model describes the system dynamics for timescales longer than an hour, but 4 additional variables are needed to capture the dynamics on the timescale of minutes. Such "time hierarchies" in biological systems were also discussed by Maria (2006), particularly with respect to genetic regulatory network (GRN) models (Maria 2008, 2009). Maria argues that the level of detail within lumped sub-modules should be adjusted according to the available experimental information which is perhaps important for parameter estimation problems. Brochot et al. (2005) suggest that the use of lumping to develop reduced models can assist in overcoming problems of statistical identifiability within parameter estimation for pharmacokinetic models. For example, when model parameters are highly correlated or have multiple peak posterior distributions, parameter estimation can require a large number of runs in order to explore the space of possible parameter values. A reduced model is therefore computationally beneficial. However, Maria warns that the application of lumping to models of metabolic processes must account for the physical significance of species and their interactions, as well as the systemic properties of the metabolic pathway, rather than being based on purely mathematical analysis of system timescales (Maria 2006). One important aspect of lumping in biological and biochemical systems therefore, may be the need to relate the lumped parameters and variables back to those of the original model.

Dokoumetzidis and Aarons (2009b) further highlight the need for variables and parameters within reduced biological models to retain a specific physiological

meaning. They develop an approach for proper lumping, where each of the original species contributes to only one of the pseudo-species within the lumped system, meaning that the original species form groups which have a clear physical interpretation. Their algorithm is based on a formal lumping approach as outlined in Sect. 7.7.2. Many possible lumping matrices are explored, and an optimisation approach is used to select the reduced model with the smallest error when compared to the original model. To avoid a combinatorial explosion (see Sect. 7.6), the lumps are added one at a time in a greedy-type approach. However, for a system with 30 variables and 20 lumps, over 8000 model evaluations are still required. The approach was demonstrated for a model describing the signalling pathways of NF-κB. A useful development to this approach was made in Dokoumetzidis and Aarons (2009a) where parameter uncertainties were accounted for. Here a Bayesian framework was used to produce lumping schemes which, whilst not necessarily optimal for the nominal parameter values, were optimal on average over the prior parameter distribution (i.e. incorporating uncertainties). This was compared with a standard non-Bayesian lumping method which produced a model that was good for the nominal values but was very poor for other values within the prior distribution. The approach was demonstrated for a physiologically based pharmacokinetic (PBPK) model for barbiturates. Their study raises the very important issue of model reduction under uncertainty which is particularly critical if the reduced model is to be used within the context of parameter estimation.

An algorithm for lumping coupled with parameter optimisation and variable elimination was also developed in Dano et al. (2006) and demonstrated for a 20-variable model of yeast glycolytic oscillations. A key aim of their approach is to ensure that the lumping and reduction procedures preserve the dynamic behaviour of the model, an issue which was also discussed more formally in Toth et al. (1997). The model was first lumped using a method similar to Sunnaker et al. (2010), and then parameter optimisation was performed in order to preserve the dynamic properties of the model such as its oscillatory behaviour and the structure of the bifurcation diagram. Variables are then eliminated from the dynamic model using QSSA relationships, and an optimisation approach is also used to test all physically realistic models and to search for the smallest one which preserves the dynamic behaviour of the model. The combinatorial explosion which is typically found in optimisation problems (Sect. 7.6) is avoided by sequentially applying the QSSA to the least important species until the point at which the oscillatory behaviour is lost upon further elimination. This type of methodology would be greatly assisted by formalised methods for the selection of QSS-species which will be discussed in the following section.

7.8 The Quasi-Steady-State Approximation

We hinted in Sect. 2.3.6 that the timescale separation present in most kinetic systems can be exploited in terms of model reduction. The next sections will therefore cover the use of timescale analysis for the reduction of the number of

variables within kinetic models. This can have the added advantage of reducing the stiffness of the equation systems (see Sect. 6.7), since often the fast variables are removed from the system of differential equations and determined through algebraic relations with respect to the slower variables. We start first with the application of the QSSA, which is one of the simplest methods for exploiting timescale separation and is based on associating fast and slow timescales to individual species (see Sect. 6.3 for a full discussion of this point).

7.8.1 Basic Equations

Consider the following general initial value problem:

$$\frac{\mathrm{d}\mathbf{Y}}{\mathrm{d}t} = \mathbf{f}(\mathbf{Y}, \mathbf{p}), \quad \mathbf{Y}(0) = \mathbf{Y}^0 \tag{7.69}$$

On applying the QSSA, we define non-QSSA variables (the *slow variables*) and QSSA variables (the *fast variables*) as $\mathbf{Y} = (\mathbf{Y}^{(1)}, \mathbf{Y}^{(2)})$. The distinction between fast and slow variables was discussed in Chap. 6. The right-hand side of the system of ODEs (7.69) can be divided accordingly: $\mathbf{f} = (\mathbf{f}^{(1)}, \mathbf{f}^{(2)})$. The concentrations of the non-QSS-species are calculated by solving the system of ODEs $\mathbf{f}^{(1)}$, whilst the concentrations of the QSS-species are calculated by solving the algebraic system of equations obtained by setting the right-hand side of equations $\mathbf{f}^{(2)}$to zero:

$$\frac{\mathrm{d}\mathbf{Y}^{(1)}}{\mathrm{d}t} = \mathbf{f}^{(1)}(\mathbf{Y}, \mathbf{p}), \quad \mathbf{Y}^{(1)}(0) = \mathbf{Y}_0^{(1)} \tag{7.70}$$

$$\mathbf{0} = \mathbf{f}^{(2)}(\mathbf{Y}, \mathbf{p}) \tag{7.71}$$

The system of differential (7.70) and algebraic (7.71) equations is coupled through common variables and therefore can only be solved together. Various numerical methods exist for directly solving such differential algebraic equations (DAEs) (Gear and Petzold 1984), although other tricks can be introduced to improve the numerical efficiency of employing the QSSA as discussed below.

Application of the QSSA is successful if the solution of ODE (7.69) is almost identical to the solution of the coupled DAEs (7.70 and 7.71). What is considered as "almost identical" may depend on the actual problem and the accuracy required, but in reaction kinetic modelling, a 1 % error for all species at any time is usually considered acceptable. It was emphasised in Sect. 7.2 that the aim of chemical kinetic simulations is the accurate calculation of the concentrations of important species or those of important reaction features. Therefore, the statement above can be refined so that the application of the QSSA is successful if the solutions of Eqs. (7.69) and (7.70–7.71) are almost identical considering the concentrations of important species and the important features.

7.8.2 *Historical Context*

The first application of the QSSA is usually attributed to Bodenstein (Bodenstein 1913; Bodenstein and Lutkemeyer 1924), but Chapman and Underhill (1913) and Semenov (1939, 1943) were also early users of the technique. Further pioneers of the application of the QSSA are Michaelis and Menten (1913) and Briggs and Haldane (1925). The history of the application of the QSSA can be divided into three periods (Turányi et al. 1993b). In the early period (1913–1960), accurate experimental data for various applications were obtained and compared with solutions of simple kinetic systems of differential equations that were formulated to model the experimental behaviour. Due to the limited availability of computer power during this time, the kinetic ODEs had to be solved analytically and using the QSSA helped to convert the systems into an analytically solvable form.

From the 1960s onwards, computers became available for many researchers, but the stiff systems of ODEs that describe many kinetics applications often could not be simulated using available computer codes during this early period of numerical analysis. By applying the QSSA, the stiff systems of ODEs could be converted to non-stiff ones (Snow 1966; Blouza et al. 2000), and numerical solutions to these ODEs could be obtained using traditional ODE solvers.

The publication of the Gear algorithm (Gear 1971) allowed the numerical solution of stiff systems of differential equations and facilitated the comparison of solutions of the kinetic system of differential equations with and without the application of the QSSA. In early numerical experiments, the two solutions were often different, and therefore, Edelson et al. demanded the cease of the application of the QSSA (Edelson 1973; Farrow and Edelson 1974). However, the QSSA is still widely used (Mendiara et al. 2004; Machrafi et al. 2005; Ströhle and Myhrvold 2006; Ciliberto et al. 2007) for the interpretation and simplification of reaction mechanisms and speeding up reaction kinetic simulations. Peters et al. (Peters 1985; Paczko et al. 1986; Peters and Kee 1987; Peters and Rogg 1993) simplified several detailed combustion mechanisms to skeleton mechanisms with only $2-4$ lumped reaction steps by using the QSSA, allowing the early use of combustion kinetics in 3D computational fluid dynamic (CFD) simulations with complex geometries. The explicit or hidden application of the QSSA is present in thousands of articles on chemical kinetic modelling, and there are more than one hundred articles dealing with the theory of the QSSA (see e.g. Miller and Alberty 1958; Segel 1988; Segel and Slemrod 1989; Borghans et al. 1996; Tzafriri and Edelman 2004, 2005; Flach and Schnell 2006; Li et al. 2008a; Goussis 2012; Li and Li 2013). It is a commonly used technique with perhaps a large potential for model reduction, and therefore, it is worthwhile establishing sound principles on which to base its application. Early failures of the application of the method are more likely to be due to its inappropriate use, rather than a breakdown of the technique itself.

7.8.3 The Analysis of Errors

Several early articles dealt with the applicability of the QSSA for certain groups of species. Detailed reaction mechanisms were simulated with and without the application of the QSSA (see e.g. Farrow and Edelson 1974; Sundaram and Froment 1978; Savage 1990), and the two solutions were compared. This determines the applicability of the QSSA for a given system at given conditions, but unfortunately does not provide general conclusions. In other publications, the applicability of the QSSA was investigated for small skeleton models such as the Michaelis−Menten scheme (see e.g. Georgakis and Aris 1975) and on the basis of singular perturbation theory (see the review of Klonowski (1983)). The main result of the latter approach is that using the Tihonov theorem (Tihonov 1952; Heineken et al. 1967; Vol'pert and Hudjaev 1985), a necessary condition can be given for the applicability of the QSSA. However, this theory cannot be applied for the calculation of the error induced by the application of the QSSA for an arbitrary reaction mechanism which will be covered below.

An early article on the error caused by the application of the QSSA was written by Frank-Kamenetskii (1940), who is perhaps better known for theories on reactor stability and flame modelling. This very brief article received only a few citations over several decades following its publication (Benson 1952; Sayasov and Vasil'eva 1955; Rice 1960). Turányi and Tóth (1992) published an English translation of Frank-Kamenetskii's article with detailed comments. Further development and generalisation (Turányi et al. 1993b) of the reasoning of Frank-Kamenetskii allows the calculation of the error caused by the QSSA and is detailed below.

On the application of the QSSA and using the notation introduced in Sect. 7.8.1, the Jacobian can be divided into four submatrices:

$$\mathbf{J} = \begin{pmatrix} \mathbf{J}^{(11)} & \mathbf{J}^{(12)} \\ \mathbf{J}^{(21)} & \mathbf{J}^{(22)} \end{pmatrix} = \begin{pmatrix} \dfrac{\partial \mathbf{f}^{(1)}}{\partial \mathbf{Y}^{(1)}} & \dfrac{\partial \mathbf{f}^{(1)}}{\partial \mathbf{Y}^{(2)}} \\ \dfrac{\partial \mathbf{f}^{(2)}}{\partial \mathbf{Y}^{(1)}} & \dfrac{\partial \mathbf{f}^{(2)}}{\partial \mathbf{Y}^{(2)}} \end{pmatrix} \tag{7.72}$$

At the beginning of reaction kinetic simulations, usually the concentrations of only a few species (e.g. reactants, diluent gases, etc.) are defined, and other concentrations are set to zero. The QSSA is not usually applicable from the beginning of the simulation since at this point, the trajectories are quite far from any underlying slow manifolds (see Sect. 6.5). Hence, the kinetic system of ODEs (7.69) is usually solved first, and at time t_1 is switched to the solution of the DAE system (7.70–7.71). We denote $\mathbf{Y}(t_1)=(\mathbf{Y}^{(1)}(t_1), \mathbf{Y}^{(2)}(t_1))$ to be the solution of Eq. (7.69) at time t_1. When the system of Eqs. (7.70–7.71) is used, then the concentrations of the QSS-species are calculated first via the solution of algebraic system of Eqs. (7.71), and the result is concentration vector $\mathbf{y}^{(2)}(t_1)$. The concentrations of the non-QSS-species are identical to the solution of system of ODEs (7.69) at time

t_1, and therefore vector $\mathbf{y}(t_1) = (\mathbf{Y}^{(1)}(t_1), \mathbf{y}^{(2)}(t_1))$ is the initial value of the DAE system of Eqs. (7.70–7.71).

The *local error* of the QSSA at time t_1 is given by the following vector (Turányi et al. 1993b):

$$\Delta\mathbf{y}^{(2)}(t_1) = \mathbf{y}^{(2)}(t_1) - \mathbf{Y}^{(2)}(t_1) \tag{7.73}$$

We now calculate the Taylor expansion of function $\mathbf{f}^{(2)}$ at variable values $\mathbf{y}(t_1)$:

$$\frac{\mathrm{d}\,Y_i^{(2)}}{\mathrm{d}\,t}(t_1) = \left[f_i^{(2)}(\mathbf{Y})\right]_{\mathbf{Y}=\mathbf{y}(t_1)} + \sum_k \left[\frac{\partial f_i^{(2)}(\mathbf{Y})}{\partial Y_k}\right]_{\mathbf{Y}=\mathbf{y}(t_1)} \Delta Y_k^{(2)}(t_1) \tag{7.74}$$

where the expansion is applied for the QSSA variables only. Since vector $\mathbf{y}(t_1)$ is a root of the system of algebraic Eqs. (7.71), then $\left[f_i^{(2)}(\mathbf{Y})\right]_{\mathbf{Y}=\mathbf{y}(t_1)} = 0$ for each i. The second- and higher-order terms in the Taylor expansion are neglected. This is a usual step in physical chemical derivations, but in this context it is justified, since if the mechanism contains not more than bimolecular steps and does not contain second-order consumption steps such as the reaction type $2\mathrm{A} \rightarrow \mathrm{B}$, then the third and higher terms of the Taylor expansion are all zero.

Equation (7.74) can also be written in matrix form:

$$\frac{\mathrm{d}\,\mathbf{Y}^{(2)}}{\mathrm{d}\,t} = \mathbf{J}^{(22)}\Delta\mathbf{y}^{(2)} \tag{7.75}$$

where $\mathrm{d}\,\mathbf{Y}^{(2)}/\mathrm{d}\,t$ is the production rate of the QSS-species at time t_1 and $\mathbf{J}^{(22)}$ is the submatrix of the Jacobian belonging to the QSS-species at values $\mathbf{y}(t_1)$. It is more practical, however, to evaluate the matrix $\mathbf{J}^{(22)}$for the concentration vector $\mathbf{Y}(t_1)$, which results in an almost identical matrix. If the production rate $\mathrm{d}\,\mathbf{Y}^{(2)}/\mathrm{d}\,\mathrm{t}$ of the QSS-species and matrix $\mathbf{J}^{(22)}$are known, then the local error $\Delta\mathbf{y}^{(2)}$ of the QSSA at any time t_1 can be calculated by solving the algebraic system of Eq. (7.75).

The local error of the QSSA is not equal to the difference between the solution of the systems of Eqs. (7.69) and (7.70–7.71) at later times, which we call the *global error* of the QSSA (Turányi et al. 1993b). If the local error is large at the initial time, then the initial condition of Eqs. (7.70–7.71) will be wrong, and therefore, the global error is also expected to become large over time. In addition, if the agreement between Eqs. (7.69) and (7.70–7.71) is good until time t_2 and then the local error suddenly increases, the global error may also become large over time. This implies that successful application of the QSSA (i.e. where the global error is well controlled) means that the local error should remain small during the whole interval of its application.

Using the algebraic system of Eq. (7.75), the local error can be calculated for all QSS-species. If this equation is used for species i only, the following equation is obtained:

$$\frac{\mathrm{d}y_i}{\mathrm{d}t} = J_{ii}\,\Delta y_i \tag{7.76}$$

where J_{ii} is the i-th element of the diagonal of the Jacobian. The local error of the QSS-species can therefore be calculated as follows:

$$\Delta y_i = \left(-\frac{\mathrm{d}y_i}{\mathrm{d}t}\right)\left(-\frac{1}{J_{ii}}\right) \tag{7.77}$$

It was shown in Sect. 6.2 that $(-1/J_{ii})$ is equal to the lifetime of species i, and therefore, Eq. (7.77) means that if the QSSA is applied for a single species, then the absolute value of the local QSSA error is equal to the product of the species lifetime and its production rate. The local error is therefore small if the species is consumed in fast reactions and has a short lifetime. In this case the production rate of the QSS-species can be large, and therefore, it may undergo significant concentration changes during the simulation. This point is perhaps counter-intuitive since the term "steady-state" usually implies low rates of change. Tomlin et al. (1992), for example, showed that in the simulation of oscillatory hydrogen ignitions, the QSSA can be applied even for species that have a large production rate as long as they have a short lifetime. The local error of the QSSA can also be small, if the species is not very reactive, but also its production rate is small. In this case the QSSA is close to a "real" stationary approximation. This is the case when the QSSA is applied in polymerisation kinetic systems (Stockmayer 1944).

Figure 7.8 shows a visualisation of Eq. (7.77), i.e. the production rate of a QSS-species as a function of its concentration. The real production rate f_i belongs

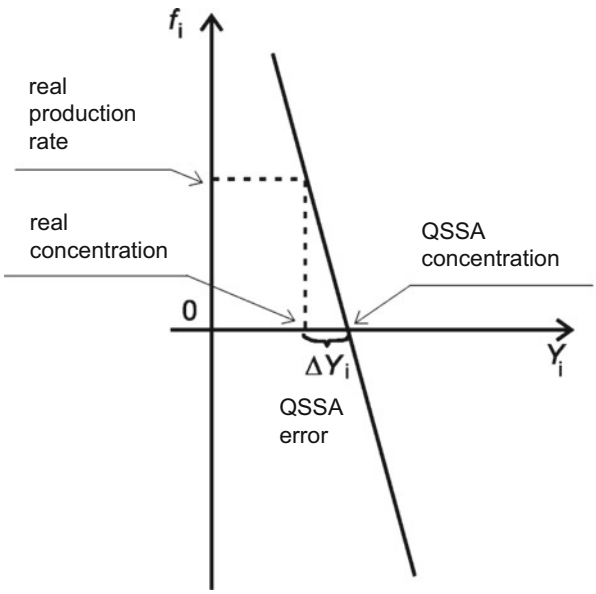

Fig. 7.8 The relationship between the concentration and the production rate of a species, and the error of the QSSA

to the real concentration $Y_i(t_1)$, whilst the zero production rate belongs to the QSSA concentration $y_i(t_1)$, calculated from Eq. (7.71). The figure shows that if function $f_i(Y_i)$ is steep, that is, slope $-J_{ii}$ is large (and hence the species lifetime is short), then the deviation between the real and the approximated concentrations is small. This means that the local error of the QSSA will be small, even if the real production rate of the QSS-species is large. If the production rate of the QSS-species is small, then the local error can be small, even if the slope of function $f_i(Y_i)$ is small. If the production rate is zero, then we apply the real steady-state approximation instead of the QSSA. Several reaction kinetics textbooks claim that the algebraic system of Eqs. (7.70–7.71) is applicable for the calculation of the concentration of the QSS-species because the production rate of the QSS-species is really almost zero. As Fig. 7.8 shows, the quasi-steady-state approximation is successful if the real and the approximated concentrations are close to each other, and it might be true even where the production rate is large, if function $f_i(Y_i)$ is very steep.

If any of the initial concentrations of intermediate species within the mechanism are zero, then the QSSA is usually only applicable after a time duration called the *induction period*. Using the equations above, the induction period can be estimated to be about ten times the lifetime of the QSS-species with the longest lifetime (Turányi et al. 1993b).

The selection of QSS-species is perhaps the most important part of the application of the QSSA. The following algorithm was suggested in Turányi et al. (1993b). First using Eq. (7.77), the local error of the QSSA (related to each species separately) is calculated across the domain of application. A group of candidate QSS-species is selected according to a user-defined tolerance. Up to 10 % error has been suggested to be tolerable within applications in combustion (Hughes et al. 2009). Then local error is calculated for this group of species using Eq. (7.75). If the approximated local error remains small, then the QSSA is applied for this group of species (Whitehouse et al. 2004a, b). The selection can be checked by comparing the solutions of systems of Eqs. (7.69) and (7.70–7.71), for the important species and important features over selected conditions. DAE solvers such as DASSL can be used for this purpose (Maly and Petzold 1996).

Due to the local error of the QSSA, the concentrations of the QSS-species calculated by Eq. (7.70–7.71) are slightly different from the "real" concentrations, which can be considered as a continuous perturbation of the trajectory of the non-QSS-species. Using the Green function (see Sect. 5.2.3), or in other words the initial concentration sensitivities, it is possible to assess (Turányi et al. 1993b) whether the concentration perturbation causes a significant deviation in the trajectories of the non-QSS-species.

7.8.4 Further Recent Approaches to the Selection of QSS-Species

As discussed in Sect. 2.3.5, conserved properties result in the linear combination of species concentrations or other variables of the system remaining constant throughout the trajectory. Such constants are called first integrals in mathematics. As Straube et al. (2005) demonstrated, the presence of QSSA relations leads to further linear functions of the concentrations being approximately constant during the solution of the kinetic system of ODEs. Straube et al. called these functions quasi-integrals. This means that identification of QSS-species can be based on the identification of the corresponding quasi-integrals. The unique feature of this approach is that in this case, the identification of the QSSA relations is not directly based on the investigation of timescales.

The relationship between the QSSA and the calculated concentrations of the important species was handled in a different way by Løvås and co-workers (Løvås et al. 2000, 2002a, b; Løvås 2009), who introduced the *level of importance* (LOI) *index*. This index is the product of the lifetime of a species and a local sensitivity term:

$$(\mathrm{LOI})_{ij} = \vartheta_i \sum_{l=1}^{N_R} \nu_{jl} \frac{\partial Y_i}{\partial \ln A_l} \tag{7.78}$$

The summation refers to all the N_R reaction steps. For the calculation of lifetime ϑ_i, not only the chemical lifetime τ_i is taken into account but also the residence time in a reactor and the species' rate of diffusion. The half-normalised local sensitivity coefficient $\partial Y_i/\partial \ln A_l$ shows the effect of perturbing the A-factor of reaction step l on concentration Y_i, and ν_{ij} is the corresponding stoichiometric coefficient. The index $(\mathrm{LOI})_{ij}$ estimates the error of the calculation of the concentration of species j due to the application of the QSSA on species i.

According to Løvås and co-workers (2002a), a species having a short lifetime is related to a small local error of the QSSA, but this small error may cause large errors in the simulated concentrations if these species exhibit large sensitivities. In several combustion systems, the QSSA error of the H-atom has such a property. In this case the LOI is large, and the QSSA is not applicable for such a species as found also in Tomlin et al. (1992). The opposite situation may arise when the species has a long lifetime, therefore a large local QSSA error, but this large error does not spread to the simulation results. An example might be that in ethylene/air and ethane/air premixed flames, the molecule C_2H_2 can be treated as a QSS-species (Wang and Rogg 1993). In this case the LOI is small, and the QSSA is applicable for this species. The LOI seems to be practically useful and has been applied to several systems. A mathematical derivation of the approach would be a useful development.

Montgomery et al. (2006) used a *genetic algorithm* for the selection of QSS-species. Based on the difference between the simulation results without and with the application of the QSSA, the selection of the QSS-species was optimised until the simulation error decreased below a certain threshold. CSP analysis can also be used for the selection of QSS-species and is covered in more detail in Sects. 6.4 and 7.9. The validity of the QSSA in solution-phase bimolecular reactions was also studied in Tzafriri and Edelman (2005).

Vora and Daoutidis (2001) developed a nonlinear model reduction method for non-isothermal reaction systems that exhibit dynamics on two different timescales. The method identifies the independent algebraic constraints (possibly of QSSA origin) that define the low-dimensional state space where the slow dynamics of the reaction system are constrained to evolve.

7.8.5 *Application of the QSSA in Spatially Distributed Systems*

The propagation of errors in spatially distributed systems is also important and has been the subject of several studies. Yannacopoulos et al. (1996a, b) carried out a mathematical study of the general case and found that in common with the spatially homogeneous case, the higher the net rate of production of the QSS-species, the larger the possible error. Steep spatial gradients in concentrations also led to larger overall errors. They also state that the higher the minimum diffusion rate of the species, the lower the possible error, which relates to the idea that steep spatial gradients (and therefore large errors) are smoothened by strong diffusion processes. In Yannacopoulos et al. (1995), a method was suggested to describe the transient relaxation to the slow manifold (i.e. the induction period) based on algebraic sets and perturbation theory. Its application was demonstrated for a simple enzyme substrate model and a two-dimensional oscillatory system as well as spatially distributed systems. The method is equivalent to finding higher-order approximations to the fast dynamics of the system, whereas the QSSA represents a zeroth-order approximation. The additional accuracy of the higher-order approximation was found to reduce the propagation of errors in reaction–diffusion systems. The main reason for this is a better approximation to the initial stages of the fast dynamics during the induction period where the QSSA errors may be higher. Although it was stated above that the QSSA should not be applied during this induction period, in practice it is often applied during this period for spatially homogeneous systems with little consequence on the long time errors. However, because of the spatial dependence of the solution in reaction–diffusion systems, transient dynamics before relaxation to the slow manifold can have a very important effect on the solution at long times. In these types of cases, it is important to find a reduced system which is a good approximation to the full system almost everywhere, i.e. it is necessary to take into account the transient dynamics of the

relaxation to the slow manifold explicitly using higher-order approximations (Yannacopoulos et al. 1995). Other methods for determining higher-order approximations have been developed based on nonlinear perturbation theory as discussed in Sect. 7.7.5.

7.8.6 *Practical Applications of the QSSA*

The classical textbook approach to the application of the QSSA is to describe the concentrations of QSS-species via explicit algebraic expressions as functions of the slower species. When the QSSA is used only for a few species or the QSS-species are not strongly coupled to each other, then it is usually possible to calculate their concentrations sequentially, in an order that allows explicit equations to be obtained. Historically the QSSA was applied by directly solving such algebraic expressions (e.g. Peters and Williams 1987); however, this often resulted in large simplifications of the starting schemes to facilitate analytical solutions or truncation of the QSSA expressions. Since we are now moving towards modelling more and more complex systems, it is unlikely that these traditional methods will find general application. On the other hand, Hughes et al. (2009) demonstrated that such an approach based on algebraic equations could be applied to highly complex hydrocarbon oxidation schemes when algebraic manipulation packages such as MAPLE (Maple) are employed in order to provide a level of automation to the procedures. In their approach the use of explicit expressions to describe the concentrations of the QSS-species was coupled with reaction lumping in order to directly remove the QSS-species from the reaction scheme. A simple example of this type of reaction lumping based on the QSSA was demonstrated in Sect. 2.3.4 and showed that the lumped rate parameters derived in this way are often complicated nonlinear functions of the original rate parameters. They do not necessarily correspond to those of a single rate-determining step, and hence, the approach is slightly more complex than that described in Sect. 2.3.3.

Hughes et al. (2009) demonstrated the application of this approach for the reduction of a skeletal scheme describing the oxidation of *n*-heptane from 218 species to 110 species which is a substantial reduction. This extensive application was possible since often in hydrocarbon oxidation schemes in both combustion and atmospheric applications, the QSS-species are present in parallel pathways with little coupling between them. Therefore, finding analytical solutions is possible with the aid of algebraic manipulation packages. The types of species which can be removed tend to be fast radicals such as alkyl radicals, alkyl hydroperoxy radicals and hydroperoxyalkyl peroxy radicals (Hughes et al. 2009). Peroxy radicals, however, are shown to have higher QSSA errors and are often rate determining. They therefore cannot be removed using the QSSA. A similar approach was also taken by Whitehouse et al. within application to the Master Chemical Mechanism (MCM) describing tropospheric hydrocarbon degradation (Whitehouse et al. 2004c). It should be pointed out that such a simple approach is very difficult to apply to

highly coupled QSS-species and so may not be applicable to all possible QSS-species.

In fact in general, the QSSA results in implicit nonlinear algebraic equations (Pantea et al. 2014), the solution of which may require significant CPU time. It is possible to solve the coupled DAE system using easily available numerical methods such as DASSL as discussed above, but since this does not lead to substantial CPU savings, the use of such an approach is usually confined to testing the validity of applying the QSSA to selected groups of species over limited sets of conditions. Numerical schemes based on the QSSA have also been developed as discussed in Sandu et al. (1997a, b) and Jay et al. (1997). However, since the performance of traditional QSSA solvers was worse than many of the other explicit and implicit methods for solving the stiff atmospheric systems tested, we do not discuss them in detail here, and refer the reader to the papers of Sandu and co-workers for further details. A higher-order extension was also proposed in Jay et al. (1997), which was shown to improve upon earlier schemes.

In general, larger CPU savings will be made by solving for the QSS-species separately and substituting their concentrations into the ODEs for the slow species. Methods based on either inner or fixed point iteration methods (see e.g. Chap. 6 in Peters and Rogg 1993) or matrix manipulations (Chen 1988) have often been used in the past. The former of these methods uses iteration cycles to solve the coupled implicit equations, whereas the latter relies on matrix manipulations. The formulation of these methods is discussed in Jay et al. (1997), and they have been commonly applied in atmospheric chemistry (Jay et al. 1997) and combustion (Løvås et al. 2002b). Chen and Tham (2008) elaborated a method for the effective solution of the system of algebraic equations resulting from the QSSA. They stated that neither fixed point iteration nor matrix inversion methods are generally effective. They identified the strongly coupled QSS-species first, and their concentrations were calculated using matrix inversion. Fixed point iteration was used for the calculation of the concentrations of the other QSS-species. Also, if a nonlinear system of algebraic equations has polynomial equations on the right-hand side, then a numerically efficient way of solving it is to transform its coefficient matrix to an upper triangle matrix using a Gröbner basis (Becker and Weispfenning 1993).

Lu and Law (2006c) suggested another approach for the numerically efficient application of the QSSA. In their approach, the nonlinear algebraic equations for the QSS-species concentrations are first approximated by a set of linear equations, and these linearised equations are analytically solved with a directed graph (see Sect. 7.5), which is abstracted from the couplings between QSS-species. To improve computational efficiency, groups of strongly connected QSS-species are first identified. The intergroup couplings are then sorted topologically, and the inner group couplings are solved using variable elimination by substitution in a near-optimal sequence. The method was applied to generate a 16-step reduced mechanism for ethylene/air combustion, with the reduced scheme showing good accuracy for simulations of auto-ignition and perfectly stirred reactors compared to the initial scheme (Lu and Law 2006c).

Zambon and Chelliah (2007) also elaborated a method for the explicit, iteration-free calculation of the QSS concentrations. The method is based on modifications to the original matrix-based methods of Chen (1988) and is implemented in the Matlab coding environment utilising its symbolic programming capabilities. The method was used to develop an 18-step scheme for ethylene/air combustion from a skeletal scheme containing 31 species and 128 reversible elementary reactions, i.e. a similar level of reduction to that achieved by Lu and Law (2006c).

Kalachev and Field (2001) reduced a simplified reaction model of tropospheric chemistry. Using non-dimensionalisation and timescale-based variable reduction, a simple 4-variable model was obtained. The features of this model were investigated and compared with other small skeleton tropospheric chemical models.

Radulescu et al. (2008) suggested the application of a series of methods for the model reduction of biochemical networks. First, linear kinetic models are identified as subsystems of multi-scale nonlinear reaction networks. For the nonlinear systems, the solutions of the fast variables are calculated using the quasi-stationarity equations. The solutions of some of the slow variables are smoothed by averaging. The method was used for the analysis of a model of the NF-κB pathway. Boulier et al. (2011) proposed a new method for the derivation of reduced schemes based on the QSSA by means of differential and algebraic elimination. The approximations obtained are simpler than the classic equations for the Michaelis–Menten enzymatic reaction system. Zhang et al. (2013) suggested a hybrid kinetic mechanism reduction scheme based on on-the-fly reduction and the QSSA. The globally identified QSS-species were separated from the system of ODEs and solved via a set of algebraic equations.

7.9 CSP-Based Mechanism Reduction

Computational singular perturbation or CSP analysis also provides information on the contribution of the rates of the reaction steps to the various timescale modes within a model. It can therefore be used to identify redundant species and reactions as part of a model reduction procedure. The CSP methodology has been introduced in Sect. 6.4, and here we discuss aspects related to mechanism reduction. We continue the use of notations that were introduced in Sect. 6.4.

In the CSP methodology, several characteristic values (called indices) were derived (Kourdis and Goussis 2013), which allow the analysis and reduction of reaction mechanisms.

The fast amplitudes can be calculated by equation

$$z^m = \mathbf{b}^m \ \mathbf{f}, \qquad m = 1, \ \ldots \ , M \tag{7.79}$$

where M is the number of fast modes and $\mathbf{f}$ is the right-hand side of the kinetic system of differential equations. When the solution has reached the slow invariant manifold (SIM), then the amplitude of the fast modes is nearly zero:

$$z^m = z_1^m + z_2^m + \quad \ldots \quad + z_{N_R}^m \approx 0 \tag{7.80}$$

The term z_k^m can be calculated from

$$z_k^m = (\mathbf{b}^m \boldsymbol{\nu}_k) \; r_k \tag{7.81}$$

where r_k is the rate of reaction step k and $\boldsymbol{\nu}_k$ is the k-th column of the stoichiometric matrix. The term z_k^m denotes the contribution of the k-th reaction step to the m-th fast amplitude. Usually, only few terms are significant, and these can be identified (Goussis and Lam 1992) by the *CSP Participation Index*:

$$P_k^m = \frac{z_k^m}{\sum_j^{N_R} \left| z_j^m \right|} \tag{7.82}$$

The sum of the absolute values of P_k^m is equal to unity. A relatively large $|P_k^m|$ value indicates that the k-th reaction step is a significant participant in the m-th equilibrium.

The contribution of the k-th reaction step to the evolution on the SIM of the n-th variable can be evaluated with the help of the CSP Importance Index:

$$f_{\text{slow}}^n = f_{\text{slow}}^{n,1} + f_{\text{slow}}^{n,2} + \quad \ldots \quad + f_{\text{slow}}^{n,N_R} \tag{7.83}$$

The quantity $f_{\text{slow}}^{n,k}$ can be calculated from the following equation

$$f_{\text{slow}}^{n,k} = \sum_{j=M+1}^{N_S} a_j^n \left(\mathbf{b}^j \boldsymbol{\nu}_k\right) \; r_k, \quad k = 1, \ldots, N_R \tag{7.84}$$

where r_k is the rate of reaction step k, $\boldsymbol{\nu}_k$ is the k-th column of the stoichiometric matrix and a_j^n denotes the n-th element of column vector $\mathbf{a}_j$ in matrix $\mathbf{A}_s$. The *CSP Importance Index* is defined as

$$I_k^n = \frac{f_{\text{slow}}^{n,k}}{\sum_j^{N_R} \left| f_{\text{slow}}^{n,k} \right|} \tag{7.85}$$

The sum of the absolute values of I_k^n is equal to unity. A relatively large $|I_k^n|$ value indicates that the k-th reaction step has a significant contribution to the change of Y_n on the SIM.

In relation to the M-dimensional fast subspace $T_Y F$, there are several variables (i.e. species concentrations) that have a large contribution to the exhausted modes.

The number of such variables is greater than or equal to M. These variables can be identified with the help of the *CSP Pointer*:

$$\mathbf{D}_m = \mathrm{diag}[\mathbf{a}_m \ \ \mathbf{b}^m] \tag{7.86}$$

A value of D_m^i close to unity indicates that the i-th variable is strongly connected to the m-th mode and its corresponding timescale. In early publications related to CSP, D_m^i was called a "radical pointer", and it was used for the identification of QSS-species. Later, Lu and Law (2008a) demonstrated that the radical pointer identifies not only the QSS-species but also non-QSS-species participating in fast equilibria.

Using the CSP method, a non-stiff reduced model can be obtained that well describes the change of modes belonging to the characteristic timescale of the system (Valorani et al. 2005; Goussis and Valorani 2006). This method has been used for the reduction of mechanisms describing the production of nitrogen oxides in premixed methane−air flames (Goussis and Skevis 2005), ignition processes (Treviño 1991; Treviño and Solorio 1991; Treviño and Mendez 1991, 1992; García-Ybarra and Treviño 1994; Treviño and Liñan 1994; Wu et al. 2013), the tropospheric carbon bond mechanism (Neophytou et al. 2004; Mora-Ramirez and Velasco 2011), the Regional Atmospheric Chemistry Mechanism (Løvås et al. 2006) and biochemical models describing the circadian rhythm (Goussis and Najm 2006).

In recent papers, Goussis investigated the relationship between the QSSA and the partial equilibrium approximation (PEA) using CSP (Goussis and Maas 2011; Goussis 2012). It was shown that the QSSA is a limiting case of the PEA. Algorithms were reported for the identification of the variables in QSS and/or of the processes in partial equilibrium. Bykov and Gol'dshtein (2013) also discussed the relationship between the QSSA and PEA within the framework of the classical theory of singularly perturbed systems.

7.10 Numerical Reduced Models Derived from the Rate Equations of the Detailed Model

Several of the mechanism reduction methods discussed so far (see Sects. 7.2–7.6) result in a smaller reaction mechanism, which is a subset of the original detailed mechanism obtained by the removal of redundant species and reactions. Other methods provide a smaller mechanism consisting of lumped species and/or lumped reaction steps (Sect. 7.7). A further group of methods was then discussed which identify fast timescales within the model (see Sects. 7.8 and 7.9), and the resulting reduced model is a new set of differential equations with accompanying algebraic equations. In some cases these equations can be converted back to a reaction

mechanism via reaction lumping, but often an easily understandable kinetic structure is lost.

In the following sections, further methods are presented which result neither in a smaller reaction mechanism nor in a new set of differential equations. Instead, these methods provide a numerical relationship between a vector that defines the state of the model and the outputs of the chemical kinetic model. These reduced models will be termed here as numerical reduced models. Such relationships can be obtained directly from the kinetic and thermodynamic equations that define the system (see this section) or can be deduced by processing simulation results (see Sects. 7.11–7.13).

7.10.1 Slow Manifold Methods

Several of the numerical-based methods exploit the presence of slow manifolds within chemical kinetic systems which can help to reduce the dimensionality of the system (see Sects. 6.5 and 7.7.3) whilst retaining the ability to reproduce the important system dynamics. A slow manifold is rapidly approached during a simulation as the fast system timescales collapse. Let us assume that we have identified a point in the space of variables that is on (or close to) an N_z-dimensional manifold. The state of the system can then be characterised by the following variable vector

$$\alpha_1, \alpha_2, \quad \ldots \quad, \alpha_{N_Z}, g_1(\boldsymbol{\alpha}), g_2(\boldsymbol{\alpha}), \quad \ldots \quad, g_{N_Z}(\boldsymbol{\alpha}), Y_1, Y_1, \quad \ldots \quad, Y_{N_S}, \tag{7.87}$$

Here vector $\boldsymbol{\alpha}$ is the vector of the parameterising variables of the manifold, vector $\mathbf{g}(\boldsymbol{\alpha})$ is its time derivative, and the N-dimensional vector $\mathbf{Y}$ defines chemical concentrations and other variables of the thermokinetic state of the system, such as temperature or the enthalpy of the system. Knowing the N_z-dimensional manifold means that we have at least a numerical approximation of function $\mathbf{Y} = \mathbf{h}(\boldsymbol{\alpha})$ that projects the variables of the manifold onto the space of concentrations. The function $\boldsymbol{\alpha}=\overline{\mathbf{h}}(\mathbf{Y})$ defines the relationship between the concentrations and the coordinates of the manifold.

If at least one point $\boldsymbol{\alpha}_0$ of the manifold is known, then we can calculate the progress of the kinetic system using the following system of differential equations with N_z variables:

$$\frac{\mathrm{d}\boldsymbol{\alpha}}{\mathrm{d}t} = \mathbf{g}(\boldsymbol{\alpha}) \quad \boldsymbol{\alpha}(t_0) = \boldsymbol{\alpha}_0 \tag{7.88}$$

This means that the number of equations which needs to be solved is much less than the original kinetic system as discussed in Sect. 7.7.3. The calculated $\boldsymbol{\alpha}$ values can be converted to the full concentration vector at any time point using function $\mathbf{h}$. The initial value problem in Eq. (7.88) contains only $N_z \ll N$ variables, but the values of

all concentrations can be obtained as though the original kinetic system of differential equations had been solved. Reduced models based on low-dimensional manifolds can usually be simulated faster than the full systems of differential equations because the resulting dynamical system contains fewer variables and is usually much less stiff. Explicit integration methods could therefore potentially be used.

In the derivation above, there is an assumption that the manifold remains attractive as time progresses. This is not true for explosive or excitable systems, but it is valid for all other chemical kinetic systems. For explosive systems, the approach may still be valid, but the dimensionality of the slow manifold chosen would have to be large enough to contain the explosive modes. This point was demonstrated in Brad et al. (2007) where a low-dimensional repro-model describing the oscillatory ignition of CO–H_2 mixtures was developed using the ILDM concept. A manifold dimension of 4 was required in order to capture the complex dynamics associated with oscillatory ignition, but the initial system dimensionality was 14, and hence, substantial reductions and computational time savings were achieved.

Reduced systems modelling based on the initial value problem in Eq. (7.88) requires the application of three functions. Function $\dot{\boldsymbol{\alpha}}=\mathbf{g}(\boldsymbol{\alpha})$ defines the time derivative of $\boldsymbol{\alpha}$, function $\mathbf{Y}=\mathbf{h}(\boldsymbol{\alpha})$ calculates the concentrations from the parameters of the manifold (mapping $\Re^{Nz} \rightarrow \Re^{\mathrm{N}}$), whilst function $\boldsymbol{\alpha}=\overline{\mathbf{h}}(\mathbf{Y})$ (mapping $\Re^{\mathrm{N}} \rightarrow \Re^{Nz}$) defines the relationship between the concentrations and the coordinates of the manifold.

The approach above has several degrees of freedom:

1. *Method for the identification of the manifold*. There are many different mathematical approaches for the identification of the location of low-dimensional manifolds and thus for the definition of function $\mathbf{h}$. Several such methods will be discussed in Sects. 7.10.2 and 7.10.4.
2. *Selection of the parameterising variable* $\boldsymbol{\alpha}$. This has implications for the final description of the function $\boldsymbol{\alpha}=\overline{\mathbf{h}}(\mathbf{Y})$. Usually variables $\boldsymbol{\alpha}$ are selected to be identical to, or functions of, monotonically changing concentrations. For example, in several combustion systems, the concentrations of H_2O and CO_2 are continuously increasing, and therefore, the concentrations of these two species are chosen as the parameters of a two-dimensional manifold. Mathematically this means that function $\overline{\mathbf{h}}$ truncates the whole concentration vector to the concentrations of H_2O and CO_2, i.e. projects the whole concentration vector to a two-element vector that contains the H_2O and CO_2 concentrations only. This approach is not applicable when CO_2 is a diluent in high-temperature combustion systems because then the concentration of CO_2 may be a maximum function of the progress of the reaction. In this case, for example, H_2O and the sum of the concentrations of CO and CO_2 can be used as the two parameters of the manifold.

   In principle, the function $\overline{\mathbf{h}}$ can be any linear or nonlinear function. The requirement is that it should provide an unambiguous representation of the

manifold. In a limited range, the concentration of any species may be a parameter of the manifold. A systematic method to define the parameterising variables was suggested in Najafi-Yazdi et al. (2012). This method is based on a principal component analysis (PCA) of species mass fractions in composition space. The method yields the minimum number of linearly independent progress variables for a user-prescribed desirable accuracy. Niu et al. (2013) discussed using automated methods for defining progress variables in which all species of a chemical scheme are involved. The requirement is a monotonic change in their concentrations and a low gradient in the progress variable space. A set of weighting coefficients is determined for every species of the detailed chemical scheme, in order to construct the progress variable space.

3. *Representation of functions* $\dot{\boldsymbol{\alpha}}=\mathbf{g}(\boldsymbol{\alpha})$ and $\mathbf{Y}=\mathbf{h}(\boldsymbol{\alpha})$. If the parameterising variables $\boldsymbol{\alpha}$ of the manifold are identical to some of the concentrations, then their time derivatives can be calculated from the right-hand side of the kinetic system of differential equations. In general, the function can be obtained from the transformation function $\overline{\mathbf{h}}$ and the right-hand side of the kinetic system of differential equations. During the simulations, $\mathbf{g}$ can be calculated from $\mathbf{h}$ and the kinetic system of ODEs or, alternatively, $\mathbf{g}$ is also pre-calculated and stored as a fitted function. The requirement is that a mathematical function and its computational implementation is needed that calculates $\dot{\boldsymbol{\alpha}}$ and $\mathbf{Y}$ from the vector $\boldsymbol{\alpha}$ in a fast and accurate way.

7.10.2 Intrinsic Low-Dimensional Manifolds

Using the intrinsic low-dimensional manifold (ILDM) algorithm of Maas and Pope introduced in Sect. 6.5 and detailed below, the location of the slow manifolds in the concentration space can be determined. If we denote N_z to be the dimension of the slow manifold, then N_z variables should be selected for its representation (Golub and Van Loan 1983; Rhodes et al. 1999), and the concentrations of the other variables will be determined as a function of these variables.

Usually, the values of the N_z parameterising variables are selected according to a grid, whilst the values of all other concentrations are calculated by solving the appropriate system of algebraic equations. The original idea of Maas and Pope (Maas and Pope 1992) was that if a point $\mathbf{Y}$ in the concentration space belongs to the slow manifold, then the eigenvectors $\mathbf{w}_f^i$ of the Jacobian belonging to the fast modes are all orthogonal to the vector of reaction rates $\mathbf{f}(\mathbf{Y})$, and therefore

$$\mathbf{W}_f(\mathbf{Y})\ \ \mathbf{f}(\mathbf{Y}) = 0 \tag{7.89}$$

The matrix $\mathbf{W}_f$ consists of vectors $\mathbf{w}_f^i$. In early applications of the method, it was found that the angles between vectors $\mathbf{w}_f^i$ can be small causing numerical problems or degenerate systems. Therefore, the Schur decomposition (Golub and Van Loan

1983) of the Jacobian was used instead of the eigenvalue−eigenvector decomposition as discussed in Sect. 7.7.3. We can choose a decomposition $\mathbf{Q}^{\mathrm{T}}$ such that

$$\mathbf{Q}^{\mathrm{T}}\mathbf{J}\mathbf{Q} = \begin{pmatrix} \mathbf{J}'^{(11)} & \mathbf{J}'^{(12)} \\ 0 & \mathbf{J}'^{(22)} \end{pmatrix} \tag{7.90}$$

where $\mathbf{J}'^{(11)}$ corresponds to the N–N_z most negative eigenvalues (i.e. the fastest relaxing timescales) and $\mathbf{J}'^{(22)}$ corresponds to the N_z positive or small negative eigenvalues. If the point representing the actual state of the system (e.g. the concentration set) is on the slow manifold, then the vector of the rate of its change (e.g. vector of production rates) is perpendicular to the space defined by the fast modes, and thus, the slow manifold is defined by

$$\mathbf{Q}_f^{\mathrm{T}}\mathbf{f}(\mathbf{Y},\mathbf{k}) = 0 \tag{7.91}$$

The slow manifold is therefore defined by points in composition space where the chemical source term only has a component in the direction of the slow processes. The slow variables are projected accordingly onto the manifold defined by Eq. (7.91) yielding

$$\mathbf{Q}_S^{\mathrm{T}}\frac{\mathrm{d}\mathbf{Y}}{\mathrm{d}t} = \mathbf{Q}_S^{\mathrm{T}}\mathbf{f}(\mathbf{Y},\mathbf{k}) \tag{7.92}$$

Equation (7.91) is difficult to solve numerically although several methods have been suggested (Maas and Pope 1992; Maas 1998; Gicquel et al. 1999).

Using the method above, the values of all other variables belonging to the slow manifold are given as a function of the N_z parameterising variables defined on a grid. This means that the location of the manifold is given as a function of the parameterising variables. Also, the changes in the variables (e.g. the production rates of the species) can be calculated at each grid point. Usually this information is stored in a look-up table which is then used as a replacement for the original equation system. An appropriate search code can then be used to retrieve the values of the N_z parameterising variables, locate the nearest tabulated grid points, and calculate the values of all variables and the corresponding time derivatives using linear interpolation between the points. The errors inherent within such an approach could however be large if a too low a manifold dimension is assumed that is unable to represent the full dynamics of the system. The higher the tabulation dimension used, the lower the errors should be, although this has obvious implications for the computational cost of storage and retrieval algorithms (see Sects. 7.12 and 7.13). Interpolation errors should be kept small as long as the resolution of the tabulation grid is small enough.

The high-temperature combustion of several simple fuels has been simulated using the ILDM method (Ishmurzin et al. 2003). The results suggest that for models of adiabatic combustion in closed systems, the number N_z of necessary

parameterising variables is one for the combustion of hydrogen (Eggels and de Goey 1995), two for the combustion of wet carbon monoxide (Maas and Pope 1992) and three for the combustion of methane (Riedel et al. 1994). This shows that the chemical kinetics of the combustion of these species can be described by surprisingly few variables for certain applications if the temperature is high (e.g. $T \geq$ about 1,000 K). For open systems or systems which attempt to describe the low-temperature ignition behaviour of fuels, the required dimension may be higher. For example, Brad et al. (2007) found that modelling the oscillatory ignition of wet carbon monoxide required four variables. In their paper they also discussed the problems of fitting/tabulation errors for systems which demonstrate excitability (i.e. local increases in dimension), where small errors in one part of the variable phase space may be amplified at later points in the trajectory.

It is worthwhile to compare the application of ILDM-based methods with other approaches based on timescale analysis. For example, a typical detailed mechanism for the high-temperature combustion of methane, without the chemistry describing the reactions of nitrogen- and sulphur-containing species, contains about 30 reactive species. The QSSA has been found to be applicable for about 15 species, and therefore, even after the application of the QSSA, the kinetic system of differential equations contains about 15 variables. On the other hand, a manifold-based differential equation, with similar accuracy over a given range of conditions, may contain only 3 variables (Riedel et al. 1994). One reason for the difference is that the QSSA provides analytical expressions that should be applicable within a wide domain of concentrations of the non-QSS-species and therefore may be more restrictive than the criteria used for the generation of the ILDM over a restricted domain. In addition, the application of the QSSA assumes that the fast timescales are related to single species separately. In Chap. 6, however, we discussed how timescales may actually relate to linear or nonlinear functions of species concentrations. Therefore, the restriction of associating each fast timescale with a single species may lead to too stringent requirements when using dimension reduction strategies. Another requirement of the QSSA is that these fast timescales should be present for all investigated concentrations of the non-QSS-species. Using ILDM approaches, the fast processes can be different in different regions of concentration space. The combination of these advantageous features can result in dynamical models based on ILDM methods requiring fewer variables than those based on the QSSA.

Reduced models based on low-dimensional manifolds can usually be simulated faster than full systems of differential equations because the resulting dynamical system contains fewer variables and is usually not stiff (see Sect. 6.7). However, the search and retrieval algorithms required to access the look-up tables can consume significant amounts of computer time. As an example, the simulation of methane combustion based on the ILDM method was eight times faster than that using a detailed mechanism (Riedel et al. 1994). Special algorithms have been developed to speed up the search and retrieval process (Androulakis 2004). In situ tabulation methods have also been developed as discussed in Sect. 7.12 below.

Recent developments of methods based on the direct calculation of low-dimensional manifolds have branched out in several directions. One direction

has been the application of the method for more complex fuels. The method was successfully applied for the development of reduced models describing the combustion of high-molecular-weight hydrocarbons, such as *iso*-octane and *n*-dodecane (Blasenbrey and Maas 2000). Nafe and Maas (2003) also showed that the ILDM created for the description of the oxidation of smaller hydrocarbons can be used as a first approximation for the ILDM describing model dynamics for the combustion of larger hydrocarbons. Surovtsova and co-workers (2009) applied the ILDM method to several biochemical systems and implemented the method (together with a modified version) within the computer code COPASI (Hoops et al. 2006).

Improvements in the numerical methods for the calculation of low-dimensional manifolds have also been achieved. The original method of Maas and Pope works well if there is a clear separation between the fast and slow timescales, and therefore, the trajectories quickly approach the slow manifold. This is usually the case for high-temperature combustion. An improved algorithm is needed, if the manifold is not strongly attracting, i.e. there is weak timescale separation and the trajectories approach the manifold slowly. This is often the case for low-temperature combustion and other relatively slow kinetic processes. A further development of the ILDM algorithm applicable for slower processes was suggested by Maas and co-workers (Nafe and Maas 2002; Bykov and Maas 2007b; König and Maas 2009).

Most of the manifold-based methods simulate the slow subspace by solving differential equations and describe the fast subspace with functional relations. Using the method of *global-quasi-linearisation* (GQL) (Bykov et al. 2007), the fast subsystem is solved by integration (which is less stiff compared to the original system), and the slow variables are assumed to be linear functions of time during the local time integration step. The decomposition is based on comparing the values of the right-hand sides of the original system of equations, leading to the separation of "fast" and "slow" variables. The hierarchy of the decomposition is allowed to vary with time. The error between the solutions of the full system and those of the decomposed system of equations was shown to be negligibly small for practical applications. The efficiency of this approach was demonstrated on the wet carbon monoxide combustion system (Bykov et al. 2007; Bykov and Maas 2009a) and modelling the auto-ignition of a cyclohexane−air mixture (Bykov et al. 2013).

The advantage of the ILDM method is that it allows the modelling of dynamical systems using a number of differential equations (ODEs or PDEs) which is equal to the dynamical dimension of the simulated system (see Sect. 6.5). The disadvantage of the ILDM method is that the creation of the database that contains the manifolds requires significant human effort for any new detailed mechanism, and a specialised computer program is needed. When multivariate manifolds are stored in look-up tables, the database can be extremely large, and retrieval in the database is slow. So far, $N_z = 5$ is the highest number of parameterising variables that has been used for the tabulation of an ILDM (Blasenbrey 2000). An alternative approach is to store the data on the slow manifolds in the form of fitted functions (see Sect. 7.13). For example, Niemann et al. (1997) developed an approach where the space of

variables used to parameterise the ILDM was divided into many domains, and the ILDM was described in each domain using high-order orthonormal polynomials.

A second potential disadvantage of the ILDM is that it does not represent the exact invariant manifold of the system but rather is an approximation to it. The exact slow invariant manifold (SIM) is that to which propagated trajectories are attracted, whereas the ILDM is an approximation based on infinitesimally propagated trajectories (Skodje and Davis 2001). Thus once a trajectory has reached an invariant manifold, it does not leave it (Gorban et al. 2004b). The SIM is therefore a global attractor, whereas the ILDM is a local attractor. Several methods for determining SIMs have been developed using geometric approaches and will be discussed in Sect. 7.11.

7.10.3 Application of ILDM Methods in Reaction Diffusion Systems

Available methods for the reduction of reaction mechanisms are usually first tested on spatially homogeneous systems, but their most important practical application is the simulation of spatially inhomogeneous reaction−diffusion systems. In isothermal or adiabatic spatially homogeneous systems, the timescales are determined exclusively by the chemical reactions. If a chemical reaction occurs in a spatially inhomogeneous system, then mixing and diffusion timescales are also present as discussed in Sect. 6.6. Therefore, when using mechanism reduction methods based on timescales in spatially inhomogeneous systems, the physical timescales are also important. Maas and Pope discussed this question in one of their early articles (Maas and Pope 1994). In this early work, they assumed that the presence of species diffusion does not change the location of the manifold in the concentration space but rather shifts the point belonging to the actual state of the system along the manifold. Later investigations by, e.g., Ren and Pope (2007b) suggested that where clear timescale separations do exist, compositions in the reaction–diffusion system are perturbed from the chemical ILDM by $O(\varepsilon)$ due to molecular diffusion—the so-called "close-parallel" assumption (Ren and Pope 2006b). Also, whilst convection processes do not have a direct effect on composition, they can have significant indirect effects via the diffusion process by changing the gradients of composition. Therefore, in a reactive flow, the enhanced diffusion caused by convection may further pull the compositions away from the chemical ILDM (Ren and Pope 2007b). In addition, as discussed in Sect. 6.6, the chemical slow manifold may not give a good approximation to the full system of equations in cases where there is little timescale separation between the important chemical timescales and those related to the flow. One solution may be to use a higher-dimensional chemical manifold, hence ensuring that only timescales that are significantly faster than the flow have been equilibrated, but this could lead to too

high a dimension being required for the chemical ILDM in some cases. More general approaches have therefore been developed for reactive flow systems.

One such approach is the *reaction–diffusion manifold* (REDIM) *method*. Using the notation of Bykov and Maas (2007a), the evolution equation for the scalar field of a reacting flow is given by

$$\frac{\partial \boldsymbol{\psi}}{\partial t} = \mathbf{F}(\boldsymbol{\psi}) - \vec{\boldsymbol{\upsilon}} \cdot \operatorname{grad}\boldsymbol{\psi} + \frac{1}{\rho}\operatorname{div}\mathbf{D}\operatorname{grad}\boldsymbol{\psi} \tag{7.93}$$

where $\boldsymbol{\psi} = (\psi_1, \psi_2, \ldots, \psi_{N_S+2})^{\mathrm{T}}$ is the thermokinetic state, which can, e.g., be expressed by the specific enthalpy h, the pressure p and the mass fractions w_i of the N_S chemical species: $\boldsymbol{\psi} = (h, p, w_1, \ldots, w_{N_S})^{\mathrm{T}}$, $\mathbf{F}$ denotes the chemical source term, $\vec{\boldsymbol{\upsilon}}$ the velocity, ρ the density and $\mathbf{D}$ the matrix of transport coefficients (cf. Sect. 6.6).

The assumption that an invariant slow manifold of low dimension exists in the state space yields

$$\left(\mathbf{I} - \boldsymbol{\psi}_{\boldsymbol{\theta}}(\boldsymbol{\theta})\,\boldsymbol{\psi}_{\boldsymbol{\theta}}^{+}(\boldsymbol{\theta})\right) \cdot \left[\mathbf{F}(\boldsymbol{\psi}(\boldsymbol{\theta})) - \frac{1}{\rho}\operatorname{div}\left(\mathbf{D}\boldsymbol{\psi}_{\boldsymbol{\theta}}(\boldsymbol{\theta})\operatorname{grad}\boldsymbol{\theta}\right)\right] = 0, \tag{7.94}$$

where $\boldsymbol{\psi}_0(\boldsymbol{\theta})$ is an initial guess for the manifold in terms of reduced composition variables $\boldsymbol{\theta}$ (e.g. as estimated using the chemical ILDM). $(\mathbf{I} - \boldsymbol{\psi}_{\boldsymbol{\theta}}\boldsymbol{\psi}^{+})$ is a projection operator, which eliminates all components of the evolution of $\boldsymbol{\psi}$ tangent to the manifold. Here $\boldsymbol{\psi}_{\boldsymbol{\theta}}$ is a matrix which spans the tangent space of the manifold, and $\boldsymbol{\psi}^{+}$ is a pseudo-inverse, with the condition that $\boldsymbol{\psi}^{+}\boldsymbol{\psi}_{\boldsymbol{\theta}} = \mathbf{I}$. Bykov and Maas (2007a, 2009b) describe an approach to solve Eq. (7.94) using a time-stepping method:

$$\begin{aligned} &\frac{\partial \boldsymbol{\psi}(\boldsymbol{\theta}, t)}{\partial t} = \left(\mathbf{I} - \boldsymbol{\psi}_{\boldsymbol{\theta}}(\boldsymbol{\theta})\boldsymbol{\psi}^{\boldsymbol{\theta}+}(\boldsymbol{\theta})\right) \cdot \left[\mathbf{F}(\boldsymbol{\psi}(\boldsymbol{\theta})) - \frac{1}{\rho}\operatorname{div}\left(\mathbf{D}\boldsymbol{\psi}_{\boldsymbol{\theta}}(\boldsymbol{\theta})\operatorname{grad}\boldsymbol{\theta}\right)\right] \\ &\boldsymbol{\psi}(\boldsymbol{\theta}, 0) = \boldsymbol{\psi}_0(\boldsymbol{\theta}) \end{aligned} \tag{7.95}$$

with initial and boundary conditions given, e.g., by an extended chemical ILDM manifold (Bykov and Maas 2007a, b). In order to find the manifolds, estimates for the gradients of $\boldsymbol{\theta}$ have to be supplied, although it can be shown that the higher the dimension of the manifold, the smaller its sensitivity with respect to the gradient estimate (Bykov and Maas 2007b, 2009b).

Once the manifold has been identified, the governing equation for the scalar field of the reacting flow can be projected onto the manifold (Bykov and Maas 2007b, 2009a, b; Maas and Bykov 2011):

$$\frac{\partial \boldsymbol{\theta}}{\partial t} = \boldsymbol{\psi}_{\boldsymbol{\theta}}^{+}\mathbf{F}(\boldsymbol{\psi}(\boldsymbol{\theta})) - \vec{\boldsymbol{\upsilon}}\operatorname{grad}\boldsymbol{\theta} - \boldsymbol{\psi}_{\boldsymbol{\theta}}^{+}\frac{1}{\rho}\operatorname{div}(\mathbf{D}\boldsymbol{\psi}_{\boldsymbol{\theta}}\operatorname{grad}\boldsymbol{\theta}) \tag{7.96}$$

The REDIM method has been applied to systems with complex transport models (Maas and Bykov 2011). Its concepts have some similarities to the strategies used in

flamelet-generated manifolds (van Oijen and de Goey 2000; Verhoeven et al. 2012) or the flamelet prolongation of ILDMs (Gicquel et al. 2000). The flamelet approach will be discussed later in Sect. 7.12.4 since it is not specifically derived using the system equations.

An extended ILDM method was also developed by Bongers et al. (2002) for specific application in diffusion flames. In their work, the manifold is constructed in composition phase space (PS) instead of composition space, and hence, the chemical ILDM method is extended to the PS-ILDM method. The composition phase space includes not only the species mass fractions and enthalpy but also the diffusive fluxes of species and the diffusive enthalpy flux. The extended equation system therefore is of dimension $2(N_S + 1)$ where N_S is the number of species and hence is twice the dimension of the original system of equations. However, the extension allows the resulting ILDM to take account of diffusion processes that would not be represented by the purely chemical ILDM. Therefore, a low-dimensional slow manifold may be found, even in regions of the flame where there are strong interactions between chemistry and flow. The method is demonstrated for a premixed CO/H_2 flame with preferential diffusion.

7.10.4 Thermodynamic Approaches for the Calculation of Manifolds

The results of a chemical kinetic model can be obtained by solving the corresponding differential equations, and therefore, it is logical that reduced mechanisms can be deduced from these equations. It is perhaps surprising that successful model reduction strategies can be developed based on the thermodynamic functions of high-temperature gas kinetic systems. The *rate-controlled constrained equilibrium* (RCCE) method is such an approach and was first proposed by Keck in the 1970s (Keck and Gillespie 1971) as an alternative formulation for the simulation of chemical kinetic systems. It has more recently been used for the purposes of chemical model reduction and, in common with slow manifold, QSSA- and CSP-based methods, aims to exploit the timescale separation in kinetic systems (Jones and Rigopoulos 2005a, b). It therefore falls into the class of dimension reduction methods along with techniques such as ILDM. However, a different formulation is used in RCCE to derive the low-dimensional models. In RCCE the kinetically controlled species evolve according to differential equations involving detailed chemical kinetics, whilst equilibrated species are determined by minimising the free energy of the mixture, subject to the additional constraints [i.e. in addition to the conservation of mass, energy and elements (Jones and Rigopoulos 2007; Rigopoulos 2007)]. A brief description of the concepts involved in RCCE-based methods is given here as well as a summary of its main applications for chemical mechanism reduction to date. For a full discussion of the foundations

of the method, the reader is referred to the reviews of Keck (1990) and Beretta et al. (2012).

Using the normal formulation for chemical rate equations, the local equilibration of a species can be expressed by setting the right-hand side of its rate equation (i.e. its net production rate) to zero (see Sect. 2.3). However, the equilibrium state of a chemical system can also be determined using the maximum entropy principle of statistical thermodynamics (Chiavazzo et al. 2007). For a full equilibrium state, several constraints exist on the system. The first is element conservation as discussed in Sect. 2.3. Two thermodynamic constraints must also be specified, which, if expressed in terms of enthalpy and pressure, result in the Gibbs free energy being minimised for closed systems (Jones and Rigopoulos 2005a). Calculation of the final equilibrium state therefore does not involve knowledge of a detailed chemical mechanism. The equilibrium composition can instead be calculated by minimising its Gibbs free energy subject to constraints imposed by the mass of each element, and the pressure p and enthalpy being maintained constant at their specified values. This minimisation can be carried out using the method of Lagrange multipliers, and the equilibrium molar concentrations Y_j' can be shown to satisfy the following expression:

$$Y_j^{'} = \frac{p}{\rho RT}\left(\frac{-\mu_j^{\ominus}}{RT}\right)\exp\left[\sum_{i=1}^{M_e}\left(a_{ij}^{e}\lambda_i^{e}\right)\right] \quad (j = 1, \ldots N_S) \tag{7.97}$$

where λ_i^{e} are Lagrange multipliers referred to as element potentials, N_S is the number of species, M_e is the number of elements and $\mu_j^{\ominus}$ is the chemical potential in the standard state which is a function of temperature (see Jones and Rigopoulos (2007) for full derivation). The matrix a_{ij}^{e} contains the contributions of each element i in species j. Element constraints can be represented as

$$E_i = \sum_{j=1}^{N}\left(a_{ij}^{e}Y_j\right) \quad (i = 1, \ldots, M_e) \tag{7.98}$$

The conservation of pressure and enthalpy leads to 2 additional constraints.

If we wish to represent the system in a non-equilibrium state, then further constraints must be introduced. These constraints are usually expressed as linear combinations of species concentrations:

$$C_i = \sum_{j=1}^{N_S}\left(a_{ij}^{c}Y_j\right) \quad (i = 1, \ldots, M_c) \tag{7.99}$$

where M_c is the number of additional constraints. The molar concentrations resulting from constrained equilibrium Y_j^{*} are expressed as

$$Y_j^* = Y_j' \exp\left[\sum_{i=1}^{M_c}\left(a_{ij}^c \lambda_i^c\right)\right] \quad (j = 1, \ldots, N) \tag{7.100}$$

where $\lambda_i{}^c$ are additional Lagrange multipliers usually called constraint potentials. In the constrained equilibrium state, the species mole fractions are determined by M_c Lagrange multipliers.

In common with slow manifold-type methods, RCCE uses the assumption that fast reactions exist that relax the chemical system to the associated constrained equilibrium state on timescales which are shorter than those on which the constraints are changing (Tang and Pope 2004). The RCCE therefore comprises two concepts:

1. The constraints evolve according to chemical kinetics information.
2. At any time point, the state of the system is a constrained thermodynamic equilibrium state.

The implication of (1.) is an ODE which describes how the constraints evolve in time:

$$\frac{\mathrm{d}C_i}{\mathrm{d}t} = \sum_{j=1}^{N}\left(a_{ij}^c W_j\right) \quad (i = 1, \ldots, M_c) \tag{7.101}$$

where W_j is the production rate for species j (Jones and Rigopoulos 2005a). The implication of (2.) is that a system of algebraic equations exist which must be satisfied in order for the composition to remain on the constrained equilibrium manifold. Equation (7.100) defines such a sub-manifold in composition space, the constrained equilibrium manifold (CEM), on which the dynamical evolution of the system is allowed to take place. Equation (7.100) must be satisfied along with element constraints on the CEM:

$$E_i = \sum_{j=1}^{N}\left(a_{ij}^e Y_j^*\right) \quad (i = 1, \ldots, M_e) \tag{7.102}$$

and further constraints:

$$C_i = \sum_{j=1}^{N}\left(a_{ij}^c Y_j^*\right) \quad (i = 1, \ldots, M_c) \tag{7.103}$$

as well as the conservation of pressure and enthalpy. A non-equilibrium closed system will relax to a final equilibrium through a sequence of RCCE states expressed by CEMs. Hence, thermodynamic arguments are employed to calculate the partial equilibrium state through constraints, but chemical kinetics determines

the dynamic evolution of the system, i.e. how the constraints evolve in time, through Eq. (7.101).

Equations (7.100–7.103) form a differential algebraic system of equations where the number of constraints used determines the dimension of the reduced system. Since the RCCE formulation leads to a general system of ODEs, it is also necessary to select which variables the constraints should be applied to, since different selections may lead to different model reduction errors. Most commonly, constraints are applied to individual species, but this may be more related to practicalities of implementation rather than inherent properties of the system. There is in principle no reason why constraints should not be applied to combinations of species (e.g. lumped variables). To summarise (Jones and Rigopoulos 2007), an RCCE system comprises a set of ODEs or PDEs that describe the dynamics of the kinetically controlled species taken directly from a detailed mechanism without any approximations and a set of algebraic equations for the computation of the equilibrated species, derived on a physical basis via the maximum entropy principle of thermodynamics.

In Jones and Rigopoulos (2005a), RCCE was applied to the simulation of methane laminar flames. The first two constraints chosen were necessarily CH_4 and O_2 since initial and boundary conditions must correspond to a constrained equilibrium state for the set of constraints selected. Further constraints were then tested on a trial-and-error basis until the reduced model with the lowest error compared to the full model was obtained. Systems using 9 and 7 constraints were tested and found to give good agreement with the full model containing 63 species. The same set of constraints was also found to be satisfactory for the modelling of a methane ignition problem. The RCCE method was also applied in Ugarte et al. (2005) to a model of the combustion of a stoichiometric mixture of formaldehyde and oxygen which contained 29 species and 139 reactions over a wide range of temperatures and pressures. Reduced models containing between 1 and 6 RCCE constraints were tested along with three fixed element constraints (carbon, oxygen and hydrogen). Overall eight constraints were needed to give good agreement with ignition delays predicted by the full model, although slightly more were required for the prediction of minor species.

The selection of constraint species by trial and error, however, could be time consuming, and it would be useful to be able to automatically select the optimal set of constraints which minimises the simulation error for a given reduced model dimension. Hiremath et al. (2010, 2011) address this issue by developing a "greedy" algorithm to select a "good" set of constrained species. Whilst this may not be the globally optimal set, it is an improvement on trial-and-error approaches and was demonstrated for a methane combustion model to produce the lowest reduction error over a wide range of temperatures and pressures for partially stirred reactor studies. The selection of constraints was also achieved using an LOI in Rigopoulos and Løvås (2009) and more recently in Løvås et al. (2011), where the constraints were selected adaptively in different regions of the composition space. Here a cross-over between QSSA and RCCE methods occurs since the LOI is related to

the species lifetime (see Eqn (7.78)), and hence, the constrained species approximately correspond to non-QSS-species.

One advantage of RCCE is that it provides a consistent framework to derive equations describing the reduced model based on the second law of thermodynamics. This means that approaches such as tabulation or complex algebraic manipulations based on the QSSA can be avoided. One drawback of the RCCE approach, however, as pointed out by Tang and Pope (2004), is that the CEMs are not inertial manifolds but only approximations to them. What this means is that the RCCE manifolds produced are not the exact ones to which trajectories approach in a simulation of the full system. However, the same could be said of the ILDM formulation which also gives only an approximation to the exact inertial manifold. For this reason, extensions to RCCE have been proposed (Ren et al. 2007) which use CEMs as a starting point for trajectory-based methods which calculate the corresponding inertial manifold (see later discussion in Sects. 7.11 and 7.12).

7.11 Numerical Reduced Models Based on Geometric Approaches

7.11.1 Calculation of Slow Invariant Manifolds

As pointed out in the previous section, one potential disadvantage of ILDM and RCCE methods is that they do not represent the exact invariant manifold of the system but rather an approximation to it. The exact slow invariant manifold (SIM) is that to which propagated trajectories are attracted, and once a trajectory has reached an invariant manifold, it does not leave it (Gorban et al. 2004b). Singh et al. (2002) demonstrate, for example, that an ILDM is not in general a SIM but approaches one in the limit of large stiffness, i.e. clear timescale separation between slow and fast dynamics. Several methods for determining such globally attracting SIMs have been developed which fall into the class of geometric methods. Such geometric methods include trajectory-based methods, iterative methods and the invariant constrained equilibrium edge pre-image curve (ICE-PIC) method. Davis and Skodje (1999) argue that geometric approaches are more general than other approaches such as ILDM, since motion on a one-dimensional manifold need not conform to a single exponential or a simple rate law except when close to the final equilibrium point.

A full mathematical description of the definition of the invariance of an SIM is given in Chiavazzo et al. (2007). Based on the concept of invariance, it follows that the SIM can be obtained through the simulation of trajectories rather than via the algebraic equations defined for the ILDM above. Hence, locating the invariant manifold can be obtained by simulating the progress of reaction trajectories from suitable initial conditions as they proceed towards equilibrium. Trajectory-based methods for converging to the SIM using a predictor corrector algorithm were

discussed in Davis and Skodje (1999) with application to a hydrogen oxidation mechanism. They demonstrated a higher degree of accuracy of the SIMs obtained in this approach compared to QSSA- or ILDM-based reduction methods.

An alternative approach was also formulated by Fraser and co-workers (Fraser 1988; Roussel and Fraser 1990, 1991a, b, 2001; Fraser and Roussel 1994) who suggested that the slow invariant manifold could be viewed as an attracting fixed point of a functional mapping. Thus, an initial guess for the slow manifold (e.g. based on the QSSA) could be iteratively improved. A method based on functional equation truncation was also developed by Roussel and Tang (2006). Davis and Skodje (1999) modified this method to allow its use for high-dimensional systems. Both the trajectory-based approaches and an updated algorithm based on Fraser's original work were shown in their work to be more accurate than the ILDM and QSSA for the test cases studied. A full discussion of the different approaches is given in Skodje and Davis (2001).

A related approach termed the *method of invariant grids* (MIG) is also discussed in Gorban and Karlin (2003), Gorban et al. (2004a, c), Chiavazzo et al. (2007, 2009) based on the *method of invariant manifold* (MIM). In MIG, a quasi-equilibrium approach is used to define a first approximation to the SIM on a grid in concentration space, and then improved estimations of the SIM are obtained using either Newton iteration or relaxation methods. The MIG was compared to CSP-based methods, the ILDM method and the entropy-based methods in Chiavazzo et al. (2007).

Singh et al. (2002) suggested a method where diffusion is taken into account during the determination of the slow manifold. They called this manifold the infinite-dimensional *approximate slow invariant manifold* (ASIM), and it is an extension of the functional iteration techniques introduced by Roussel and co-workers (Fraser 1988; Roussel and Fraser 1990, 1991a, b, 2001; Fraser and Roussel 1994) discussed above. When applied to reactive flow systems, their method results in an elliptic system of partial differential equations describing motion on the infinite-dimensional ASIM which are obtained by equilibrating the fast dynamics of the closely coupled reaction/convection/diffusion system. They demonstrate the method for a model of ozone decomposition in a premixed laminar flame and observe smaller errors in the simulation of key flame features than when using the purely chemical ILDM. Similar approaches based on finding the ASIM were also developed by Ren and Pope (2005, 2006b, 2007a, b) for reaction−diffusion systems. A full discussion of the differences between the ILDM, the close-parallel assumption and ASIM methods for reaction–diffusion systems is given in Ren and Pope (2007b). The conclusion drawn is that whilst the full ASIM approach gives accurate predictions of the full composition even close to the solution boundaries, it is by far the most computationally expensive of the three approaches. Ren and Pope (2007b) propose some simplifications to the general approach adopted in Singh et al. (2002) in order to improve the efficiency of the method based on the formulation of explicit governing PDEs for the reduced composition (slow variables) rather than the full composition.

7.11.2 The Minimal Entropy Production Trajectory Method

A geometric-based method for the calculation of one-dimensional manifolds based on thermodynamic principles was also developed, namely, the *minimal entropy production trajectory* (MEPT) *method* (Lebiedz 2004). This method can be interpreted as the demand that under the given constraints, all thermodynamic forces and dynamic modes of the system remain maximally relaxed except one, the progress variable, which is parameterised. This is equivalent to finding a trajectory approaching equilibrium for which the squared deviation of the entropy production from zero is minimal for a weighted sum of single reaction step contributions, which is called the MEPT. The approach can be loosely linked with the application of simple reduction rules such as partial equilibrium or quasi-equilibrium assumptions (see Sects. 2.3.2 and 2.3.4) since it can be interpreted as finding the model configuration with as many elementary reaction steps as possible being close to quasi-equilibrium in a chemical sense. Such a model is determined using an optimisation algorithm.

These methods were further extended in Ugarte et al. (2005), Ren et al. (2007) and Reonhardt et al. (2008) to two-dimensional manifolds which are computed as families of MEPTs using a multiple shooting method with a range of initial values. Hence, a discrete grid of initial values of the reaction progress variables is used, and then optimal trajectories (based on the MEPT principle) are calculated which span the two-dimensional manifold. However, Al-Khateeb et al. (2009), who investigated the relationship between thermodynamics and a reactive system's slow invariant manifold, suggest that such a manifold cannot be a good representation of the SIM. In their work they conclude that the MEPT is not attractive along its complete trajectory, and thus does not correspond to the SIM of the system. A mathematical analysis is provided which shows that equilibrium thermodynamic potentials do not alone determine reactive systems' dynamics during their approach towards the physical equilibrium and are not attractive manifolds describing the slow dynamics, even near the equilibrium point. It is worth noting the similarities between the minimal entropy production trajectory (MEPT) method, the RCCE (Sect. 7.10.4) and the entropy production-based skeletal mechanism reduction method (Sect. 7.4).

7.11.3 Calculation of Temporal Concentration Changes Based on the Self-Similarity of the Concentration Curves

Harstad and Bellan (2010a, b) investigated the concentration−time curves obtained during the simulation of the ignition of large alkanes. They found that on plotting the concentration of several species as a function of a selected dominant variable (e.g. the normalised temperature), the resulting curves were similar to each other,

which means that one curve can be transformed to the other by a linear projection. They distinguished local and global self-similarity; the former means that it occurs only in some regions of the (p_0, T_0, φ) space, whilst the latter is valid in the entire investigated space. The concentrations of the large hydrocarbon intermediates were calculated with the similarity equations, whilst those of the small radicals were calculated using the QSSA approximation. This allowed them to create a reduced model in which differential rate equations were solved for only 11 species. This approach was used for formulating reduced models for the ignition of *n*-heptane (Harstad and Bellan 2010b) and various mixtures of *iso*-octane, *n*-heptane and *n*-pentane or *iso*-hexane (Harstad and Bellan 2010a) over a wide range of equivalence ratios, initial pressures and temperatures. The approach was developed further by Kourdis and Bellan (Kourdis and Bellan 2014), who improved the numerical methodology and extended it to further hydrocarbons.

Bellan et al. present the existence of self-similarity as an empirical observation resulting from the inspection of simulation results, and they do not provide a mathematical foundation to the method. Similar concentration curves may be a result of the existence of very different timescales, and the application of QSSA or partial equilibrium may result in linear relations between the concentrations. However, in these articles self-similarity was found among long lifetime ("heavy") species, and therefore, the existence of self-similarity seems to be a consequence of possible lumping relationships within the system variables. Although the self-similarity concept seems to be related to the lumping of species, it is not equivalent to it, since the derived linear functions contain the concentrations of all heavy species and not only a selection of them.

7.12 Tabulation Approaches

In the previous two sections, several methods for model reduction were discussed which in some way exploited the inherent low-dimensional manifolds that are present in kinetic systems. In general, for high-dimensional nonlinear models, such methods have to be applied numerically rather than by solving coupled set of algebraic equations symbolically. Further speed-ups can be gained through the use of storage and retrieval algorithms defining behaviour on the low-dimensional manifolds. Within this class of methods, the simulations are usually carried out in two steps. First, the system of equations is solved over many possible reaction conditions, and the simulation results are stored using an appropriate information storage and retrieval system. When further simulations are carried out at similar conditions, the results can be deduced from the stored outputs.

Meisel and Collins were among the first authors who used this principle and called it the repro-modelling approach. Meisel and Collins suggested that within a large complex model, it is worth identifying very time-consuming subtasks which are used frequently, where the results depend only on the values of a few variables (Meisel and Collins 1973). It is immediately obvious that the presence of

low-dimensional manifolds in a system will lead to this type of behaviour. These subtasks can be solved at many possible values of their variables, and the results are fitted or stored as a function of a reduced number of variables (e.g. the parameterising variables of the slow manifold). The fitted functions/tables can then be used several thousand times during the simulation of the complex model, and solutions are likely to be cheaper to retrieve, compared to the integration of a stiff set of differential equations. Various strategies for storage and retrieval have been developed which will be discussed in this and the following section. We start here with tabulation methods.

7.12.1 The Use of Look-Up Tables

The relationship between the state of a model and the vector of chemical kinetic information can be stored in tables. Such tables are called look-up tables in the simulation of turbulent flames. When the simulation code receives the input vector, it locates points within the table that are close to the input point within a high-dimensional space. The output vector is composed using linear interpolation between the output vector elements at the storage points.

During the creation of look-up tables, several aspects have to be taken into account (Atanga 2012):

1. The information storage structure of the database must be optimised.
2. The CPU time needed to retrieve a stored value must be minimal.
3. The accuracy of the retrieved value has to meet specific criteria.
4. The required memory needed to store all the desired data must be affordable.

However, the search and retrieval algorithms required to access the look-up tables can consume significant amounts of computational time. Special algorithms have been developed to speed up the search and retrieval process (Androulakis 2004). The success of the methods is judged by their ability to give accurate representations of the full kinetic system with the lowest computational calculation and storage requirements. The time investment in generating the equivalent model is also important for some applications, although for models used in repeated design or operational control calculations this may be of lower priority.

Early applications of tabulation methods in turbulent combustion simulations employed tabulations of large regions of the physically realisable composition or thermochemical phase space. As a result, they tended to use highly reduced global mechanisms in order to generate the look-up tables, in order to avoid the dimensionality of the table becoming too large. In early implementations (Taing et al. 1993; Chen et al. 1995), a regular mesh was used to cover the realisable region of the composition space, with the reaction mapping determined by offline integration of a highly reduced model for storage within the look-up table. In such cases the success of the tabulated model is limited by the accuracy of the reduced scheme employed to generate it. Examples include tabulations of a 3-step scheme

describing H_2/CO combustion used in *pdf* calculations of turbulent non-premixed flames in Taing et al. (1993) and the 1- and 2-step schemes describing the chemistry of turbulent hydrogen jet flames in Chen et al. (1995). A similar methodology is the *flow-controlled chemistry tabulation* (FCCT) *method* (Enjalbert et al. 2012). Using this approach, the stored chemistry is based on the simulation results of partially stirred reactors. For the simple reactor simulations, the mixing, the conditions of the chemical reaction and the inflow/outflow were selected according to conditions expected within the turbulent flame to be modelled.

An alternative, and potentially more accurate approach, would be to utilise the concepts embodied in the low-dimensional manifold methods described in Sect. 7.10 to identify a reduced number of variables for which the dynamics must be described. A variety of methods can then be used to generate either tabulations or training data, and a fitted algebraic model can be developed for the minimal number of required variables. The advantage over the use of global mechanisms comprising only a few steps is that full or skeleton chemical mechanisms could potentially be used to generate the fitting data, bypassing the assumptions made in the generation of global schemes. This is achievable since often homogeneous simulations can be carried out using a detailed model, with the input–output relations of only a few key variables used for tabulating the systems dynamics on the slow manifold which is usually of a much lower dimension than the full composition space.

Tabulated chemistry was used in the simulation of cool flames (Colin et al. 2005), which was based on the representation of ignition quantities such as cool flame ignition delay, fuel consumption and reaction rates. The values used in the tables were extracted from complex chemistry calculations for *n*-heptane. The approach was extended to the *variable volume tabulated homogeneous chemistry* (VVTHC) *approach* in Jay and Colin (2011). This approach provides the evolution of major species and radicals from the onset of auto-ignition up to the end of the expansion stroke for compression ignition and spark ignition engine applications. It was first tested for homogeneous engine cases where it compared very well to complex chemistry simulations. It was implemented in a piston engine combustion model and used for the calculation of the burned gases volume variation behind a propagating flame at constant pressure and in reproducing the subsequent composition evolution of kinetic differential equations. For this reason, tabulation approaches are very often utilised within engineering simulations such as, for example, engine piston simulations (Mosbach et al. 2008).

Tabulation was successfully used for the description of the oxidation of *n*-heptane, *iso*-octane, *n*-decane and *n*-dodecane. The agreement was good compared with the results of detailed chemical calculations for all alkanes when only 20 progress variable light species were used (Kourdis and Bellan 2014). Tabulation was applied by Xuan and Blanquart (2014) for the calculation of the concentrations of polycyclic aromatic hydrocarbons (PAHs) in non-premixed flames.

A special utilisation of the tabulation of the final result of a combustion model was incorporated into the *NO relaxation approach* (NORA) *method* in order to predict thermal NO in combustion chambers (Vervisch et al. 2011). In the NORA methodology, the NO reaction rate is written as a linear relaxation towards the

equilibrium value Y_{NO}^{eq} with a characteristic time τ. Both parameters are tabulated as functions of equivalence ratio, pressure, temperature and dilution mass fraction. The table is generated on the basis of spatially homogeneous calculations but later used within turbulent combustion models designed to simulate piston engine applications. The approach has advantages for simulating NO emissions where global kinetic models or tabulations have been used to simulate the turbulent fuel combustion since sometimes radical concentrations may not be available for the post combustion NO_x simulations when using such approaches.

7.12.2 In Situ Tabulation

Early applications of tabulation methods in turbulent combustion simulations employed tabulations of large regions of the physically realisable composition or thermochemical phase space, thus necessitating the use of highly reduced global mechanisms in the generation of the look-up tables. The use of full mechanisms with potentially higher numbers of independent variables was limited in these early applications by the storage requirements of the tabulation. This problem was addressed in later developments of tabulation methods based on in situ tabulation (Pope 1997), where only accessed regions of composition space are tabulated. This allows higher-dimensional starting mechanisms to be used since these accessed regions are substantially smaller than the physically realisable region in most applications due to the presence of low-dimensional manifolds.

The first application of in situ adaptive tabulation (ISAT) was introduced by Pope within a particle *pdf* (probability density function) model for turbulent combustion (Pope 1997). Operator splitting is commonly used in the solution of such systems so that the mixing and reaction terms are solved separately for a given time step Δt (see Sect. 6.8). In practice the time step is chosen to be small in comparison to the mixing timescale. Following the application of operator splitting, it is possible to seek efficient methods for the solution of the purely chemical part of the model equations, i.e. a reduced chemical model. As pointed out by Pope, in a particle *pdf* model of turbulent combustion, solution of the chemical reaction term may be required billions of times, which indicates the need for efficient computational methods. The same issue may also arise in Eulerian grid codes where similar chemical compositions may be found within many grid cells during a full reactive flow simulation (e.g. in atmospheric chemistry models). Both methods suggest that during reactive flow calculations, regions of composition space may be revisited many times, a feature which may be exploited in the development of efficient solution methods.

The basic idea underpinning ISAT is the in situ tabulation of accessed regions of composition space for a particular model application. The tabulation is achieved by integrating the chemical source terms when a region is first accessed and then storing the reaction mapping and sensitivity information in a binary tree data

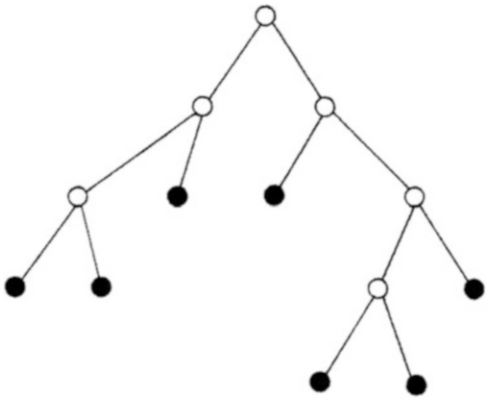

Fig. 7.9 A sketch of a binary tree used within the ISAT approach. At each leaf (*filled circle*), there is a record; at each node (*empty circle*), there is information about the cutting plane. Reprinted from Pope (1997) by permission of Taylor & Francis Ltd, www.tandfonline.com

structure. Subsequent estimations of the reaction mapping terms for points within a small distance of the previously tabulated ones are achieved using multilinear interpolation. Any reaction mapping that cannot be interpolated with sufficient accuracy is generated by direct integration and added to the table. The method therefore achieves the tabulation in situ rather than using offline calculations that were employed within earlier tabulation approaches. It can be linked to the tabulation of low-dimensional manifolds discussed in Sects. 7.10 and 7.11, since in reality it is this manifold that will be accessed during the integration rather than the full composition space. This allows significant reduction of the tabulation effort and facilitates the use of detailed starting mechanisms that were not used within early implementations of tabulation methods (Taing et al. 1993; Chen et al. 1995). Using in situ methods, the accessed region is tabulated rather than the physically realisable region. The presence of low-dimensional manifolds within the chemical system ensures that the accessed region is usually much smaller than the realisable region.

The interpolation error that is incurred for accessed regions between mesh points can be controlled by adaptive refinement of the mesh. The need for mesh refinement is determined by establishing the region of accuracy for the tabulated points within the mesh. This is defined as the connected region containing initial conditions φ^0 consisting of perturbed points φ^q for which the local error in the reaction mapping terms ε does not exceed the specified tolerance ε_{tol}. In the ISAT method, the region of accuracy is assumed to be a hyper-ellipsoid, which is related to the mapping gradient matrix and the concentration sensitivities over the given time step. The ISAT table consists of a binary tree: a set of records (one for each leaf of the tree) and a set of cutting planes (one for each node of the tree) as shown in Fig. 7.9.

Each record consists of the tabulation point (composition), the reaction mapping, the mapping gradient matrix and the specification of an ellipsoid of accuracy within which a linear approximation to the reaction mapping is valid. For each time step during the calculation, a query is made for the given composition, and if the point lies within the *ellipsoid of accuracy* (EOA) of a point within the table, then a linear approximation to the mapping gradient is retrieved. Otherwise a direct integration

of the reaction mapping is made and the actual error measured. If this error is less than the specified tolerance for an already existing point, then the EOA for this point is grown. Otherwise a new point is generated.

The approach was initially tested for methane−air combustion with 14 degrees of freedom in a pairwise-mixing stirred reactor (Pope 1997). In this example the control of local errors controls the global simulation errors well. The speed-up factor of the method increases dramatically with the number of queries made to the chemical source term, with speed-ups of up to 10^3 achieved for a large number of queries. Cannon et al. (1999) compared the use of in situ methods to conventional tabulation techniques for NOx predictions in CO combustion using a 5-step mechanism, showing that the storage requirements using the adaptive methods were up to three orders of magnitude lower than conventional techniques due to the much smaller size covered by the accessed region of composition space.

The ISAT method has been subsequently applied in a range of applications with several additional developments to the methodology. In Yang and Pope (1998), a method based on principal directions (ISATPD) was proposed in order to reduce the dimensionality of the in situ tabulation. This method is based on the fact that, in the principal directions of composition space, the trajectory of the composition point is essentially restricted to a low-dimensional space, even though the original composition dimension may be very high. The data is therefore projected onto principal directions (singular vectors) in order to improve the storage requirements leading to more efficient search and retrieval algorithms. Androulakis (2004) demonstrated the importance of the leading singular vectors for a range of mechanisms, illustrating that the number of leading eigenvectors is much smaller than the full dimensionality of the problems studied. The use of the method by Yang and Pope allowed skeletal mechanisms to be used for the tabulation rather than the global schemes used in earlier applications of tabulation, thus improving the accuracy of the reduced chemical model.

Further developments include the use of ISAT in a range of turbulent combustion simulations. Pope and co-workers (Saxena and Pope 1999; Xu and Pope 2000; Tang et al. 2000) have coupled the ISAT method with Monte Carlo joint *pdf* calculations of turbulent reacting flows using an operator splitting approach, allowing the representation of the finite rate kinetics necessary to capture important features such as local flame extinctions and pollutant formation. Speed-ups of up to a factor of 60 were reported in Saxena and Pope (1999) compared to conventional chemistry calculations. Similar speed-ups were reported by Wang and Fox (2003) in a *pdf* model for predicting reactive precipitation in time-evolving flows and Xie et al. (2004) in a finite volume model of multi-phase fluidised beds. Higher speed-ups (up to 165) have been reported for premixed combustors (James et al. 2001) indicating that the accessed regions of composition space are smaller for premixed flames compared to diffusion flames. A detailed analysis of speed-up factors and possible improvements to the search and retrieval algorithms based on *binary search trees* (BSTs) was given by Chen (2004). The method suggested was based on ensuring that the table entry closest to the inquiry point is retrieved, which potentially increases the number of retrieval operations compared to directly

integrated steps. This is achieved by conducting a reverse traversal of the binary tree structure when a retrieval fails, in order to find a table entry closer to the inquiry. Speed-ups of up to a factor of 5 compared to conventional BSTs were reported.

A detailed error analysis of ISAT was performed in Saxena and Pope (1999) for a pairwise-mixing stirred reactor (PMSR) utilising a reduced 16 species scheme for methane combustion. The analysis showed a straightforward relationship between local interpolation errors and global errors for this case study. Slightly larger relative global errors were incurred for the minor species compared to the major ones. The conclusion of the work was that the global accuracy can be adequately controlled for species of interest by suitably choosing a local error tolerance. Liu and Pope (2005) performed further detailed error analysis of ISAT for turbulent *pdf* calculations of a piloted jet methane/air flame using a skeleton methane mechanism. They discussed various methods for growing EOAs with the standard ellipsoid method giving similar results compared to more conservative methods such as conical growing. They also discussed possible sources of the large local errors that occasionally occur during retrieval, citing non-convex regions of accuracy as the main reason. Again for this example, the global errors are reported to scale linearly with respect to local errors. Improvements in the search strategies and error correction algorithms were also suggested in Lu and Pope (2009).

A range of other applications of ISAT to combustion-related problems exist in the literature. ISAT has also been employed using the Strang operator splitting methods (Strang 1968) for reaction–diffusion systems (Singer and Pope 2004; Singer et al. 2006) and for unsteady reacting flows in one and two dimensions with relevance to potential application in direct numerical simulation (DNS) codes. Masri et al. (2004) incorporated the ISAT technique into the commercial CFD code FLUENT using a hybrid Reynolds-averaged Navier–Stokes (RANS) *pdf* approach with application to flame lift-off. Their work demonstrated the ability of ISAT to represent chemistry with sufficient detail to model auto-ignition phenomena within turbulent jets of H_2/N_2 mixtures into co-flows of hot gas mixtures. Engine simulations using ISAT were performed in Contino et al. (2011). Mazumder (2005) adapted the ISAT technique to heterogeneous surface reactions with application to the catalytic combustion of a methane–hydrogen mixture on platinum using a 19-species reaction mechanism. The heterogeneous part of the problem was different from the solution of gas-phase chemistry since it required the solution of nonlinear algebraic equations instead of a standard initial value problem. In this case the use of operator splitting was prohibited due to the fact that the surface processes were kinetically rather than diffusion limited. Transport and surface chemistry therefore needed to be solved together, leading to coupled nonlinear algebraic relationships. However, since ISAT can generally be used to map input–output relationships, the technique was easily adapted by Mazumder to represent the relationship between input parameters and predicted outputs of the resulting set of coupled nonlinear equations. In this case the inputs were the diffusion velocities and concentrations of the gas-phase species and the wall temperature, and the outputs the wall concentrations of all the species. ISAT was also applied to the

catalytic combustion of methane on a platinum surface in Kumar and Mazumder (2011), this time using an unstructured CFD approach. Cunha and da Silva (2014) also tested the ISAT method, focusing on the issues of accuracy, efficiency and memory usage in the simulation of homogeneous stirred reactor models using the GRI 3.0 methane combustion mechanism. They found that the ISAT implementation had an absolute global error smaller than 1 %, whilst 34 % of the computational time was saved.

More recent applications of ISAT type methods have been coupled to the types of dimension reduction techniques described in previous sections in order to exploit the existence of low-dimensional manifolds in composition space. The use of in situ tabulation then equates to the tabulation of reaction mappings for the reduced variables within accessed regions of the low-dimensional manifold, rather than the tabulation of the whole realisable region of the manifold. To a certain extent, the issue of dimensionality was addressed in the ISATPD method, although in this case the reduced representation was in the singular vector space rather than the original composition or thermochemical space. More recent methods address the adaptive tabulation of low-dimensional manifolds in the original thermochemical space. Tang and Pope (2002) developed a method for the tabulation of rate-controlled constrained equilibrium (RCCE) manifolds as discussed in Sect. 7.10.4. This allowed detailed rather than reduced kinetic schemes to be used for the in situ tabulation, since the table is generated for only a small number of constraints or constraint potentials necessary to describe the chemical system. The method was tested for the comprehensive methane scheme GRIMech 1.2 (32 variables) using 16 constraint potentials, with the results compared against the tabulation of a 17-variable mechanism reduced by conventional techniques including the QSSA. The relative accuracy of the two methods depends on the assumptions made with the conventional mechanism reduction compared to those made in the constrained equilibrium approach, with comparable results achieved in the pairwise-mixing stirred reactor case studied by Tang and Pope.

7.12.3 Controlling Errors and the Invariant Constrained Equilibrium Pre-image Curve (ICE-PIC) Method

An extremely important issue with regard to all tabulation or fitting methods is that the global errors should not grow beyond an acceptable level during a time-dependent simulation. Since most of the methods described in this and the next section are based on controlling the local fitting error, it follows that the relationship between local and global errors is important. In applications which tend towards an equilibrium point, one would expect this relationship to be favourable since reaction trajectories tend to converge, at least within a region of the equilibrium point which may be quite large. The discussion of the ISAT method above indicated that for most applications tested, the global modelling error scaled linearly with the

overall tolerance chosen for the ellipsoid of accuracy. However, for systems exhibiting complex dynamics such as oscillatory or even chaotic behaviour, the relationship between local and global errors may be more complex. Brad et al. (2007) demonstrated that for CO/H_2 combustion in a continuously stirred tank reactor (i.e. an open system), trajectories could diverge substantially over short time intervals during the early stages of ignition, indicating that the local fitting error had to be more tightly controlled within these low-temperature regions in order to control the overall modelling error. It may follow therefore that controlling the local error using the same tolerance in all regions of thermochemical space is not optimal, since in higher-temperature regions where nearby trajectories rapidly converge, larger local errors may be tolerated.

Ensuring mass conservation has been reported to be an important feature of controlling the global error (Tonse et al. 1999; Brad et al. 2007) when using tabulation/fitting methods. In the context of the use of low-dimensional manifolds, this involves modelling not only the key variables but also the other variables (which are usually fast variables) in order to reconstruct the whole composition space. Several methods can be used to generate concentrations of the fast variables. If available, algebraic expressions based on the QSSA can be employed. Where such expressions are highly coupled, then alternative approaches have been suggested based on ILDM tabulations, RCCE and local repro-models. The reconstruction of these species should however be achieved locally within the context of operator splitting, without the need for them to be included in complex flow calculations.

An alternative method for species reconstruction based on pre-image curves was developed by Ren and Pope within the invariant constrained equilibrium edge pre-image curve (ICE-PIC) method (Ren and Pope 2005; Ren et al. 2006; Pope and Ren 2009). This is a trajectory-based method, where a very good approximation to the invariant manifold is determined by computing trajectories of the full system from appropriate initial conditions. The method can be applied to local reconstruction of species on, or close to, the inertial manifold, since the local initial conditions of the trajectories are defined using a pre-image curve. The method is local in nature and therefore may be more computationally efficient than the global methods used to determine SIMs such as those based on trajectory or functional iteration methods (see Sect. 7.11.1). Al-Khateeb et al. (2009), however, compared SIMs with ICE-PIC-generated manifolds for a simple hydrogen–oxygen reactive system, and showed that the ICE-PIC-generated manifold did not contain the SIM over its whole range and that the error of the ICE-PIC manifold grew away from the equilibrium point of the system. Nevertheless, since the ICE-PIC method uses trajectories, it provides a closer approximation to the SIM than RCCE methods.

The pre-image curve provides the initial conditions for trajectory simulations and is not necessarily unique, as initial points from a sizeable region of the pre-image manifold will give rise to reaction trajectories that end up on or very close to the SIM if the manifold is strongly attractive (Ren and Pope 2005). This is illustrated in Fig. 7.10 where many trajectories are seen to end up close to the point A which lies on the SIM. For a given composition of the reduced variables, the

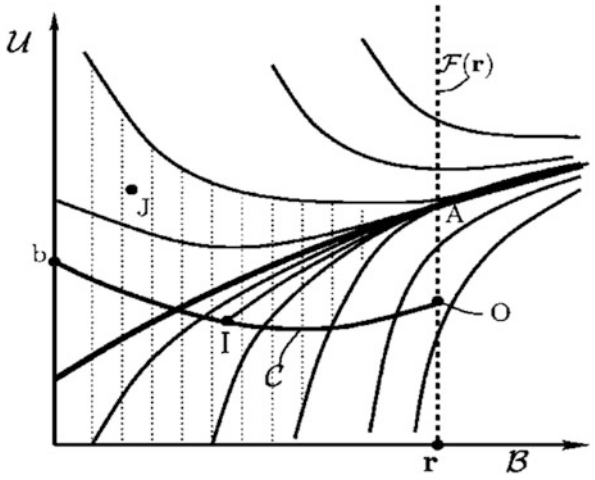

Fig. 7.10 A sketch of the composition space where B indicates the represented subspace (reduced variables ($\mathbf{r}$)) and U, the unrepresented subspace (e.g. fast species, etc.). The dashed line is the feasible region ($F(\mathbf{r})$) corresponding to the reduced composition $\mathbf{r}$, and C is the pre-image curve. The other *curves* are reaction trajectories, which intersect $F(\mathbf{r})$. There is a strongly attracting manifold (*bold line*) so that all trajectories originating in the shaded region intersect $F(\mathbf{r})$ close to the point "A" which lies at the intersection of the SIM and the feasible region. Reproduced from Ren and Pope (2005) with permission from Elsevier

pre-image curve is generated by first finding the corresponding point on the constrained equilibrium manifold, i.e. the feasible composition of maximum entropy (see Sect. 7.10.4). The pre-image curve with the minimum curvature is then calculated, with the initial direction based on the constrained equilibrium manifold, and subject to the requirement that each point on the curve is a pre-image point of the corresponding point on the inertial manifold. Such a curve is illustrated by C in the schematic in Fig. 7.10.

A reaction trajectory from the boundary end of the pre-image curve is then calculated until it reaches the appropriate point (i.e. that with the given reduced variable composition) on or close to the inertial manifold, and the full thermo-chemical state is determined at this point. The method is shown to achieve significantly higher accuracy than the RCCE and ILDM methods for the reconstructed species for a methane ignition problem and a 1D laminar hydrogen−oxygen flame, particularly at lower temperatures (Ren and Pope 2005). The ICE-PIC method was extended to a trajectory-based method in the full composition space in Hiremath and Pope (2013) taking it closer to a global invariant manifold method. Here the reaction mapping involves solving the full system of rate equations for all species in the full composition space which is found to give a more accurate representation of the SIM. The reaction mapping computation is tabulated in this method using the ISAT algorithm.

7.12.4 Flamelet-Generated Manifolds

The above approaches to tabulation, whilst mostly applied in the simulation of combustion problems, have a general foundation that would be relevant to many kinetic systems. However, a special class of tabulation methods has been developed for flame simulations. If a fast exothermic reaction takes place between two components (e.g. a fuel and an oxidiser) of a gaseous system, then flames are observed. In premixed flames the fuel and the oxidiser are premixed before combustion takes place, whilst in non-premixed (diffusion) flames, the fuel and the oxidiser diffuse into each other, and the flame occurs at the boundary or flame front. Premixed and non-premixed flames are two extreme cases, but in many practical flames, continuous states between these two extremes will exist. Flames can be classified as laminar or turbulent according to the characteristics of the flow. Flames are special types of reaction−diffusion systems, characterised by high spatial gradients in temperature and species concentrations, and consequently reaction rates will have a high spatial variability.

Often, for the purposes of simplifying the modelling task, the edge of a turbulent flame is approximated by an ensemble of discrete, steady laminar flames, called flamelets (Libby and Bray 1980; Liew et al. 1981). The individual flamelets are assumed to have a similar structure to laminar flames for the same concentration and temperature conditions so that detailed calculations of the flamelet chemistry can be obtained from lower-dimensional numerical calculations. Laminar opposed-flow diffusion flamelets for non-premixed combustion can then be embedded within a turbulent flame, for example, using statistical *pdf* methods. This approach is adopted in the description of the chemical processes in flames through *flamelet-generated manifolds* (FGM) (van Oijen et al. 2001), also known as *flame-prolongated ILDMs* (FPI) (Gicquel et al. 2000; Pera et al. 2009). In these methods, spatially one-dimensional, premixed and non-premixed flames are first simulated using a detailed reaction mechanism. Counter-flow diffusion flame simulations are often used for this purpose (Verhoeven et al. 2012).

The flamelets are usually computationally cheap to produce, even using detailed mechanisms containing several hundred reaction steps, since they are based on one-dimensional simulations. These simulations can therefore be performed over a wide range of conditions, e.g. using a large number of boundary conditions, pressures and temperatures, so that the simulations cover the expected conditions within the three-dimensional turbulent flames of interest. The results of the calculations are stored in databases, and these empirical manifolds are used for the simulation of two- and three-dimensional flames, when direct simulation would require far more computational time. For the simulation of two- and three-dimensional turbulent flames, the values of only a few variables are usually calculated such as the local enthalpy and conversion. It is then assumed that the local structure of a flame having complex geometry is similar to those of a one-dimensional flame, and the concentrations of the calculated variables are obtained from the database. A number of applications of flamelet-generated

manifolds have been published, and the accuracy of this approximation was investigated over various conditions for modelling the combustion of fuels such as hydrogen, methane (Bilger 1990; Gicquel et al. 2000, 2006; van Oijen and de Goey 2000, 2002; van Oijen et al. 2001; de Goey et al. 2003; Bongers et al. 2005; Fiorina et al. 2005; Godel et al. 2009; Verhoeven et al. 2012), benzene (Xuan and Blanquart 2014) and even diesel oil (Bekdemir et al. 2011). In another approach (Michel et al. 2008, 2009, 2010), flamelet-like libraries were generated based on perfectly stirred reactor (PSR) calculations in terms of auto-ignition delays and steady-state profiles of the progress variable. Lamouroux et al. (2014) stored flamelets using the tabulated chemistry approach. The chemical information is then applied in a turbulent combustion model within the large eddy simulation (LES) framework. The use of in situ flamelet-generated manifolds was suggested in Lodier et al. (2011). A procedure for building converged composition space solutions for premixed flamelets was proposed and tested. This method provides the framework for an efficient in situ calculation of complex chemistry with differential diffusion to be applied to three-dimensional unsteady flame simulations.

7.13 Numerical Reduced Models Based on Fitting

Although sophisticated methods for the storage and retrieval of tabulated data have been developed, there is still a computational overhead in using these techniques. An alternative approach to storage and retrieval is the use of functional representations of the time-dependent kinetic changes or the look-up table contents, using, for example, polynomial functions or artificial neural networks. In such representations, only the coefficients of the functions need be stored rather than the data itself, and hence, the memory requirements and computational costs of evaluating the fitted functions should be lower than for standard tabulation methods. However, the overall accuracy of the operational model will depend on achieving high accuracy of the fits across the model domain. This repro-modelling principle can be used for the development of general algorithms for performing fast kinetic simulations (Turányi 1994, 1995). If a detailed mechanism has been reduced to a skeletal mechanism, its differential (or algebraic-differential) equation can be transformed to a difference equation that can be evaluated very quickly. One disadvantage of these methods is that unlike tabulations, they are not guaranteed to be completely accurate everywhere and should not be extrapolated beyond the conditions under which the functional fits were obtained. They have, however, been successfully applied within repro-modelling approaches for kinetic models, and several of the most widely used methods will therefore be discussed here.

7.13.1 Calculation of Temporal Concentration Changes Using Difference Equations

The characteristic timescale of a system is the time period during which the events occur that are of interest to us. For the simulation of the same physical system, several different timescales can be selected according to the purpose of the modelling. The requirement is that during this period all interesting changes should be completed. A mathematical model of a particular phenomenon should represent the changes to its important features over the characteristic timescale. In the case of kinetics, this may include changes in species concentrations or temperature. Usually these changes are simulated by integrating the kinetic differential equations for the system, but the changes can also be stored and re-accessed.

One possible approach for storing the solution of a kinetic model is according to the following general algorithm:

1. Time step Δt is selected to achieve good resolution of the characteristic timescale of the system.
2. Several thousand, spatially homogeneous simulations are carried out with a series of initial concentrations and/or temperatures, which are typical for the circumstances of applications of the final intended model.
3. The $\mathbf{Y}(t)$, $\mathbf{Y}(t+\Delta t)$ concentration vector pairs are stored in a database.
4. A function $\mathbf{G}$ is fitted to the data and can then be used to predict the change in concentration after time step Δt : $\mathbf{Y}(t+\Delta t) = \mathbf{G}(\mathbf{Y}(t))$.

In spatially homogeneous simulations, the concentration−time curves (with resolution Δt) can be obtained via a recursive evaluation of function $\mathbf{G}$. If operator splitting is used in a reactive flow model (i.e. the solution of the flow and chemistry steps are separated), then this fitted function can be applied instead of typically using implicit integration methods to solve the chemical rate equations. Potentially large savings in computational effort can be achieved.

This method was called the repro-modelling approach in Dunker (1986) and Turányi (1994). The applicability of repro-modelling depends on the determination of function $\mathbf{G}$. This function converts n old concentrations to n new concentrations and thus is an $\Re^n \rightarrow \Re^n$ mapping. However, it may be equally good to develop piecewise fits using n pieces of $\Re^n \rightarrow \Re$ functions. In order to be successful, the fitted function has to give an accurate approximation within the domain of applicability for the final intended model. The selection of the initial simulation conditions is therefore critical, since often, fitted functions may exhibit odd behaviour if utilised outside of the original fitting domain. The function should also be quick to evaluate, and several possibilities exist for suitable functional representations of $\mathbf{G}$ as discussed later.

An early application of this idea was used by Dunker (1986), who applied it to the modelling of tropospheric ozone formation. He started from a lumped mechanism containing 47 species and identified 10 parameterising variables (species concentrations or functions of species concentrations). All in all, 20,736 grid points

were selected in the 10-dimensional space, and the following equation was used to calculate the change of concentrations $\Delta\mathbf{y}$ during each time step Δy:

$$\mathbf{y}(t+\Delta t) = \mathbf{Y}(t+\Delta t) + \sum_{i=1}^{N} \frac{\partial \mathbf{Y}(t+\Delta t)}{\partial y_i^0(t)} \left(y_i^0(t) - Y_i^0(t)\right) + \frac{1}{2}\sum_{i=1}^{N}\sum_{j=1}^{N} \frac{\partial^2 \mathbf{Y}(t+\Delta t)}{\partial y_i^0(t)\ \partial y_j^0(t)} \left(y_i^0(t) - Y_i^0(t)\right)\left(y_j^0(t) - Y_j^0(t)\right) \tag{7.104}$$

where N is the number of parameterising variables, $y_i^0(t)$ is the concentration of the i-th parameterising variable and $Y_i^0(t)$ is the coordinate of the nearest grid point. The constant term of the Taylor expansion was calculated by solving the original kinetic system of ODEs, and the other terms used are the appropriate initial concentration sensitivities [also called Green functions, see Eq. (5.10)]. The use of low-order polynomials in this application led to different sets of polynomials being required for neighbourhoods of different nodes in the computational grid. Nevertheless, using this approach, the ozone concentration−time profiles could be calculated 300 times faster than simulations of the original mechanism.

Using the method outlined above, a repro-model was created (Turányi 1994) from a skeleton model (Turányi et al. 1993a) of the Belousov−Zhabotinsky oscillating reaction. In order to generate the repro-model, the original model was first simulated 200 times using different initial concentrations, and the concentration values were saved in a database after each $\Delta t = 0.1$ s simulation time. In this way 20 thousand ($\mathbf{Y}(t)$, $\mathbf{Y}(t+\Delta t)$) data sets were collected. These data were fitted by a trivariate, up to 8th-order polynomial. A single evaluation of this polynomial shows how the concentration set changes over a $\Delta t = 0.1$ s time step. The sequential calling of the polynomials produces concentration time curves, which are in good accordance with solution of the kinetic system of ODEs (Fig. 7.11). The repro-modelling-based simulation in this case was 50 times faster than the solution of the ODEs.

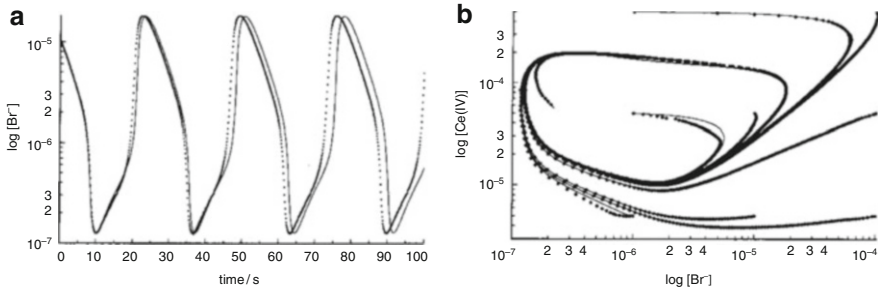

Fig. 7.11 Simulation of a skeletal model of the Belousov–Zhabotinsky reaction based on the solution of the kinetic system of ODEs (*solid line*) and using a repro-model (*dots*). (**a**) Concentration–time curves; (**b**) the solution in phase space. Reprinted from Turányi (1994) with permission from Elsevier

7.13.2 Calculation of Concentration Changes by Assuming the Presence of Slow Manifolds

An alternative to using in situ tabulation as discussed above was to tabulate the systems dynamics on the slow manifold which is usually of a much lower dimension than the full composition space. A related approach is the parameterisation of a tabulated ILDM as discussed in this section or the fitting of dynamics on low-dimensional invariant manifolds using trajectory-generated data, i.e. on an SIM (Lowe and Tomlin 2000a, b; Skodje and Davis 2001; Büki et al. 2002; Brad et al. 2007). Ideally it would be useful to evaluate the minimum number of variables required to accurately describe the dynamics within the manifold a priori, so that different dimensions do not have to be tested. A number of studies of chemical reaction systems have been carried out using timescale analysis along trajectories in order to determine the intrinsic dimension of the slow manifolds (Tomlin et al. 2001; Büki et al. 2002; Zsély et al. 2005; Ren and Pope 2006a; Brad et al. 2007; Davis and Tomlin 2008a, b). A method for the determination of the dimension of the manifold was introduced in Sect. 6.5. This dimension can be surprisingly low (1−3) for models such as those describing the high-temperature combustion of fuels such as hydrogen (Büki et al. 2002; Ren and Pope 2006a), wet carbon monoxide (Brad et al. 2007) and hydrocarbons (Ren and Pope 2006a). The fitted difference equations can therefore be of low dimension.

Yang et al. (2013) discussed the various ways for the determination of manifolds from simulation data; they call the manifolds identified this way the *empirical low-dimensional manifolds* (ELDMs). The simplest ELDM is the plane manifold obtained from the principal component analysis (PCA) (Sutherland and Parente 2009; Parente et al. 2009, 2011; Bilgari and Sutherland 2012; Coussement et al. 2012, 2013; Mirgolbabaei and Echekki 2013, 2014; Mirgolbabaei et al. 2014). A correlation analysis of two-dimensional direct numerical simulation (DNS) data of a turbulent non-premixed H_2/air flame with detailed chemistry was used to find the ELDMs (Maas and Thévenin 1998). Proper orthogonal decomposition (POD) analysis has also been applied to obtain low-dimensional representations of DNS data for H_2/air flames (Frouzakis et al. 2000; Danby and Echekki 2006) and to simplify an atmospheric chemistry mechanism (Sportisse and Djouad 2000). Yang et al. (2013) applied both PCA and multivariate adaptive spline regression (MARS) to DNS databases of a non-premixed CO/H_2 temporally evolving jet flame and of an ethylene lifted jet flame.

In such methods a suitable data set for fitting the low-dimensional surrogate model is generated over a wide range of temperatures, pressures and mixture compositions, by integrating the system of differential equations from a variety of initial conditions chosen to include all behavioural properties of the system. Once the trajectories have settled onto the lower-dimensional manifold, the concentrations are stored and can be fitted using the repro-modelling approach (Turányi 1995; Lowe and Tomlin 2000a, b; Büki et al. 2002). The collected data can also be used to determine the maximum dimension of the slow manifold N_z (see Sect. 6.5).

The recommended algorithm is similar to the previous one:

1. Time step Δt is selected to achieve good resolution of the characteristic time-scale of the system.
2. Several thousand, spatially homogeneous simulations are carried out with a series of initial concentrations and/or temperatures, which are typical for the circumstances of applications of the final intended model.
3. The $\mathbf{Y}(t)$, $\mathbf{Y}(t+\Delta t)$ concentration vector pairs are stored in a database.
4. An analysis of the data (e.g. using methods outlined in Sect. 6.5) leads to the determination of highest dynamical dimension N_Z.
5. Some variables of the model (e.g. concentrations) are selected as the parameterising variables. These variables are denoted as $\alpha_1, \alpha_2, \ldots, \alpha_{N_Z}$.
6. Function $\mathbf{G}_1$ is fitted to the data and can then be used to predict the change in parameterising variables after time step Δt : $\boldsymbol{\alpha}(t+\Delta t) = \mathbf{G}_1(\boldsymbol{\alpha}(t))$.
7. The same set of recorded concentrations is used to obtain fitted function $\mathbf{G}_2$ that relates all concentrations to the parameterising variables: $\mathbf{Y} = \mathbf{G}_2(\boldsymbol{\alpha})$. This $\mathbf{G}_2$ function is similar to function that was introduced at the beginning of Sect. 7.10.

Functions $\mathbf{G}_1$ and $\mathbf{G}_2$ can be any appropriate mathematical function, and a variety of possible choices is discussed below. In spatially homogeneous simulations, the time dependence of the N_Z parameterising variables can be obtained via the sequential calling of function $\mathbf{G}_1$, whilst the values of all variables (concentrations) can be reconstructed using function $\mathbf{G}_2$. In spatially inhomogeneous calculations using operator splitting (see Sect. 6.8), functions $\mathbf{G}_1$ and $\mathbf{G}_2$ are part of the chemical term.

7.13.3 Fitting Polynomials Using Factorial Design

The use of polynomial fits is a possible alternative to the application of tabulations. If the values of the input variable vector are assumed to be independent from each other, then for each variable a minimum $x_i^{\min}$ and maximum $x_i^{\max}$ value can be defined. The $(x_i^{\min}, x_i^{\max})$ sets for all variables define a hyper-rectangle in the space of input variables. This is also called the full factorial design arrangement of the variable values (Box et al. 1978). Frenklach et al. (1992) suggested the creation of fitted second-order polynomials for the construction of surrogate models where the variable vectors used as the independent variables of the fitting were arranged according to a full factorial design. In this way all possible variable value combinations were well represented. This method has been shown to provide reliable and accurate response surfaces. However, its application may become computationally expensive when the number of variables is large. Surrogate models based on factorial design have been and are routinely used in model optimisation studies by Frenklach et al. (Frenklach et al. 2004; Feeley et al. 2004, 2006; Russi et al. 2008, 2010; You et al. 2011, 2012). In the field of model reduction, Marsden

et al. (1987) suggested a similar method for the creation of a repro-model for ozone production in the troposphere using a 15-variate polynomial which was fitted to a series of simulations, arranged according to a factorial design.

7.13.4 Fitting Polynomials Using Taylor Expansions

A kind of cross-over between tabulation and polynomial storage methods is the application of a collection of Taylor expansions. The exact values are tabulated at some fixed points **x** of the input vector, but the values in between the tabulated points are determined not by linear interpolation but according to the following Taylor expansion:

$$Y_i(\mathbf{x}+\Delta\mathbf{x}) = Y_i(\mathbf{x}) + \sum_{j=1}^{m} \frac{\partial Y_i}{\partial x_j}\Delta x_j + \frac{1}{2}\sum_{k=1}^{m}\sum_{j=1}^{m} \frac{\partial^2 Y_i}{\partial x_k \partial x_j}\Delta x_k \Delta x_j + \ldots \qquad (7.105)$$

Here $Y_i(\mathbf{x})$ is the stored exact value, $\Delta\mathbf{x}$ is the deviation of the queried point from the stored point, and $\partial Y_i/\partial x_j$ and $\partial^2 Y_i/\partial x_k \partial x_j$ are the first-order and second-order local sensitivity coefficients, respectively. There are several efficient numerical methods for the calculation of the first-order local sensitivity coefficients (see Sect. 5.2). The second-order local sensitivity coefficients can be calculated from the first-order coefficients using a finite-difference approximation. The Taylor series approximations have the general disadvantage that the accuracy significantly decreases further from the central point.

Davis et al. proposed the application of a Taylor expansion for constructing kinetic response surfaces used in the development and optimisation of reaction kinetic models (Davis et al. 2004). They termed it the sensitivity analysis-based (SAB) method. Tests indicated that for gas-phase combustion models, the response surface obtained with the SAB method was as accurate as the factorial design method previously used in reaction model optimisation, but using the sensitivity coefficients calculated by the combustion simulation codes allowed significant computational savings. This method was used in all later mechanism optimisation studies by Wang et al. and Sheen et al. (Davis et al. 2004; Sheen et al. 2009, 2013; Sheen and Wang 2011a, b).

7.13.5 Orthonormal Polynomial Fitting Methods

The previous two polynomial fitting methods resulted in second-order polynomials. In some applications, however, second-order approximations are not accurate enough, and higher-order polynomials have to be applied. Since general high-order polynomials will have a large number of coefficients, it follows that the

approach becomes feasible only if a large number of these can be set to zero. Methods for the determination of the coefficients of high-order polynomials have to be suitable for fitting a polynomial function to tens of thousands of data points and determining coefficients for the effective variables only, usually using a least-squares-based method. The application of *orthonormal polynomials* (Turányi 1994) can be advantageous for this task, since their coefficients can be determined independently from each other. A method for fitting multivariate orthonormal polynomials for many data points is therefore outlined below.

We first denote $\mathbf{x}^i = (x_1^i, x_2^i, \ldots, x_m^i)$, $i = 1, \ldots, n$ to be a data set and $\varphi_j, j = 1,\ldots,l$ to be a set of $\Re^m \rightarrow \Re$ functions with appropriate weights w_i, $i = 1,\ldots,n$. The scalar product of functions φ_j and φ_k can be interpreted in the following way:

$$\left(\varphi_j, \varphi_k\right) = \sum_{i=1}^{n} w_i \varphi_j\left(\mathbf{x}^i\right) \varphi_k\left(\mathbf{x}^i\right) \tag{7.106}$$

This means that the scalar product is determined not only by functions φ_j and φ_k but also the data set and the values of weights w_i. Functions φ_j and φ_k are orthonormal with respect to scalar product (7.106), if

$$\left(\varphi_j, \varphi_k\right) = \begin{cases} 0 & \text{if } j \neq k \\ 1 & \text{if } j = k \end{cases} \tag{7.107}$$

Any function F: $\Re^m \rightarrow \Re$ can be approximated using the set of orthonormal functions $\varphi_j, j = 1,\ldots,l$ by a Fourier expansion:

$$F \approx \sum_{j=1}^{l} \left(F, \varphi_j\right) \ \varphi_j \tag{7.108}$$

The deviation between function F obtained from the full model and its approximation can be characterised by the error r:

$$r = \left\| F - \sum_{j=1}^{l} \left(F, \varphi_j\right) \ \varphi_j \right\| \tag{7.109}$$

where $\|\|$ denotes the Euclidean norm. This error is also called the root mean square (*r.m.s.*) error. For each $l \leq n$, the approximation in Eq. (7.108) is the best, according to the following relationship

$$r \leq \left\| F - \sum_{j=1}^{l} a_j \varphi_j \right\| \tag{7.110}$$

where coefficients $a_j, j = 1,\ldots,l$ are arbitrary real numbers.

The application of Fourier expansion (7.108) requires orthonormal functions, which can be generated from independent functions using the Gram−Schmidt orthonormalisation process. We denote f_j, $j = 1,\ldots, l$ to be a set of linearly independent functions. Using these functions, orthonormal functions can be generated as follows:

$$\begin{aligned}
\varphi_1 &= c_{11} f_1 \\
\varphi_2 &= c_{21} f_1 + c_{22} f_2 \\
\varphi_3 &= c_{31} f_1 + c_{32} f_2 + c_{33} f_3 \\
&\vdots \\
\varphi_l &= \sum_{j=1}^{l} c_{lj} f_j
\end{aligned} \tag{7.111}$$

Coefficients c are calculated using the equations below according to the Gram−Schmidt process:

$$\begin{aligned}
\varphi_1' &= f_1 && \varphi_1 = \varphi_1' / \left\| \varphi_1' \right\| \\
\varphi_2' &= f_2 - (\varphi_1, f_2)\, \varphi_1 && \varphi_2 = \varphi_2' / \left\| \varphi_2' \right\| \\
&\vdots \\
\varphi_l' &= f_l - \sum_{j=1}^{l-1} (\varphi_j, f_l)\, \varphi_j && \varphi_l = \varphi_l' / \left\| \varphi_l' \right\| \\
c_{11} &= 1 / \left\| \varphi_1' \right\| \\
c_{21} &= -(\varphi_1, f_2)\, c_{11} / \left\| \varphi_2' \right\| \\
c_{22} &= 1 / \left\| \varphi_2' \right\| \\
c_{lk} &= \left[-\sum_{j=1}^{l-1} (\varphi_j, f_l)\, c_{jk} \right] / \left\| \varphi_l' \right\| && k \neq l \\
c_{ll} &= 1 / \left\| \varphi_l' \right\|
\end{aligned} \tag{7.112}$$

A possible set of linearly independent functions are the monomials of a polynomial. For example, the monomials of a trivariate, second-order polynomial are the following: $1, x, y, z, x^2, xy, xz, y^2, zy$ and z^2. The general form of the monomials is given by

$$M_j = \prod_{k=1}^{m} x_k^{\mu_j^k}, \quad \mu_j^k \in \{0, 1, 2, \ldots, l\} \tag{7.113}$$

The order of the monomial is $\sum_{k=1}^{m} \mu_j^k$, whilst the order of the polynomial is equal to the highest-order monomial within the polynomial.

In reaction kinetics simulations, we might wish that the relative accuracy of the fitted concentrations should be equal for both low and high concentrations (e.g. radicals and products). For this reason, a weighting function $w_i = 1/F^2(\mathbf{x}^i)$ is

normally used. The overall aim is to get a good fit using as few monomials as possible. Therefore, each polynomial is generated by initially fitting a constant to the data and calculating the *r.m.s.* error from Eq. (7.109). A new term is then added, an orthonormal polynomial is generated and the new *r.m.s.* error calculated. If the change in *r.m.s.* error is greater than a pre-set tolerance, then this term is accepted, and a new term is tested. In this way, the polynomial is built up with terms of progressively increasing order – from first-order terms in each variable up to typically fourth- or fifth-order terms in combinations of variables. The fitting is stopped when the error becomes lower than a given threshold. This means that the order of the polynomial need not be selected before the fitting process but rather the algorithm automatically finds the smallest order polynomial that fulfils the accuracy requirement.

The final step is the conversion of the appropriate orthonormed polynomial to a "usual" polynomial:

$$F \approx \sum_{j=1}^{l} a_j \varphi_j = \sum_{j=1}^{l} a_j \sum_{h=1}^{j} c_{jh} M_h = \sum_{j=1}^{l} b_j M_j \tag{7.114}$$

where $a_j = (F, \varphi_j)$ and $b_j = \sum_{s=j}^{l} a_s c_{sj}$.

The method above has several advantageous features. It provides the best least-squares fit to the data, and the computational expense increases quadratically with the number of accepted monomials but only linearly with the number of rejected ones.

The evaluation of polynomials is more effective using Horner's rule. For example, the evaluation of polynomial $a\,x^3 + b\,x^2 + c\,x + d$ requires 6 multiplications and 3 additions, whilst the Horner nested polynomial representation $((ax + b)x + c)x + d$ requires only 3 multiplications and 3 additions. When using higher-order polynomials with many variables, even larger efficiency gains can be made using Horner representations. It is therefore worthwhile converting the polynomial formed in equation (7.114) into its equivalent Horner form since this will speed up the evaluation of the expression and hence the information retrieval. Symbolic computer packages (including the Symbolic Math Toolbox of Matlab) are able to convert a polynomial to its Horner representation. A Fortran program was also written (Turányi 1994) that produces the Horner representation of a polynomial as Fortran code from its matrix of coefficients. One possible problem with the Horner representation is that the error caused by the finite representation of real numbers in computers is higher in the Horner form, causing values calculated in this way to be erratic for numerical reasons in some cases. Before using the Horner form, it is therefore important to evaluate whether the two forms of the polynomial provide almost identical values.

Repro-modelling using higher-order polynomial fits has found several applications in complex reactive flow modelling. Clifford et al. (1998) simulated the spread

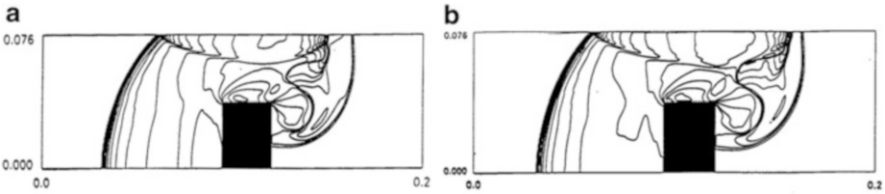

Fig. 7.12 The upper part of the detonation wave travelled further, whilst the lower part reflected back from the obstacle. A part of the wave also reflected back from the ceiling. The density maps were calculated using (**a**) a detailed mechanism including 9 species and (**b**) a repro-model. The latter calculation was one hundred times faster. Reprinted from Clifford et al. (1998) with permission from Elsevier

of a detonation wave at 2.5 Mach in hydrogen−oxygen−argon mixtures, its collision with an obstacle and reflection. The spatially 2D simulations were carried out using either a detailed reaction mechanism or a repro-model. The repro-model consisted of 4th-order polynomials, and its variables were the pressure, temperature and conversion factor β. In spatially homogeneous calculations, application of the repro-model was 1,500 times faster than the simulation of the detailed model. The time-dependent density maps obtained in 2D simulations were almost identical when calculated with a detailed mechanism (Fig. 7.12a) and the repro-model (Fig. 7.12b), but the repro-model-based simulation was 100 times faster. Imbert et al. (2008) calculated the ignition times in detonation waves in a similar way using polynomial approximations over a wide range of conditions.

A similar method was also used for the generation of a repro-model describing the oscillatory ignition of CO–H_2 mixtures in a continuously stirred tank reactor (CSTR) at very low pressures (Brad et al. 2007). Using a 4-variable repro-model based on 6th-order polynomials, successful representation of the regions of steady state, cool flames and large temperature oscillations was achieved based on fits to a 14-variable full model. In this particular example, separate repro-models were developed for different regions of the concentration/temperature space due to the need to control fitting errors to a very high degree of accuracy in some regions. For example, within low-temperature regions at the start of the ignition period, smaller partitioned sets were required in order to achieve local fitting errors as low as 0.1 %. It was found that in such regions, small differences in predicted concentrations could lead to large shifts in the ignition point. However, as a result of achieving low local fitting errors, only small shifts in the phase of the oscillatory trajectories were found when using the repro-model as shown in Fig. 7.13. The application demonstrates, however, that particular care may be required when applying repro-models to ignition applications.

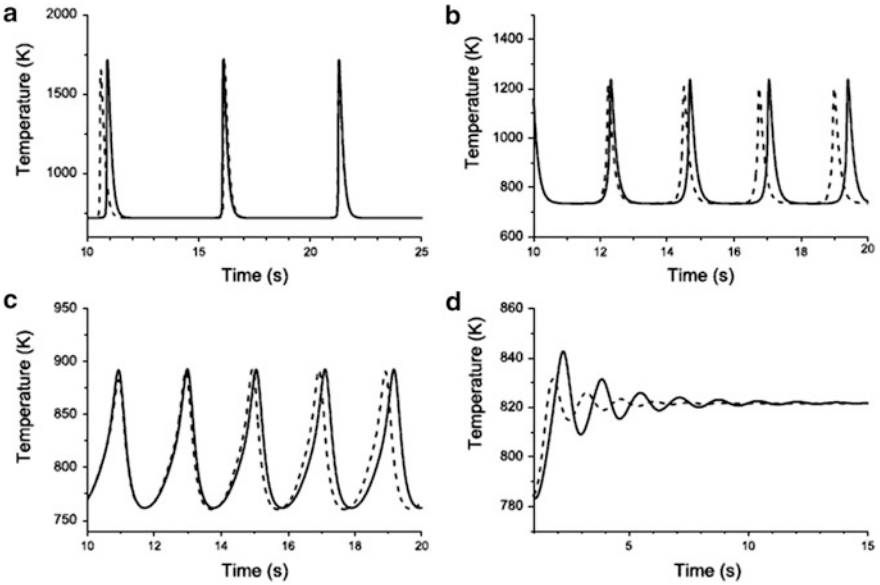

Fig. 7.13 Comparison between model simulations based on ordinary differential equations describing the reduced scheme (*solid*) and fitted polynomial repro-model (*dashed*) for oscillatory ignition of CO–H_2 mixtures at $p = 25$ Torr and 0.5 % H_2 and initial temperatures (**a**) 720 K, (**b**) 735 K, (**c**) 750 K, (**d**) 770 K. Reprinted from Brad et al. (2007) with permission from Elsevier

7.13.6 High-Dimensional Model Representations

The method described in the previous section has several advantages; the fitted function is the best approximation, and most of the coefficients within the high-order polynomial are likely to be zero. However, in high-dimensional nonlinear cases with many variables and the requirement of a high-order approximation, the number of nonzero coefficients can be very large, making the creation and evaluation of multivariate high-order polynomials very expensive. In such cases, rapidly convergent hierarchical correlated function expansions in the input variables, or high-dimensional model representations (HDMR), can be used.

The functional form of the HDMR expansion and its use for global sensitivity analysis was already discussed in Sect. 5.5.5, but a similar approach can also be taken to develop reduced model representations. The purpose is to create a fast equivalent operational model (FEOM) based on the HDMR, giving sufficient accuracy with respect to the full chemical model, but with much lower computational expense. HDMR builds approximations recursively, based on the assumption that high-order-correlated effects of the inputs are expected to have negligible impact on the output. Applications have shown that the order of the correlations between the independent variables dies off rapidly, and therefore, only a few terms are usually required to represent even highly nonlinear input–output relationships.

Tests on several systems including application to a stratospheric chemical model (Shorter et al. 1999) and a tropospheric alkane oxidation model (Wang et al. 2005) indicate that the few lowest-order terms are often sufficient to represent the model in equivalent form to good accuracy. The approach was applied in Li et al. (2008b) to the simulation of ignition within homogeneous H_2/air mixtures over wide ranges of temperatures and pressures ($1{,}000 < T_0 < 1{,}500$ K, $0.1 < P < 100$ atm) and in Gomez and Tchijov (2010) to a 3-dimensional model describing the diffusion and advection of reactive air pollutants.

The application of HDMR tools can therefore dramatically reduce the computational effort needed to represent the input–output relationships of a physical system. One potential advantage of such methods is that only low-order expansion functions or coefficients must be stored, and therefore, for high-dimensional systems, storage requirements may potentially be low compared to standard tabulation and potentially even adaptive tabulation methods. In order to reduce computational effort, the terms in the expansion are usually represented by fitted orthogonal polynomial functions (Li et al. 2002). The successful application of these methods in chemically reactive atmospheric models (Wang et al. 2001) suggests their potential for success within other applications of chemical kinetic modelling. The methods could be coupled with ILDM-based or other methods for the selection of key model variables in order to reduce the number of functional expansions required (Tomlin et al. 2001). Additional information may also be obtained from the terms in the expansion which reveal cooperations between variables and highlight the extent of nonlinearity of the input–output relationships. As with all operational model representations, the success of the HDMR method depends on using a large enough region of the input variable phase space so as to be relevant in the full model. None of these fitting methods should be expected to extrapolate well to new conditions outside of the fitted region.

7.13.7 Artificial Neural Networks

Artificial neural networks (ANNs) are designed to attempt to recreate the way a human brain works by constructing a network of neurons or nodes linked to each other by a series of "synapses". This artificial model of a brain can then be "trained" by presenting it with examples and adjusting the effect the neurons have on each other until the system "recognises" the examples. Through this process, ANNs have been successfully used in image recognition and for modelling systems where governing equations are yet to be developed or require excessive computing power to solve. Therefore, the ANNs should be in principle capable of representing highly nonlinear functions such as those which arise in chemical kinetic systems. A schematic diagram of the architecture of an ANN with 2 input neurons, two hidden layers of 6 neurons each and 3 output neurons is given in Fig. 7.14. The strengths of connections between the different neurons are stored as weights which are determined by an appropriate learning algorithm.

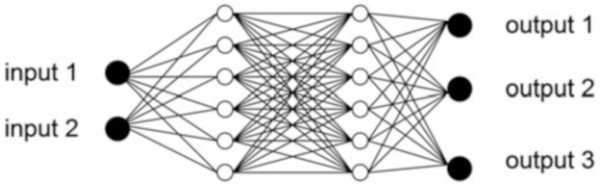

Fig. 7.14 A schematic of the architecture of an ANN with 2 input neurons, two hidden layers of 6 neurons each and 3 output neurons

The approach can be summarised mathematically as

$$y_i^l = f\left(\sum_{j=1}^{K_{l-1}} w_{ij}^l y_j^{l-1} + \varphi_i^l\right) \qquad i = 1, \ldots, K_i, l, \ldots, L \tag{7.115}$$

where y_i^l is the output of the i-th neuron of the l'-th layer, w_{ij}^l is the weight value of connection between the j-th neuron of the (l-1) layer and the i-th neuron of the l'-th layer and φ_i^l is the bias value of the i-th neuron of the l'-th layer (Christo et al. 1995, 1996a, b; Blasco et al. 1999, 2000; Chen et al. 2000; Flemming et al. 2000; Ihme et al. 2008). The nonlinear transfer function f(.) is commonly a sigmoidal or hyperbolic-tangent function. Through presenting input−output examples to the system and adjusting the synaptic weights w_{ij}^l in an appropriate manner, the system can be trained to recognise patterns or replicate complicated functions. The learning algorithm provides the means of adjusting the weights in order to reduce the fitting error of the ANN when compared to the training data. Commonly a back-propagation algorithm is used (Christo et al. 1996a) with a least-squares error function.

A possible disadvantage of using ANNs is the lack of definitive guidelines for optimising important features of the network such as the appropriate number of layers and the number of neurons (elements) in each layer (Christo et al. 1996a). Optimising the network can therefore become effectively an iterative trial-and-error procedure. For example, large numbers of weights are capable of providing a highly accurate fit to training data but can lead to poor results for unseen data (over-fitting), in perhaps an analogous way to using polynomials of too high order. Since the ANNs typically use exponential functions, their evaluation requires more computer time than using polynomials.

Despite these issues, Christo et al. (1996a) successfully applied such an approach based on a multilayer perceptron architecture in the modelling of a velocity–scalar joint *pdf* transport equation for H_2/CO_2 turbulent jet diffusion flames. They highlighted the importance of training data in the development of ANNs and introduced a procedure for the selection of training samples using dynamic randomisation. This approach aimed to reduce the possibility of the network being trapped in a local minimum by presenting a random sample of between 70 % and 80 % of the full training set during each iteration. The algorithm was shown to improve convergence compared with the use of fixed sets of selected training samples. Christo et al. used fits to a three-step global scheme for H_2/CO_2

combustion in their application so that detailed comparisons with the solution of the kinetic equations and the use of look-up tables could be afforded within the turbulent calculation. Later applications combine low-dimensional manifold theory with fitting methods potentially giving greater accuracy for a similar number of variables since prior assumptions have not been made in allowing reduction to a global scheme.

Other examples of the application of ANNs include methane combustion in a zero-dimensional calculation (Blasco et al. 1998) using a four-step global scheme, where additional ANNs for density and temperature were included. Here a second-order scaled-conjugate-gradient method was used instead of a back-propagation algorithm. Again sensitivity to the training set was noted, and particular care was taken to avoid the inclusion of data points close to steady-state regions. A comparison of different ANN architectures was given in this work with either one or two hidden layers with up to 20 neurons in each. The error of the test data set was shown to decrease with the number of hidden neurons up to 20 in two hidden layers for species composition, but above this the error in some cases increased. The explanation given is that the ANN is more likely to get trapped in a local minimum as the error surface becomes more complex with increasing numbers of neurons. Again this demonstrates that care must be taken in the design of the ANN architecture. In this particular case, tabulated chemistry was shown to give a bigger speed-up than the ANN with regard to computational effort to solve the chemical submodel, although at the expense of requiring substantially more memory. Both the ANN and tabulated models provided significant speed-up compared to integration of the full chemical rate equations. The work was further developed in Blasco et al. (1999) where the accuracy of the ANN was improved by fitting separate networks to subdomains of chemical composition space.

Defining optimal subdomains for which to develop the replacement models is a key component of balancing accuracy, and storage and retrieval efficiency. In order to address this problem, Blasco et al. attempted to develop an automatic method for partitioning thermochemical space into optimal domains based on a self-organising map (SOM) approach (Blasco et al. 2000). The SOM performs a mapping between the high-dimensional thermochemical space and a two-dimensional (2D) map whilst attempting to preserve the topology of the original space. The idea is to ensure that points which are close to each other in the original space remain so in the equivalent 2D space. The SOM is then used in the retrieval stage to define which ANN to be used. Three different resolutions of subdomains with 16, 100 and 400 regions were tested, based on each mass fraction and the time step, as opposed to just the mixture fraction tested in previous work. A multilayer perceptron technique was then used to fit ANNs to each subdomain. The use of 100 subdomains with 10 or 20 hidden neurons was shown to give the lowest overall error. The use of subdomains was shown to substantially reduce the error compared to a single ANN across for the whole thermochemical space, as well as the CPU effort required in training the ANNs. This is analogous to the subdomain strategy used in the orthonormal polynomial fitting in Brad et al. (2007) discussed above. The CPU

requirements of retrieval are equivalent for the two approaches suggesting that the use of subdomains is a successful strategy.

The use of ANNs has been coupled with several other available reduction methods. For example, in Chen et al. (2000), ANNs were used to fit the outcome of the ISAT method, the idea being to reduce the storage requirements compared to the usual look-up tables used in ISAT which is based on tabulated data and linear interpolation. The use of nonlinear functions incorporated into the ANN approach therefore facilitates single fits over a wider region than the ellipsoid of accuracy (EOA) used in the original ISAT method. Here, the trade-off is between the fact that the ISAT method contains exact solution values at the tabulated points with potentially small interpolation errors where a small EOA is used, compared to potentially larger fitting errors but much smaller tabulation requirements of ANNs. There is also a potential overhead in selecting the optimal ANN architecture. The CPU requirements of both methods were comparable for the partially stirred reactor example explored in this work (Chen et al. 2000). In general, the optimal method may well depend on the individual application and accuracy and memory requirements.

Shenvi et al. (2004) applied neural networks based on a simple multivariate polynomial architecture. The accuracy and efficiency of these ridge polynomial networks were demonstrated by modelling the kinetics of H_2–Br_2 reaction, formaldehyde oxidation and H_2–O_2 combustion. Choi and Chen (2005) also applied ANNs for the prediction of ignition delay times in homogeneously charged compression ignition (HCCI) engine combustion for a range of fuels including propane and *iso*-octane in a well-mixed reactor. Dyer and Korakianitis (2007) simulated propane−air detonation by representing heat release and species information during the reaction via a mapping methodology. Multilayer feedforward neural networks were used as function approximators to reproduce the parameters extracted from the detailed integrations and to perform the nonlinear interpolations required between reaction points. The mapping method results were accurate to within 1–3 % compared to the results of detailed integrations, and the computational effort was reduced by two orders of magnitude.

Ihme et al. (2009) carried out large eddy simulations of a methane−hydrogen flame by employing two chemistry representation methods, the conventional structured tabulation technique and ANNs. The latter was based on the optimal artificial neural networks (OANNs) approach (Ihme et al. 2008). It was demonstrated that the ANN accuracies were comparable with the use of structured tables. Compared to the tabulation technique, data retrieval from the network was computationally slightly more expensive. Zhou et al. (2013) applied ANNs for both chemical kinetics reduction and source term evaluation in direct numerical simulation (DNS) and large eddy simulation (LES) of reactive flows. The ANNs were trained with 1D disturbed flames. Then, back-propagation ANNs were used for DNS and LES modelling of H_2/air and C_3H_8/air premixed flames with various levels of turbulence. Mirgolbabaei and Echekki (2014) used ANN representation in conjunction with the reduction of the composition space with kernel principal component analysis.

In Chatzopoulos and Rigopoulos (2013), the use of ANNs was combined with the rate-controlled constrained equilibrium (RCCE) approach (see Sect. 7.10.4) in models of two non-premixed and non-piloted $CH_4/H_2/N_2$ turbulent flames. Large computational speed-ups were reported, with reasonable agreement in the simulation of major chemical species with respect to the full integration of the kinetic scheme. Some discrepancies were observed for the minor species, but the work indicates a potential of RCCE–ANN tabulation methodologies for future turbulent combustion computations.

7.13.8 Piecewise Reusable Maps (PRISM)

The functional mappings used to represent the solution of the chemical kinetic differential equations (i.e. the surrogate or repro-model) are usually prepared and fitted prior to the final intended simulations within, for example, complex multidimensional reactive flow codes. Using the ISAT approach described in Sect. 7.12.2, the tabulation is achieved during the simulation, with the advantage that only accessed regions of composition space have to be tabulated. A similar method, but using polynomial fits, is the PRISM (piecewise reusable implementation of solution mapping) approach (Tonse et al. 1999) whereby the fitted polynomial functions are developed during the calculation and then reused when the region of composition space is revisited in subsequent time steps or different spatial regions. PRISM uses second-order polynomials so that in order to cover the realisable region, multiple expressions are used, each valid over a different portion of composition space. This is achieved by partitioning the chemical composition space into predetermined non-overlapping adjacent hypercubes, with edges and corners permitted at regular intervals along the axes allowing for the simple indexing required for efficient searching during reuse. Integration of the full kinetic equations then provides the solution at selected points throughout a hypercube, in order to determine the polynomial coefficients. Factorial design methods are used to reduce the required number of computed points. Not surprisingly Tonse et al. report an increase in accuracy with reduced hypercube size. In common with other methods, however, there is a trade-off between accuracy and the efficiency of polynomial generation as well as storage and retrieval. The largest hypercubes achievable should be used to minimise the computational effort required. Improvements to efficiency were suggested in Tonse et al. (2003) and Brown and Tonse (2004) based on two alternative methods for the a priori identification of hypercubes that will have a high level of reuse. This allows for polynomial construction only for those hypercubes that are revisited enough times to make the construction worthwhile. The PRISM method has demonstrated successful application to hydrogen ignition, a 1D laminar hydrogen flame, a 2D axisymmetric turbulent jet (Tonse et al. 1999, 2003) and a turbulent premixed hydrogen flame (Bell et al. 2000). In a similar way to the other repro-modelling methods, the constructed polynomials could potentially be stored for other calculations as long as the fitted regions of

composition space are common. Lee et al. (2005, 2007) approximated the dynamics on a CSP-derived slow manifold for models describing the ignition of hydrogen–air and heptane–air mixtures using a large number of low-order polynomials, in a similar approach to the PRISM method.

7.14 Adaptive Reduced Mechanisms

In the previous sections we discussed that the size and nature of skeletal or reduced mechanisms derived using automatic reduction methods are likely to be highly dependent on the local concentration and temperature conditions. If a general purpose mechanism is required, then it must be made up of the union of the reduced mechanisms derived for each local condition. On the other hand, the existence of smaller reduced mechanisms for different local conditions could be exploited, leading to the possibility of adaptive reduction.

There are two important issues related to the use of adaptive chemistry methods:

1. *Definition of the range of applicability*. In some cases the range of applicability of the model can be related to a well-known regime of the reaction. For example, in combustion, the preflame region, the flame front and the postflame region have very different characteristics. Also, a homogeneous ignition has different features before, during and after the ignition has taken place. In atmospheric models, different regimes may be associated with different temperature and pressure conditions (e.g. tropospheric vs. stratospheric) or with highly polluted versus remote regions. A reduced model may belong to a given type of reaction regime and can be selected for use at the corresponding interval or region of time or space. A different approach could be to automatically identify the characteristics of the system from the state vector (species concentrations and temperature) and to select the corresponding reduced model accordingly, without resorting to prior definitions of chemically different regimes. This may in fact lead to better selection of appropriate reduced models since assumptions are not made about the important chemistry but rather are determined according to the mathematical principles discussed previously within this chapter.
2. *When are the reduced models created*? One possible approach to the generation of adaptive reduced models is that a series of reduced models are created offline for different domains of applicability. Then during subsequent simulations, at each time step (and/or spatial coordinate), the appropriate domain is identified, and the corresponding reduced model is used. In this case, the domain of applicability for each model needs to be stored. An alternative approach is to create the reduced models "on the fly" during the simulation. In this case the size and the features of the reduced model may continuously change during the simulation. However, there could be a computational overhead in performing the reduction analysis during the simulation.

The application of adaptive chemistry has the advantage that the reduced mechanisms used have to be valid over a narrower range of conditions than a more general reduced scheme. Therefore, they are likely to be much smaller, requiring less simulation time. However, the application of adaptive chemistry may also have disadvantages. If the reduced mechanism is generated "on the fly", then the reduction method has to be fast enough for the required computer time for the reduction *and* the simulation of the reduced model to be less than the simulation of the original model. This method has been termed *dynamic adaptive chemistry* (DAC) (Liang et al. 2009a, b; Shi et al. 2010b; He et al. 2010; Contino et al. 2011; Tosatto et al. 2011; Zhang et al. 2013, 2014; Yang et al. 2013; Ren et al. 2014a, b).

Adaptivity is an inherent feature of some model reduction methods, for example, ISAT and PRISM. However, these methods fall into the category of storage and retrieval algorithms and hence were discussed in Sects. 7.12 and 7.13 above. For skeletal reduced mechanisms (i.e. reduced models which retain a kinetic mechanism structure), adaptive reduction is perhaps less commonly applied, although several recent methodologies have been developed, which will now be discussed. Usually the types of reduction algorithms that are fast enough to be employed on the fly are not the most effective at achieving model reduction compared to more sophisticated methods. Hence, the reduced mechanisms that are obtained may not be optimal. Flux analysis could be used very rapidly (e.g. He et al. (2010)), although the more sophisticated DRG-based methods (see Sect. 7.5.1) have also recently been used in this context (Ren et al. 2014b).

On the other hand, if a "library" of reduced mechanisms is generated in advance, then the computational costs of the mechanism reduction step are less critical, and the quality of the reduced models can be ensured by using an effective reduction methodology. In this case a crucial aspect of using adaptive reduced models is the ability to select the most appropriate model from the reduced model library during a full reactive flow simulation. This involves knowing the region of applicability of each of the reduced models as well as the development of a method to select representative points to perform the reduction analysis. Operational models used in design and control often lead to repeated access to identical regions of composition/temperature space, and hence, for these types of applications, the additional effort required to establish these regions of validity may provide sufficient pay back.

In this context, optimisation-based reduction methods have been extended to provide libraries of reduced models for combustion mechanisms, each with their own region of applicability based on a linear integer programming approach (Oluwole et al. 2006) and a GA-based approach (Banerjee and Ierapetritou 2003) using earlier ideas developed in Schwer et al. (2003). Banerjee and Ierapetritou (2003) describe an approach where the feasible region for a reduced model is defined as the region of phase space over which a specified error constraint is satisfied. The feasible region can be determined by performing simulations of the full and reduced models over a grid in the major species concentrations and temperature, although using this method would be quite expensive. A method for the efficient estimation of the feasible region of a reduced model is therefore

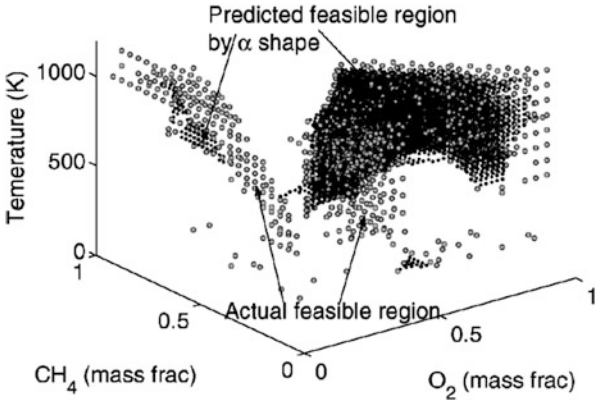

Fig. 7.15 An example of a predicted feasible region of a reduced model based on the GRI-3.0 starting mechanism for methane oxidation. Adapted from Banerjee and Ierapetritou (2006) with permission from Elsevier

required that does not involve large numbers of full versus reduced model comparisons. For the case of methane oxidation, the feasible region was found to be highly non-convex, non-smooth and in some cases disjoint. Banerjee and Ierapetritou developed a GA-based sampling technique which takes advantage of the fact that typically a small section of the entire parameter space is feasible and hence reduces the sampling burden typical of grid-based procedures (Banerjee and Ierapetritou 2006). The method is coupled to a surface reconstruction method in order to map out the entire range of validity of the reduced model. An example of the predicted feasible region for a reduced methane oxidation scheme is shown in Fig. 7.15. To save computational costs, a simplified flow model is generally adopted for the estimation of regions of validity of each reduced model. Banerjee and Ierapetritou use a pairwise-mixing stirred reactor (PMSR) model for the estimation of the feasible region since it is shown to access a considerable portion of the temperature and species composition space realised by the full reactive flow simulation (Banerjee and Ierapetritou 2006). In addition, data clustering techniques are used to identify patterns in the species concentration and temperature data sets, and hence to obtain representative points for the reduction analysis. Depending on the local condition of the PMSR, different reduced models were chosen by the flow simulation as illustrated in Fig. 7.16.

Oluwole et al. (2006) based their approach on the method of Taylor model inclusions. The approach attempts to define the largest hyper-rectangle around the reduction point that is contained in the non-convex region of validity for the reduced model. Taylor model inclusions are used to estimate the upper error bounds for the hyper-rectangle in order to ensure that they are as close to the maximum allowed error as possible, i.e. the hyper-rectangle is a large as possible. Automatic differentiation is used to compute the functions required by the Taylor models symbolically. The method is implemented in the software package RIOT [Range Identification and Optimization Tool (Schuchardt et al. 2005)]. The methods are demonstrated for a methane oxidation model (GRI 3.0) and a truncated propane oxidation scheme, and adaptive use of the model libraries are shown (Oluwole et al. 2006).

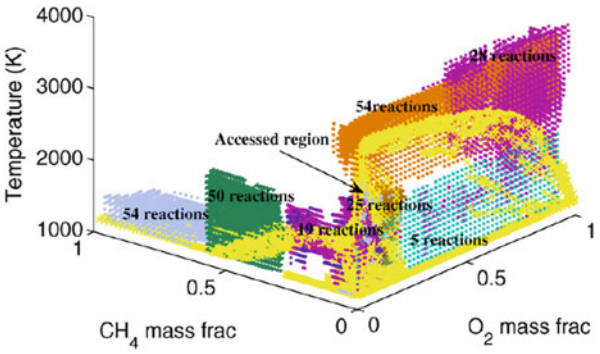

Fig. 7.16 Range of conditions addressed by different reduced methane oxidation models. Reproduced from (Banerjee and Ierapetritou 2006) with permission from Elsevier

Blurock et al. have also published several articles on methods for the identification of appropriate reduced models for given simulation conditions. Cluster analysis was used (Blurock 2004, 2006; Blurock et al. 2010) to determine the different phases of spatially homogeneous processes. Similar time steps were clustered together to form the phases of the process, and the number of phases was also determined by the clustering. He et al. (2008) pre-developed 30 reduced mechanisms for an *n*-pentane oxidation mechanism used for adiabatic plug flow reactor simulations employing a PMSR model. Similarity between flux graphs over a wide range of accessed conditions was evaluated using graph-based techniques, and a hierarchical clustering algorithm was implemented in order to group similar instantaneous flux graphs into clusters. A reduced mechanism was then generated for each cluster, and a search algorithm was defined to assign a new query point to a particular flux graph cluster, thus defining the appropriate reduced mechanism.

Several mechanism reduction approaches have been used to create dynamic adaptive chemistry schemes. Tosatto et al. (2011) used a flux-based DRG method to select reduced chemical mechanisms on a cell-by-cell basis in 2D steady and unsteady flame simulations. The largest problem considered was a JP-8 (Jet Propellant 8) flame, where the full mechanism contained 222 species. The DRGEP approach was used to produce on-the-fly reduced mechanisms for *n*-heptane (Shi et al. 2010b) and gasoline surrogate mixtures (Liang et al. 2009b; Shi et al. 2010a). Gou et al. (2013) used the PFA method for a similar purpose. Løvås et al. (Rigopoulos and Løvås 2009; Løvås et al. 2011) applied the LOI method in an adaptive way. Sportisse and Djouad (2007) used proper orthogonal decomposition (POD) analysis by dividing the composition space into subdomains and then applying different representations in the different subdomains.

Ren et al. (2014b) used dynamic adaptive chemistry (DAC) with operator splitting schemes to solve the equations governing reactive flows. Locally valid skeletal mechanisms were generated using the DRG reduction method to eliminate unimportant species and reactions from the full mechanism. The authors investigated one-dimensional, unsteady, freely propagating, premixed methane/air laminar flames with detailed chemical kinetics and realistic transport. They showed that the number of retained species was significant only near the flame front region, and speed-up factors of three to five were found. Contino et al. (2011) demonstrated the

coupling of in situ adaptive tabulation and dynamic adaptive chemistry for engine simulations. Dynamic adaptive chemistry-based models were successfully used in general turbulent reactive flow simulations (Yang et al. 2013; Ren et al. 2014a).

Lu et al. (2009) identified QSS-species and pre-equilibrium reactions on the fly, based on the investigation of system timescales. This information was used to convert the original system of differential equations to a less stiff system of differential algebraic equations. This dynamic stiffness removal method for accelerating simulations was successfully applied for predictions using an *n*-heptane oxidation mechanism in 1D and 2D turbulent direct numerical simulations.

Oluwole et al. (2012) developed a new variant of adaptive chemistry called *exact-steady-state adaptive chemistry* (ESAC). This method is applicable for fast reduced model simulations of steady-state problems. Smaller (less accurate, but faster) reduced models are used when the simulation is far from the steady state, whilst more accurate (larger and slower) models are used as the simulation approaches the final steady-state solution. The simulation is completed by applying the full kinetic model for the calculation of the steady-state solution. ESAC simulations were found to be a factor of 3–4 times faster than the equivalent full-model-everywhere simulations. Such techniques could be valuable, for example, in obtaining solutions for 2D or 3D computational fluid dynamics simulations of steady problems which are often slow to converge when using highly detailed chemistry. Oluwole et al. (2012) demonstrated application of the method for 2D steady methane and ethylene flames.

So far, the use of adaptive reduced models has mainly focused on reaction removal leading to, at best, linear reductions in computational time (Harris et al. 2000). In this case the same set of ODEs are solved at each time step, and the computational savings are made due to the lower number of operations necessary to perform Jacobian evaluations when a large number of the reaction terms have been removed. Further challenges are presented for species removal since the number of species may change in each reduced model region. In an operator splitting environment (see Sect. 6.8), where the flow and chemistry steps are solved separately, a simple solution is to consider all the species of the detailed mechanism in the flow step and only those species present in the selected reduced model in the chemistry step, with the concentration of all the other species unaltered. Banerjee and Ierapetritou (2003) successfully used this approach for a methane oxidation mechanism where up to 12 reduced models are accessed during the model simulations with the number of chemically active species varying between 6 and 29.

References

Ahmed, S.S., Mauß, F., Moréacz, G., Zeuch, T.: A comprehensive and compact n-heptane oxidation model derived using chemical lumping. PCCP **9**, 1107–1126 (2007)

Al-Khateeb, A.N., Powers, J.M., Paolucci, S., Sommese, A.J., Diller, J.A., Hauenstein, J.D., Mengers, J.D.: One-dimensional slow invariant manifolds for spatially homogenous reactive systems. J. Chem. Phys. **131**, 024118 (2009)

An, J., Jiang, Y.: Differences between direct relation graph and error-propagation-based reduction methods for large hydrocarbons. Procedia Eng. **62**, 342–349 (2013)
Anderson, J., Chang, Y.-C., Papachristodoulou, A.: Model decomposition and reduction tools for large-scale networks in systems biology. Automatica **47**, 1165–1174 (2011)
Androulakis, I.P.: Kinetic mechanism reduction based on an integer programming approach. AIChE J. **46**, 361–371 (2000)
Androulakis, I.P.: "Store and retrieve" representations of dynamic systems motivated by studies in gas phase chemical kinetics. Comput. Chem. Eng. **28**, 2141–2155 (2004)
Androulakis, I.P., Grenda, J.M., Bozzelli, J.W.: Time-integrated pointers for enabling the analysis of detailed reaction mechanisms. AIChE J. **50**, 2956–2970 (2004)
Apri, M., de Gee, M., Molenaar, J.: Complexity reduction preserving dynamical behavior of biochemical networks. J. Theor. Biol. **304**, 16–26 (2012)
Apri, M., de Gee, M., van Mourik, S., Molenaar, J.: Identifying optimal models to represent biochemical systems. PLoS One **9**, e83664 (2014)
Aris, R.: Reactions in continous mixtures. AIChE J. **35**, 539–548 (1989)
Aris, R., Gavalas, G.R.: On the theory of reactions in continuous mixtures. Philos. Trans. R. Soc. **A260**, 351–393 (1966)
Astarita, G.: Lumping nonlinear kinetics: apparent overall order of reaction. AIChE J. **35**, 529–532 (1989)
Astarita, G., Nigam, A.: Lumping nonlinear kinetics in a CSTR. AIChE J. **35**, 1927–1932 (1989)
Astarita, G., Ocone, R.: Lumping nonlinear kinetics. AIChE J. **34**, 1299–1309 (1986)
Astarita, G., Ocone, R.: Chemical reaction engineering of complex mixtures. Chem. Eng. Sci. **47**, 2135–2147 (1992)
Astarita, G., Sandler, S.I. (eds.): Kinetic and Thermodynamic Lumping of Multicomponent Mixtures. Elsevier, Amsterdam (1991)
Atanga, G.F.: Direct numerical simulation of turbulent flames on parallel computers. Ph.D. thesis, Otto-von-Guericke-Universitat (2012)
Austin, J.: On the explicit versus family solution of the fully diurnal photochemical equations of the stratosphere. J. Geophys. Res. Atmos. **96**(D7), 12941–12974 (1991)
Bahlouli, K., Atikol, U., Saray, R.K., Mohammadi, V.: A reduced mechanism for predicting the ignition timing of a fuel blend of natural-gas and *n*-heptane in HCCI engine. Energy Convers. Manage. **79**, 85–96 (2014)
Bailey, J.E.: Lumping analysis of reactions in continuous mixtures. Chem. Eng. J. **3**, 52–71 (1972)
Banerjee, I., Ierapetritou, M.G.: Development of an adaptive chemistry model considering micromixing effects. Chem. Eng. Sci. **58**, 4537–4555 (2003)
Banerjee, I., Ierapetritou, M.G.: An adaptive reduction scheme to model reactive flow. Combust. Flame **144**, 619–633 (2006)
Battin-Leclerc, F., Glaude, P.A., Warth, V., Fournet, R., Scacchi, G., Côme, G.M.: Computer tools for modelling the chemical phenomena related to combustion. Chem. Eng. Sci. **55**, 2883–2893 (2000)
Becker, T., Weispfenning, V.: Gröbner Bases (A Computational Approach to Communicative Algebra). Springer, New York (1993)
Bekdemir, C., Somers, L.M.T., de Goey, L.P.H.: Modeling diesel engine combustion using pressure dependent Flamelet generated manifolds. Proc. Combust. Inst. **33**, 2887–2894 (2011)
Bell, J.B., Brown, N.J., Day, M.S., Frenklach, M., Grcar, J.F., Propp, R.M., Tonse, S.R., Wagner, A.: Scaling and efficiency of PRISM in adaptive simulations of turbulent premixed flames. Proc. Combust. Inst. **28**, 107–113 (2000)
Benson, S.W.: The induction period in chain reactions. J. Chem. Phys. **20**, 1605–1612 (1952)
Beretta, G.P., Keck, J.C., Janbozorgi, M., Metghalchi, H.: The rate-controlled constrained-equilibrium approach to far-from-local-equilibrium thermodynamics. Entropy **14**, 92–130 (2012)
Bhattacharjee, B., Schwer, D.A., Barton, P.I., Green, W.H.: Optimally-reduced kinetic models: reaction elimination in large-scale kinetic mechanisms. Combust. Flame **135**, 191–208 (2003)

Bilgari, A., Sutherland, J.C.: A filter-independent model identification technique for turbulent combustion modeling. Combust. Flame **159**, 1960–1970 (2012)
Bilger, R.W.: On reduced mechanisms for methane-air combustion in non-premixed flames. Combust. Flame **80**, 135–149 (1990)
Blasco, J.A., Fueyo, N., Dopazo, C., Ballester, J.: Modelling the temporal evolution of a reduced combustion chemical system with an artificial neural network. Combust. Flame **113**, 38–52 (1998)
Blasco, J.A., Fueyo, N., Larroya, J.C., Dopazo, C., Chen, Y.J.: A single-step time-integrator of a methane–air chemical system using artificial neural networks. Comput. Chem. Eng. **23**, 1127–1133 (1999)
Blasco, J.A., Fueyo, N., Dopazo, C., Chen, J.-Y.: A self-organizing-map approach to chemistry representation in combustion applications. Combust. Theory Model. **4**, 61–76 (2000)
Blasenbrey, T., Maas, U.: ILDMs of higher hydrocarbons and the hierarchy of chemical kinetics. Proc. Combust. Inst. **28**, 1623–1630 (2000)
Blasenbrey, T.: Entwicklung und Implementierung automatisch reduzierter Reaktionsmechanismen für die Verbrennung von Kohlenwasserstoffen. Ph.D. thesis, Stuttgart University (2000)
Blouza, A., Coquel, F., Hamel, F.: Reduction of linear kinetic systems with multiple scales. Combust. Theory Model. **4**, 339–362 (2000)
Blurock, E.S.: Characterizing complex reaction mechanisms using machine learning clustering techniques. Int. J. Chem. Kinet. **36**, 107–118 (2004)
Blurock, E.S.: Automatic characterization of ignition processes with machine learning clustering techniques. Int. J. Chem. Kinet. **38**, 621–633 (2006)
Blurock, E.S., Tuner, M., Mauss, F.: Phase optimized skeletal mechanisms for engine simulations. Combust. Theory Model. **14**, 295–313 (2010)
Bodenstein, M.: Eine Theorie der photochemischen Reaktionsgeschwindigkeiten. Z. Phys. Chem. **85**, 329–397 (1913)
Bodenstein, M., Lutkemeyer, H.: Die photochemische Bildung von Bromwasserstoff und die Bildungsgeschwindigkeit der Brommolekel—aus den Atomen. Z. Phys. Chem. **114**, 208–236 (1924)
Bogaevski, V.N., Povzner, A.: Algebraic Method in Nonlinear Perturbation Theory. Springer, New York (1991)
Bongers, H., Van Oijen, J.A., De Goey, L.P.H.: Intrinsic low-dimensional manifold method extended with diffusion. Proc. Combust. Inst. **29**, 1371–1378 (2002)
Bongers, H., van Oijen, J.A., de Goey, L.P.H.: The Flamelet generated manifold method applied to steady planar partially premixed counterflow flames. Combust. Sci. Technol. **177**, 2373–2393 (2005)
Börger, I., Merkel, A., Lachmann, J., Spangenberg, H.-J., Turányi, T.: An extended kinetic model and its reduction by sensitivity analysis for the methanol/oxygen gas-phase thermolysis. Acta Chim. Hung. **129**, 855–864 (1992)
Borghans, J.A.M., De Boer, R.J., Segel, L.A.: Extending the quasi-steady state approximation by changing variables. Bull. Math. Biol. **58**, 43–63 (1996)
Boulier, F., Lefranc, M., Lemaire, F., Morant, P.-E.: Model reduction of chemical reaction systems using elimination. Math. Comput. Sci. **5**, 289 (2011)
Bounaceur, R., Warth, V., Glaude, P.A., Battin-Leclerc, F., Scacchi, G., Come, G.M., Faravelli, T., Ranzi, E.: Chemical lumping of mechanisms generated by computer—Application to the modeling of normal-butane oxidation. J. Chim. Phys. Phys. Chim. Biol. **93**, 1472–1491 (1996)
Box, G.E.P., Hunter, W.G., Hunter, J.S.: Statistics for Experiments. An Introduction to Design, Data Analysis, and Model Building. Wiley, New York (1978)
Brad, R.B., Tomlin, A.S., Fairweather, M., Griffiths, J.F.: The application of chemical reduction methods to a combustion system exhibiting complex dynamics. Proc. Combust. Inst. **31**, 455–463 (2007)
Briggs, G.E., Haldane, J.B.S.: A note on the kinetics of enzyme action. Biochem. J. **19**, 339–339 (1925)

Brochot, C., Tóth, J., Bois, F.Y.: Lumping in pharmacokinetics. J. Pharmacokinet. Pharmacodyn. **32**, 719–736 (2005)

Brown, N.J., Tonse, S.R.: PRISM Piecewise reusable implementation of solution mapping to improve computational economy. Abstr. Pap. Am. Chem. Soc. **228**, U308–U308 (2004)

Büki, A., Perger, T., Turányi, T., Maas, U.: Repro-modelling based generation of intrinsic low-dimensional manifolds. J. Math. Chem. **31**, 345–362 (2002)

Bykov, V., Gol'dshtein, V.: Fast and slow invariant manifolds in chemical kinetics. Comput. Math. Appl. **65**, 1502–1515 (2013)

Bykov, V., Maas, U.: The extension of the ILDM concept to reaction-diffusion manifolds. Combust. Theory Model. **11**, 839–862 (2007a)

Bykov, V., Maas, U.: Extension of the ILDM method to the domain of slow chemistry. Proc. Combust. Inst. **31**, 465–472 (2007b)

Bykov, V., Maas, U.: Investigation of the hierarchical structure of kinetic models in ignition problems. Z. Phys. Chem. **223**, 461–479 (2009a)

Bykov, V., Maas, U.: Problem adapted reduced models based on reaction-diffusion manifolds (REDIMs). Proc. Combust. Inst. **32**, 561–568 (2009b)

Bykov, V., Goldfarb, I., Gol'dshtein, V., Sazhin, S., Sazhina, E.: System decomposition technique for spray modelling in CFD codes. Comput. Fluids **36**, 601–610 (2007)

Bykov, V., Griffiths, J.F., Piazzesi, R., Sazhin, S.S., Sazhina, E.M.: The application of the global quasi-linearisation technique to the analysis of the cyclohexane/air mixture autoignition. Appl. Math. Comput. **219**, 7338–7347 (2013)

Cannon, S.M., Brewster, B.S., Smoot, L.D.: PDF modeling of lean premixed combustion using in situ tabulated chemistry. Combust. Flame **119**, 233–252 (1999)

Carslaw, N., Jacobs, P.J., Pilling, M.J.: Modeling OH, HO_2, and RO_2 radicals in the marine boundary layer 2. Mechanism reduction and uncertainty analysis. J. Geophys. Res. D **104**, 30257–30273 (1999)

Chapman, D.L., Underhill, L.K.: The interaction of chlorine and hydrogen. The influence of mass. J. Chem. Soc. Trans. **103**, 496–508 (1913)

Chatzopoulos, A.K., Rigopoulos, S.: A chemistry tabulation approach via rate-controlled constrained equilibrium (RCCE) and artificial neural networks (ANNs), with application to turbulent non-premixed $CH_4/H_2/N_2$ flames. Proc. Combust. Inst. **34**, 1465–1473 (2013)

Chen, J.Y.: A general procedure for constructing reduced reaction-mechanisms with given independent relations. Combust. Sci. Technol. **57**, 89–94 (1988)

Chen, J.Y.: Analysis of in situ adaptive tabulation performance for combustion chemistry and improvement with a modified search algorithm. Combust. Sci. Technol. **176**, 1153–1169 (2004)

Chen, J.Y., Tham, Y.F.: Speedy solution of quasi-steady-state species by combination of fixed-point iteration and matrix inversion. Combust. Flame **153**, 634–646 (2008)

Chen, J.Y., Chang, W.C., Koszykowski, M.: Numerical simulation and scaling of NOx emissions from turbulent hydrogen jet flames with various amounts of helium dilution. Combust. Sci. Technol. **111**, 505–529 (1995)

Chen, J.Y., Blasco, J.A., Fueyo, N., Dopazo, C.: An economical strategy for storage of chemical kinetics: fitting in situ adaptive tabulation with artificial neural networks. Proc. Combust. Inst. **28**, 115–121 (2000)

Chiavazzo, E., Gorban, A.N., Karlin, I.V.: Comparison of invariant manifolds for model reduction in chemical kinetics. Commun. Comput. Phys. **2**, 964–992 (2007)

Chiavazzo, E., Karlin, I.V., Frouzakis, C.E., Boulouchos, K.: Method of invariant grid for model reduction of hydrogen combustion. Proc. Combust. Inst. **32**, 519–526 (2009)

Choi, Y., Chen, J.Y.: Fast prediction of start-of-cornbustion in HCCI with combined artificial neural networks and ignition delay model. Proc. Combust. Inst. **30**, 2711–2718 (2005)

Chou, M.Y., Ho, T.C.: Continuum theory for lumping nonlinear reactions. AIChE J. **34**, 1519–1527 (1988)

Christo, F.C., Masri, A.R., Nebot, E.M., Turányi, T.: Utilising artificial neural network and repro-modelling in turbulent combustion. Proc. IEEE Int. Conf. Neural Netw. **1**, 911–916 (1995)
Christo, F.C., Masri, A.R., Nebot, E.M.: Artificial neural network implementation of chemistry with *pdf* Simulation of H_2/CO_2 flames. Combust. Flame **106**, 406–427 (1996a)
Christo, F.C., Masri, A.R., Nebot, E.M., Pope, S.B.: An integrated PDF/neural network approach for simulating turbulent reacting systems. Proc. Combust. Inst. **26**, 43–48 (1996b)
Chu, Y., Serpas, M., Hahn, J.: State-preserving nonlinear model reduction procedure. Chem. Eng. Sci. **66**, 3907–3913 (2011)
Cicarelli, P., Astarita, G., Gallifuoco, A.: Continuous kinetic lumping of catalytic cracking processes. AIChE J. **38**, 1038–1044 (1992)
Ciliberto, A., Capuani, F., Tyson, J.J.: Modeling networks of coupled enzymatic reactions using the total quasi-steady state approximation. PLoS Comput. Biol. **3**, e45 (2007)
Clifford, L.J., Milne, A.M., Turányi, T., Boulton, D.: An induction parameter model for shock-induced hydrogen combustion simulations. Combust. Flame **113**, 106–118 (1998)
Colin, O., Pires da Cruz, A., Jay, S.: Detailed chemistry-based auto-ignition model including low temperature phenomena applied to 3-D engine calculations. Proc. Combust. Inst. **30**, 2649–2656 (2005)
Contino, F., Jeanmart, H., Lucchini, T., D'Errico, G.: Coupling of in situ adaptive tabulation and dynamic adaptive chemistry: an effective method for solving combustion in engine simulations. Proc. Combust. Inst. **33**, 3057–3064 (2011)
Coussement, A., Gicquel, O., Parente, A.: Kernel density weighted principal component analysis of combustion processes. Combust. Flame **159**, 2844–2855 (2012)
Coussement, A., Gicquel, O., Parente, A.: MG-local-PCA method for reduced order combustion modeling. Proc. Combust. Inst. **34**, 1117–1123 (2013)
Crutzen, P.J.: Ozone production rates in an oxygen–hydrogen–nitrogen oxide atmosphere. J. Geophys. Res. **76**, 7311–7327 (1971)
Cunha Jr., A., da Silva, L.F.F.: Assessment of a transient homogeneous reactor through in situ adaptive tabulation. J Braz. Soc. Mech. Sci. Eng. **36**, 377–391 (2014)
Danby, S.J., Echekki, T.: Proper orthogonal decomposition analysis of autoignition simulation data of nonhomogeneous hydrogen-air mixtures. Combust. Flame **144**, 126–138 (2006)
Dano, S., Madsen, M.F., Schmidt, H., Cedersund, G.: Reduction of a biochemical model with preservation of its basic dynamic properties. FEBS J. **273**, 4862–4877 (2006)
Davis, M.J., Skodje, R.T.: Geometric investigation of low-dimensional manifolds in systems approaching equilibrium. J. Chem. Phys. **111**, 859–874 (1999)
Davis, M.J., Tomlin, A.S.: Spatial dynamics of steady flames 1. Phase space structure and the dynamics of individual trajectories. J. Phys. Chem. A **112**, 7768–7783 (2008a)
Davis, M.J., Tomlin, A.S.: Spatial dynamics of steady flames 2. Low-dimensional manifolds and the role of transport processes. J. Phys. Chem. A **112**, 7784–7805 (2008b)
Davis, S.G., Mhadeshwar, A.B., Vlachos, D.G., Wang, H.: A new approach to response surface development for detailed gas-phase and surface reaction kinetic model optimization. Int. J. Chem. Kinet. **36**, 94–106 (2004)
de Goey, L.P.H., van Oijen, J.A., Bongers, H., Groot, G.R.A.: New flamelet based reduction methods: the bridge between chemical reduction techniques and flamelet methods. In: Proceedings of ECM (2003)
Djouad, R., Sportisse, B.: Partitioning techniques for reduction in chemical kinetics. APLA: an Automatic Partitioning and Lumping Algorithm. Appl. Numeric. Math. **43**, 383–398 (2002)
Djouad, R., Sportisse, B., Audiffren, N.: Reduction of multiphase atmospheric chemistry. J. Atm. Chem. **46**, 131–157 (2003)
Dokoumetzidis, A., Aarons, L.: A method for robust model order reduction in pharmacokinetics. J. Pharmacokinet. Pharmacodyn. **36**, 613–628 (2009a)
Dokoumetzidis, A., Aarons, L.: Proper lumping in systems biology models. IET Syst. Biol. **3**, 40–51 (2009b)

Douglass, A.R., Kawa, S.R.: Contrast between 1992 and 1997 high-latitude spring halogen occultation experiment observations of lower stratospheric HCl. J. Geophys. Res. Atmos. **104**(D15), 18739–18754 (1999)

Dunker, A.M.: The reduction and parameterization of chemical mechanisms for inclusion in atmospheric reaction-transport models. Atmos. Environ. **20**, 479–486 (1986)

Dyer, R.S., Korakianitis, T.: Pre-integrated response map for inviscid propane-air detonation. Combust. Sci. Technol. **179**, 1327–1347 (2007)

Edelson, D.: On the solution of differential equations arising in chemical kinetics. J. Comput. Phys. **11**, 455–457 (1973)

Edwards, K., Edgar, T.F., Manousiouthakis, V.I.: Kinetic model reduction using genetic algorithms. Comput. Chem. Eng. **22**, 239–246 (1998)

Edwards, K., Edgar, T.F., Manousiouthakis, V.I.: Reaction mechanism simplification using mixed-integer nonlinear programming. Comput. Chem. Eng. **24**, 67–79 (2000)

Eggels, R.L.G.M., de Goey, L.P.H.: Mathematically reduced reaction mechanisms applied to adiabatic flat hydrogen/air flames. Combust. Flame **100**, 559–570 (1995)

Elliott, S., Turco, R.P., Jacobson, M.Z.: Tests on combined projection forward differencing integration for stiff photochemical family systems at long-time step. Comput. Chem. **17**, 91–102 (1993)

Elliott, S., Shen, M., Kao, C.Y.J., Turco, R.P., Jacobson, M.Z.: A streamlined family photochemistry module reproduces major nonlinearities in the global tropospheric ozone system. Comput. Chem. **20**, 235–259 (1996)

Elliott, L., Ingham, D.B., Kyne, A.G., Mera, N.S., Pourkashanian, M., Wilson, C.W.: Genetic algorithms for optimisation of chemical kinetics reaction mechanisms. Prog. Energy Combust. Sci. **30**, 297–328 (2004)

Elliott, L., Ingham, D.B., Kyne, A.G., Mera, N.S., Pourkashanian, M., Wilson, C.W.: Reaction mechanism reduction and optimization using genetic algorithms. Ind. Eng. Chem. Res. **44**, 658–667 (2005)

Elliott, L., Ingham, D.B., Kyne, A.G., Merab, N.S., Pourkashanian, M., Whittaker, S.: Reaction mechanism reduction and optimisation for modelling aviation fuel oxidation using standard and hybrid genetic algorithms. Comput. Chem. Eng. **30**, 889–900 (2006)

Enjalbert, N., Domingo, P., Vervisch, L.: Mixing time-history effects in large Eddy simulation of non-premixed turbulent flames: flow-controlled chemistry tabulation. Combust. Flame **159**, 336–352 (2012)

Farkas, G.: Kinetic lumping schemes. Chem. Eng. Sci. **54**, 3909–3915 (1999)

Farrow, L.A., Edelson, D.: Steady-state approximation—Fact or fiction? Int. J. Chem. Kinet. **6**, 787–800 (1974)

Feeley, R., Seiler, P., Packard, A., Frenklach, M.: Consistency of a reaction dataset. J. Phys. Chem. A **108**, 9573–9583 (2004)

Feeley, R., Frenklach, M., Onsum, M., Russi, T., Arkin, A., Packard, A.: Model discrimination using data collaboration. J. Phys. Chem. A **110**, 6803–6813 (2006)

Fiorina, B., Gicquel, O., Vervisch, L., Carpentier, S., Darabiha, N.: Approximating the chemical structure of partially premixed and diffusion counterflow flames using FPI flamelet tabulation. Combust. Flame **140**, 147–160 (2005)

Fischer, M., Riedel, U.: Combustion chemistry and parameter estimation. In: Bock, H.G., Carraro, T., Jäger, W., Körkel, S., Rannacher, R., Schlöder, J.P. (eds.) Model Based Parameter Estimation. Theory and Applications, vol. 4, pp. 207–226. Springer, Berlin (2013)

Fish, D.J.: The automatic generation of reduced mechanisms for tropospheric chemistry modelling. Atmos. Environ. **34**, 1563–1574 (2000)

Flach, E.H., Schnell, S.: Use and abuse of the quasi-steady-state approximation. IEE Proc. Syst. Biol. **153**, 187–191 (2006)

Flemming, F., Sadiki, A., Janicka, J.: LES using artificial neural networks for chemistry representation. Prog. Comput. Fluid Dynamics **5**, 375–385 (2000)

Fournet, R., Warth, V., Glaude, P.A., Battin-Leclerc, F., Scacchi, G., Côme, G.M.: Automatic reduction of detailed mechanisms of combustion of alkanes by chemical lumping. Int. J. Chem. Kinet. **32**, 36–51 (2000)

Frank-Kamenetskii, D.A.: Условия примениности метода Боденштейна в химической кинетике (Conditions for the applicability of the Bodenstein method in chemical kinetics) Ж. Физ. Хим. **14**, 695–700 (1940)

Fraser, S.J.: The steady state and equilibrium approximations: a geometrical picture. J. Chem. Phys. **88**, 4732–4738 (1988)

Fraser, S.J., Roussel, M.R.: Phase-plane geometries in enzyme-kinetics. Canadian Journal of Chemistry-Revue Canadienne De Chimie **72**, 800–812 (1994)

Frenklach, M.: Computer modeling of infinite reaction sequences—a chemical lumping. Chem. Eng. Sci. **40**, 1843–1849 (1985)

Frenklach, M.: Reduction of chemical reaction models. In: Oran, E.S., Boris, J.P. (eds.) Numerical Approaches to Combustion Modeling, pp. 129–154. American Institute of Aeronautics and Astronautics, Inc., Washington, DC (1991)

Frenklach, M., Harris, S.J.: Aerosol dynamics modeling using the method of moments. J. Colloid Interface Sci. **118**, 252–261 (1987)

Frenklach, M., Kailasanath, K., Oran, E.S.: Systematic development of reduced mechanisms for dynamic modeling. Prog. Astronaut. Aeronautics **105**, 365–376 (1986)

Frenklach, M., Wang, H., Rabinowitz, M.J.: Optimization and analysis of large chemical kinetic mechanisms using the solution mapping method—combustion of methane. Prog. Energy Combust. Sci. **18**, 47–73 (1992)

Frenklach, M., Packard, A., Seiler, P., Feeley, R.: Collaborative data processing in developing predictive models of complex reaction systems. Int. J. Chem. Kinet. **36**, 57–66 (2004)

Frouzakis, C.E., Boulouchos, K.: Analysis and reduction of the CH_4-air mechanism at lean conditions. Combust. Sci. Technol. **159**, 281–303 (2000)

Frouzakis, C.E., Kevrekidis, Y.G., Lee, J., Boulouchos, K., Alonso, A.A.: Proper orthogonal decomposition of direct numerical simulation data: data reduction and observer construction. Proc. Combus. Inst. **28**, 75–81 (2000)

García-Ybarra, P.L., Treviño, C.: Asymptotic analysis of the boundary layer H_2 ignition by a hot flat plate with thermal diffusion. Combust. Flame **96**, 293–303 (1994)

Gear, C.W.: The automatic integration of ordinary differential equations. Numer. Mathematics **14**, 176–190 (1971)

Gear, C.W., Petzold, L.R.: ODE methods for the solution of differential algebraic systems. SIAM J. Numer. Anal. **21**, 716–728 (1984)

Georgakis, C., Aris, R.: Diffusion, reaction and the pseudo-steady-state hypothesis. Math. Biochem **25**, 237–258 (1975)

Gery, M.W., Whitten, G.Z., Killus, J.P., Dodge, M.C.: A photochemical kinetics mechanism for urban and regional scale computer modeling. J. Geophys. Res. **D94**, 12925–12956 (1989)

Gicquel, O., Thévenien, D., Hilka, M., Darabiha, N.: Direct numerical simulation of turbulent premixed flames using intrinsic low-dimensional manifolds. Combust. Theory Model. **3**, 479–502 (1999)

Gicquel, O., Darabiha, N., Thevenin, D.: Laminar premixed hydrogen/air counterflow flame simulations using flame prolongation of ILDM with differential diffusion. Proc. Combust. Inst. **28**, 1901–1908 (2000)

Gicquel, O., Ribert, O., Darabiha, N., Veynante, D.: Tabulation of complex chemistry based on self-similar behavior of laminar premixed flames. Combust. Flame **146**, 649–664 (2006)

Godel, G., Domingo, P., Vervisch, L.: Tabulation of NOx chemistry for Large-Eddy simulation of non-premixed turbulent flames. Proc. Combust. Inst. **32**, 1555–1561 (2009)

Gokulakrishnan, P., Lawrence, A.D., McLellan, P.J., Grandmaison, E.W.: A functional-PCA approach for analyzing and reducing complex chemical mechanisms. Comput. Chem. Eng. **30**, 1093–1101 (2006)

Gokulakrishnan, P., Joklik, R., Viehe, D., Trettel, A., Gonzalez-Juez, E., Klassen, M.: Optimization of reduced kinetic models for reactive flow simulations. J. Eng. Gas Turbines Power **136**, 011503 (2013)

Golub, G.H., Van Loan, C.F.: Matrix Computations, 2nd edn. John Hopkins, Baltimore (1983)

Gomez, M.C., Tchijov, V.: The FEOM technique applied to a three-dimensional model of diffusion/advection of pollutants. Environ. Model. Software **25**, 602–606 (2010)

Gorban, A.N., Karlin, I.V.: Method of invariant manifold for chemical kinetics. Chem. Eng. Sci. **58**, 4751–4768 (2003)

Gorban, A., Karlin, I., Zinovyev, A.: Invariant grids: method of complexity reduction in reaction networks. ComPlexUs **2**, 110–127 (2004a)

Gorban, A.N., Karlin, I.V., Zinovyev, A.Y.: Constructive methods of invariant manifolds for kinetic problems. Phys. Rep. **396**, 197–403 (2004b)

Gorban, A.N., Karlin, I.V., Zinovyev, A.Y.: Invariant grids for reaction kinetics. Physica A **333**, 106–154 (2004c)

Gou, X., Chen, Z., Sun, W., Ju, Y.: A dynamic adaptive chemistry scheme with error control for combustion modeling with a large detailed mechanism. Combust. Flame **160**, 225–231 (2013)

Goussis, D.A.: Quasi steady state and partial equilibrium approximations: their relation and their validity. Combust. Theory Model. **16**, 869–926 (2012)

Goussis, D.A., Lam, S.H.: A study of homogeneous methanol oxidation kinetics using CSP. Proc. Combust. Inst. **24**, 113–120 (1992)

Goussis, D.A., Maas, U.: Model reduction for combustion chemistry. In: Echekki, T., Mastorakos, E. (eds.) Turbulent Combustion Modeling, pp. 193–220. Springer, New York (2011)

Goussis, D.A., Najm, H.N.: Model reduction and physical understanding of slowly oscillating processes: the circadian cycle. SIAM Multiscale Model. Simul. **5**, 1297–1332 (2006)

Goussis, D.A., Skevis, G.: Nitrogen chemistry controlling steps in methane-air premixed flames. In: Bathe, K.J. (ed.) Computational Fluid and Solid Mechanics, pp. 650–653. Elsevier, Amsterdam (2005)

Goussis, D.A., Valorani, M.: An efficient iterative algorithm for the approximation of the fast and slow dynamics of stiff systems. J. Comput. Phys. **214**, 316–346 (2006)

Granata, S., Faravelli, T., Ranzi, E.: A wide range kinetic modeling study of the pyrolysis and combustion of naphthenes. Combust. Flame **132**, 533–544 (2003)

Griffiths, J.F.: Reduced kinetic-models and their application to practical combustion systems. Prog. Energy Combust. Sci. **21**, 25–107 (1995)

Hannemann-Tamás, R., Gábor, A., Szederkényi, G., Hangos, K.M.: Model complexity reduction of chemical reaction networks using mixed-integer quadratic programming. Comput. Math. Appl. **65**, 1575–1595 (2014)

Harris, S.D., Elliott, L., Ingham, D.B., Pourkashanian, M., Wilson, C.W.: The optimisation of reaction rate parameters for chemical kinetic modelling of combustion using genetic algorithms. Comput. Methods Appl. Mech. Eng. **190**, 1065–1090 (2000)

Harstad, K., Bellan, J.: A model of reduced oxidation kinetics using constituents and species: *Iso*-octane and its mixtures with *n*-pentane, *iso*-hexane and *n*-heptane. Combust. Flame **157**, 2184–2197 (2010a)

Harstad, K.G., Bellan, J.: A model of reduced kinetics for alkane oxidation using constituents and species: proof of concept for *n*-heptane. Combust. Flame **157**, 1594–1609 (2010b)

He, K., Ierapetritou, M.G., Androulakis, I.P.: A graph-based approach to developing adaptive representations of complex reaction mechanisms. Combust. Flame **155**, 585–604 (2008)

He, K., Androulakis, I.P., Ierapetritou, M.G.: On-the-fly reduction of kinetic mechanisms using element flux analysis. Chem. Eng. Sci. **65**, 1173–1184 (2010)

Heard, A.C., Pilling, M.J., Tomlin, A.S.: Mechanism reduction techniques applied to tropospheric chemistry. Atmos. Environ. **32**, 1059–1073 (1998)

Heineken, F.G., Tsuchiya, H.M., Aris, R.: On the mathematical status of the pseudo-steady-state hypothesis of biochemical kinetics. Math. Biosci. **1**, 95–113 (1967)

Hernández, J.J., Ballesteros, R., Sanz-Argent, J.: Reduction of kinetic mechanisms for fuel oxidation through genetic algorithms. Math. Comput. Model. **52**, 1185–1193 (2010)

Hiremath, V., Pope, S.B.: A study of the rate-controlled constrained-equilibrium dimension reduction method and its different implementations. Combust. Theory Model. **17**, 260–293 (2013)

Hiremath, V., Ren, Z.Y., Pope, S.B.: A greedy algorithm for species selection in dimension reduction of combustion chemistry. Combust. Theory Model. **14**, 619–652 (2010)

Hiremath, V., Ren, Z.Y., Pope, S.B.: Combined dimension reduction and tabulation strategy using ISAT-RCCE-GALI for the efficient implementation of combustion chemistry. Combust. Flame **158**, 2113–2127 (2011)

Ho, T.C., Aris, R.: On apparent second-order kinetics. AIChE J. **33**, 1050–1051 (1987)

Hoops, S., Sahle, S., Gauges, R., Lee, C., Pahle, J., Simus, N., Singhal, M., Xu, L., Mendes, P., Kummer, U.: COPASI—a COmplex PAthway SImulator. Bioinformatics **22**, 3067–3074 (2006)

Hu, D., Braun-Unkhoff, M., Frank, P.: Modeling study on soot formation at high pressures. Combust. Sci. Technol. **149**, 79–94 (1999)

Huang, H., Fairweather, M., Griffiths, J.F., Tomlin, A.S., Brad, R.B.: A systematic lumping approach for the reduction of comprehensive kinetic models. Proc. Combust. Inst. **30**, 1309–1316 (2005)

Hughes, K.J., Fairweather, M., Griffiths, J.F., Porter, R., Tomlin, A.S.: The application of the QSSA via reaction lumping for the reduction of complex hydrocarbon oxidation mechanisms. Proc. Combust. Inst. **32**, 543–551 (2009)

Ihme, M., Marsden, A.L., Pitsch, H.: Generation of optimal artificial neural networks using a pattern search algorithm: application to approximation of chemical systems. Neural Comput. **20**, 573–601 (2008)

Ihme, M., Schmitt, C., Pitsch, H.: Optimal artificial neural networks and tabulation methods for chemistry representation in LES of a bluff-body swirl-stabilized flame. Proc. Combust. Inst. **32**, 1527–1535 (2009)

Imbert, B., Lafosse, F., Catoire, L., Paillard, C.-É., Khasainov, B.: Formulation reproducing the ignition delays simulated by a detailed mechanism: application to *n*-heptane combustion. Combust. Flame **155**, 380–408 (2008)

Ingber, L., Rosen, B.: Genetic algorithms and very fast simulated re-annealing—a comparison. Math. Comput. Model. **16**, 87–100 (1992)

Ishmurzin, A., Schramm, B., Lebiedz, D., Warnatz, J.: Reduction of detailed reaction mechanisms for large hydrocarbons combustion by the ILDM method. In: Proceedings of ECM (2003)

Ismail, H.M., Ng, H.K., Gan, S., Lucchini, T., Angelo Onorati, A.: Development of a reduced biodiesel combustion kinetics mechanism for CFD modelling of a light-duty diesel engine. Fuel **106**, 388–400 (2013)

Jacobson, M.Z.: Fundamentals of Atmospheric Modeling, 2nd edn. Cambridge University Press, Cambridge (2005)

James, S., Anand, M.S., Razdan, M.K., Pope, S.B.: In situ detailed chemistry calculations in combustor flow analyses. J. Eng. Gas. Turbines Power-Trans. ASME **123**, 747–756 (2001)

Jay, S., Colin, O.: A variable volume approach of tabulated detailed chemistry and its applications to multidimensional engine simulations. Proc. Combust. Inst. **33**, 3065–3072 (2011)

Jay, L.O., Sandu, A., Potra, F.A., Carmichael, G.R.: Improved quasi-steady-state-approximation methods for atmospheric chemistry integration. SIAM J. Sci. Comput. **18**, 182–202 (1997)

Jenkin, M.E., Watson, L.A., Utembe, S.R., Shallcross, D.E.: A Common Representative Intermediates (CRI) mechanism for VOC degradation. Part 1: Gas phase mechanism development. Atmos. Environ. **42**, 7185–7195 (2008)

Jiang, Y., Qiu, R.: Reduction of large kinetic mechanisms of hydrocarbon fuels with directed relation graph. Acta Physico-Chimica Sinica **25**, 1019–1025 (2009)

Jones, W.P., Rigopoulos, S.: Rate-controlled constrained equilibrium: formulation and application to nonpremixed laminar flames. Combust. Flame **142**, 223–234 (2005a)
Jones, W.P., Rigopoulos, S.: Reduction of comprehensive chemistry via constraint potentials. Proc. Combust. Inst. **30**, 1325–1331 (2005b)
Jones, W.P., Rigopoulos, S.: Reduced chemistry for hydrogen and methanol premixed flames via RCCE. Combust. Theory Model. **11**, 755–780 (2007)
Kalachev, L.V., Field, R.J.: Reduction of a model describing ozone oscillations in the troposphere: example of an algorithmic approach to model reduction in atmospheric chemistry. J. Atm. Chem. **39**, 65–93 (2001)
Katare, S., Bhan, A., Caruthers, J.M., Delgass, W.N., Venkatasubramanian, V.: A hybrid genetic algorithm for efficient parameter estimation of large kinetic models. Comput. Chem. Eng. **28**, 2569–2581 (2004)
Kazakov, A., Frenklach, M.: Dynamic modeling of soot particle coagulation and aggregation: implementation with the method of moments and application to high-pressure laminar premixed flames. Combust. Flame **114**, 484–501 (1998)
Keck, J.C.: Rate-controlled constrained-equilibrium theory of chemical-reactions in complex-systems. Prog. Energy Combust. Sci. **16**, 125–154 (1990)
Keck, J.C., Gillespie, D.: Rate-controlled partial-equilibrium method for treating reacting gas-mixtures. Combust. Flame **17**, 237–248 (1971)
Kelley, A.P., Liu, W., Xin, Y.X., Smallbone, A.J., Law, C.K.: Laminar flame speeds, non-premixed stagnation ignition, and reduced mechanisms in the oxidation of *iso*-octane. Proc. Combust. Inst. **33**, 501–508 (2011)
KINALC: CHEMKIN based program for KInetic aNALysis. http://garfield.chem.elte.hu/Combustion/kinalc.htm.
Kirchner, F.: The chemical mechanism generation programme CHEMATA–Part 1: The programme and first applications. Atmos. Environ. **39**, 1143–1159 (2005)
Kirkpatrick, S.: Optimization by simulated annealing. Science **220**, 671–681 (1983)
Klonowski, W.: Simplifying principles for chemical and enzyme reaction kinetics. Biophys. Chem. **18**, 73–87 (1983)
König, K., Maas, U.: On-demand generation of reduced mechanisms based on hierarchically extended intrinsic low-dimensional manifolds in generalized coordinates. Proc. Combust. Inst. **32**, 553–560 (2009)
Kooshkbaghi, M., Frouzakis, C.E., Boulouchos, K., Karlin, I.V.: Entropy production analysis for mechanism reduction. Combust. Flame **161**, 1507–1515 (2014)
Kourdis, P.D., Bellan, J.: Heavy-alkane oxidation kinetic-mechanism reduction using dominant dynamic variables, self similarity and chemistry tabulation. Combust. Flame **161**, 1196–1223 (2014)
Kourdis, P.D., Goussis, D.A.: Glycolysis in saccharomyces cerevisiae: algorithmic exploration of robustness and origin of oscillations. Math. Biosci. **243**, 190–214 (2013)
Kumar, A., Mazumder, S.: Adaptation and application of the in situ Adaptive Tabulation (ISAT) procedure to reacting flow calculations with complex surface chemistry. Comput. Chem. Eng. **35**, 1317–1327 (2011)
Lamouroux, J., Ihme, M., Fiorina, B., Gicquel, O.: Tabulated chemistry approach for diluted combustion regimes with internal recirculation and heat losses. Combust. Flame **161**, 2120–2136 (2014)
Law, C.K.: Combustion at a crossroads: status and prospects. Proc. Combust Inst. **31**, 1–29 (2007)
Law, C.K., Sung, C.J., Wang, H., Lu, T.F.: Development of comprehensive detailed and reduced reaction mechanisms for combustion modeling. AIAA J. **41**, 1629–1646 (2003)
Laxminarasimhan, C.S., Verma, R.P., Ramachandran, P.A.: Continuous lumping model for simulation of hydrocracking. AIChE J. **42**, 2645–2653 (1996)
Lebiedz, D.: Computing minimal entropy production trajectories: an approach to model reduction in chemical kinetics. J. Chem. Phys. **120**, 6890–6897 (2004)

Lee, J.C., Najm, H.N., Lefantzi, S., Ray, J., Frenklach, M., Valorani, M., Goussis, D.: On chain branching and its role in homogeneous ignition and premixed flame propagation. In: Bathe, K. (ed.) Computational Fluid and Solid Mechanics, pp. 717–720. Elsevier, Amsterdam (2005)
Lee, J.C., Najm, H.N., Lefantzi, S., Ray, J., Frenklach, M., Valorani, M., Goussis, D.: A CSP and tabulation-based adaptive chemistry model. Combust. Theory Model. **11**, 73–102 (2007)
Li, B., Li, B.: Quasi-steady-state laws in reversible model of enzyme kinetics. J. Math. Chem. **51**, 2668–2686 (2013)
Li, G., Rabitz, H.: A general analysis of exact lumping in chemical kinetics. Chem. Eng. Sci. **44**, 1413–1430 (1989)
Li, G., Rabitz, H.: Determination of constrained lumping schemes for nonisothermal first-order reaction systems. Chem. Eng. Sci. **46**, 583–596 (1991)
Li, G.Y., Rabitz, H.: A lumped model for H_2/O_2 oxidation in the oscillatory regime. J. Chem. Phys. **102**, 7006–7016 (1995)
Li, G., Rabitz, H.: A special singular perturbation methods for kinetic model reduction: with application to an H_2/O_2 oxidation model. J. Chem. Phys. **105**, 4065–4075 (1996a)
Li, G.Y., Rabitz, H.: Combined symbolic and numerical approach to constrained nonlinear lumping - With application to an H_2/O_2 oxidation model. Chem. Eng. Sci. **51**, 4801–4816 (1996b)
Li, G., Rabitz, H.: Reduced kinetic equations of a CO/H_2/air oxidation model by a special perturbation method. Chem. Eng. Sci. **52**, 4317–4327 (1997)
Li, G., Tomlin, A.S., Rabitz, H., Tóth, J.: Determination of approximate lumping schemes by a singular perturbation method. J. Chem. Phys. **99**, 3562–3574 (1993)
Li, G., Rabitz, H., Tóth, J.: A general analysis of exact nonlinear lumping in chemical kinetics. Chem. Eng. Sci. **49**, 343–361 (1994a)
Li, G., Tomlin, A.S., Rabitz, H., Tóth, J.: A general analysis of approximate nonlinear lumping in chemical kinetics. I. Unconstrained lumping. J. Chem. Phys. **101**, 1172–1187 (1994b)
Li, G., Tomlin, A.S., Rabitz, H., Tóth, J.: A general analysis of approximate nonlinear lumping in chemical kinetics. II. Constrained lumping. J. Chem. Phys. **101**, 1188–1201 (1994c)
Li, G., Wang, S.-W., Rabitz, H.: Practical approaches to construct RS-HDMR component functions. J. Phys. Chem. A **106**, 8721–8733 (2002)
Li, B., Shen, Y., Li, B.: Quasi-steady state laws in enzyme kinetics. J. Phys. Chem. A **112**, 2311–2321 (2008a)
Li, G.Y., Rabitz, H., Hu, J.S., Chen, Z., Ju, Y.: Regularized random-sampling high dimensional model representation (RS-HDMR). J. Math. Chem. **43**, 1207–1232 (2008b)
Liang, L., Stevens, J.G., Farrell, J.T.: A dynamic adaptive chemistry scheme for reactive flow computations. Proc. Combust. Inst. **32**, 527–534 (2009a)
Liang, L., Stevens, J.G., Raman, S., Farrell, J.T.: The use of dynamic adaptive chemistry in combustion simulation of gasoline surrogate fuels. Combust. Flame **156**, 1493–1502 (2009b)
Liao, J.C., Lightfoot, E.N.: Lumping analysis of biochemical reaction systems with time scale separation. Biotechnol. Bioeng. **31**, 869–879 (1988)
Libby, P.A., Bray, K.N.C.: Implications of the laminar flamelet model in premixed turbulent combustion. Combust. Flame **39**, 33–41 (1980)
Liew, S.K., Bray, K.N.C., Moss, J.B.: A flamelet model of turbulent non-premixed combustion. Combust. Sci. Technol. **27**, 69–73 (1981)
Liu, B.J.D., Pope, S.B.: The performance of in situ adaptive tabulation in computations of turbulent flames. Combust. Theory Model. **9**, 549–568 (2005)
Liu, G., Swihart, M.T., Neelamegham, S.: Sensitivity, principal component and flux analysis applied to signal transduction: the case of epidermal growth factor mediated signaling. Bioinformatics **21**, 1194–1202 (2005)
Lodier, G., Vervisch, L., Moureau, V., Domingo, P.: Composition-space premixed flamelet solution with differential diffusion for in situ flamelet-generated manifolds. Combust. Flame **158**, 2009–2016 (2011)

Løvås, T.: Automatic generation of skeletal mechanisms for ignition combustion based on level of importance analysis. Combust. Flame **156**, 1348–1358 (2009)

Løvås, T., Nilsson, D., Mauss, F.: Automatic reduction procedure for chemical mechanisms applied to premixed methane/air flames. Proc. Combust. Inst. **28**, 1809–1815 (2000)

Løvås, T., Amneus, P., Mauss, F., Mastorakos, E.: Comparison of automatic reduction procedures for ignition chemistry. Proc. Combust. Inst. **29**, 1387–1393 (2002a)

Løvås, T., Mauss, F., Hasse, C., Peters, N.: Development of adaptive kinetics for application in combustion systems. Proc. Combust. Inst. **29**, 1403–1410 (2002b)

Løvås, T., Mastorakos, E., Goussis, D.A.: Reduction of the RACM scheme using computational singular perturbation analysis. J. Geophys. Res. Atmos. **111**(D13302) (2006)

Løvås, T., Navarro-Martinez, S., Rigopoulos, S.: On adaptively reduced chemistry in large eddy simulations. Proc. Combust. Inst. **33**, 1339–1346 (2011)

Lowe, R., Tomlin, A.: Low-dimensional manifolds and reduced chemical models for tropospheric chemistry simulations. Atmos. Environ. **34**, 2425–2436 (2000a)

Lowe, R.M., Tomlin, A.S.: The application of repro-modelling to a tropospheric chemical model. Environ. Model. Software **15**, 611–618 (2000b)

Lu, T., Law, C.K.: A directed relation graph method for mechanism reduction. Proc. Combust. Inst. **30**, 1333–1341 (2005)

Lu, T., Law, C.: Linear time reduction of large kinetic mechanisms with directed relation graph: *n*-heptane and *iso*-octane. Combust. Flame **144**, 24–36 (2006a)

Lu, T., Law, C.K.: On the applicability of directed relation graphs to the reduction of reaction mechanisms. Combust. Flame **146**, 472–483 (2006b)

Lu, T., Law, C.K.: Systematic approach to obtain analytic solutions of quasi steady state species in reduced mechanisms. J. Phys. Chem. A **110**, 13202–13208 (2006c)

Lu, T., Law, C.K.: A criterion based on computational singular perturbation for the identification of quasi steady state species: a reduced mechanism for methane oxidation with NO chemistry. Combust. Flame **154**, 761–774 (2008a)

Lu, T., Law, C.K.: Strategies for mechanism reduction for large hydrocarbons: *n*-heptane. Combust. Flame **154**, 153–163 (2008b)

Lu, T., Law, C.K.: Toward accommodating realistic fuel chemistry in large-scale computations. Prog. Energy Combust. Sci. **35**, 192–215 (2009)

Lu, L.Y., Pope, S.B.: An improved algorithm for in situ adaptive tabulation. J. Comput. Phys. **228**, 361–386 (2009)

Lu, T., Law, C.K., Yoo, C.S., Chen, J.H.: Dynamic stiffness removal for direct numerical simulations. Combust. Flame **156**, 1542–1551 (2009)

Luche, J., Reuillon, M., Boettner, J.-C., Cathonnet, M.: Reduction of large detailed kinetic mechanisms: application to kerosene/air combustion. Combust. Sci. Technol. **176**, 1935–1963 (2004)

Luo, Z.Y., Lu, T.F., Maciaszek, M.J., Som, S., Longman, D.E.: A reduced mechanism for high-temperature oxidation of biodiesel surrogates. Energy Fuels **24**, 6283–6293 (2010a)

Luo, Z.Y., Lu, T.F., Som, S., Longman, D.E., Asme: Numerical study on combustion characteristics of biodiesel using a new reduced mechanism for methyl decanoate as surrogate. Proceedings of the ASME Internal Combustion Engine Division Fall Technical Conference, pp. 873–884 (2010b)

Luo, Z.Y., Lu, T.F., Liu, J.W.: A reduced mechanism for ethylene/methane mixtures with excessive NO enrichment. Combust. Flame **158**, 1245–1254 (2011)

Luo, Z., Plomer, M., Lu, T.F., Som, S., Longman, D.E.: A reduced mechanism for biodiesel surrogates with low temperature chemistry for compression ignition engine application. Combust. Theory Model. **16**, 369–385 (2012a)

Luo, Z., Plomer, M., Lu, T.F., Som, S., Longman, D.E., Sarathy, S.M., Pitz, W.J.: A reduced mechanism for biodiesel surrogates for compression ignition engine applications. Fuel **99**, 143–153 (2012b)

Luo, Z., Som, S., Sarathy, S.M., Plomer, M., Pitz, W.J., Longman, D.E., Lu, T.F.: Development and validation of an *n*-dodecane skeletal mechanism for Diesel spray-combustion applications. Combust. Theory Model. **18**, 187–203 (2014)

Luong, M.B., Luo, Z., Lu, T.F., Chung, S.H., Yoo, C.S.: Direct numerical simulations of the ignition of lean primary reference fuel/air mixtures under HCCI condition. Combust. Flame **160**, 2038–2047 (2013)

Lv, Y., Wang, Z.H., Zhou, J.H., Cen, K.F.: Reduced mechanism for hybrid NOx control process. Energy Fuels **23**, 5920–5928 (2009)

Maas, U.: Efficient calculation of intrinsic low-dimensional manifolds for the simplification of chemical kinetics. Comput. Vis. Sci. **1**, 69–81 (1998)

Maas, U., Bykov, V.: The extension of the reaction/diffusion manifold concept to systems with detailed transport models. Proc. Combust. Inst. **33**, 1253–1259 (2011)

Maas, U., Pope, S.B.: Simplifying chemical kinetics: intrinsic low-dimensional manifolds in composition space. Combust. Flame **88**, 239–264 (1992)

Maas, U., Pope, S.B.: Laminar flame calculations using simplified chemical kinetics based on intrinsic low-dimensional manifolds. Proc. Combust. Inst. **25**, 1349–1356 (1994)

Maas, U., Thévenin, D.: Correlation analysis of direct numerical simulation data of turbulent non-premixed flames. Proc. Combust. Inst. **27**, 1183–1189 (1998)

Machrafi, H., Lombaert, K., Cavadias, S., Guibert, P., Amouroux, J.: Reduced chemical reaction mechanisms: experimental and HCCI modelling investigations of autoignition processes of *iso*-octane in internal combustion engines. Fuel **84**, 2330–2340 (2005)

Malik, A., Schramm, J., Nielsen, C., Løvås, T.: Development of surrogate for Fischer-Tropsch biofuel and reduced mechanism for combustion in Diesel engine. SAE Technical Paper 2013-2001-2599 (2013)

Maly, T., Petzold, L.R.: Numerical methods and software for sensitivity analysis of differential-algebraic systems. Appl. Numer. Math. **20**, 57–79 (1996)

Maple. http://www.maplesoft.com/

Maria, G.: A review of algorithms and trends in kinetic model identification for chemical and biochemical systems. Chem. Biochem. Eng. Q. **18**, 195–222 (2004)

Maria, G.: Application of lumping analysis in modelling the living systems—a trade-off between simplicity and model quality. Chem. Biochem. Eng. Q. **20**, 353–373 (2006)

Maria, G.: Reduced modular representations applied to simulate some genetic regulatory circuits. Rev. Chim. **59**, 318–324 (2008)

Maria, G.: Lumped dynamic model for a bistable genetic regulatory circuit within a variable-volume whole-cell modelling framework. Asia-Pac. J. Chem. Eng. **4**, 916–928 (2009)

Marsden, A.R., Frenklach, M., Reible, D.D.: Increasing the computational feasibility of urban air-quality models that employ complex chemical mechanisms. JAPCA **37**, 370–376 (1987)

Masri, A.R., Cao, R., Pope, S.B., Goldin, G.M.: PDF calculations of turbulent lifted flames of H_2/N_2 fuel issuing into a vitiated co-flow. Combust. Theory Model. **8**, 1–22 (2004)

Mauersberger, G.: ISSA (iterative screening and structure analysis)—a new reduction method and its application to the tropospheric cloud chemical mechanism RACM/CAPRAM 2.4. Atmos. Environ. **39**, 4341–4350 (2005)

Maurya, M.R., Bornheimer, S.J., Venkatasubramanian, V., Subramaniam, S.: Mixed-integer nonlinear optimisation approach to coarse-graining biochemical networks. IET Syst. Biol. **3**, 24–39 (2009)

Mauryaa, M.R., Katare, S., Patkar, P.R., Rundell, A.E., Venkatasubramanian, V.: A systematic framework for the design of reduced-order models for signal transduction pathways from a control theoretic perspective. Comput. Chem. Eng. **30**, 437–452 (2006)

Mazumder, S.: Adaptation of the in situ adaptive tabulation (ISAT) procedure for efficient computation of surface reactions. Comput. Chem. Eng. **30**, 115–124 (2005)

Meisel, W.S., Collins, D.C.: Repro-modeling: an approach to efficient model utilization and interpretation. IEEE Trans. **SMC-3/4**, 349–358 (1973)

Mendiara, T., Alzueta, M., Millera, A., Bilbao, R.: An augmented reduced mechanism for methane combustion. Energy Fuels **18**, 619–627 (2004)

Michaelis, L., Menten, M.: Die Kinetik der Invertinwirkung. Biochem. Z. **49**, 333–369 (1913)

Michel, J.-B., Colin, O., Veynante, D.: Modeling ignition and chemical structure of partially premixed turbulent flames using tabulated chemistry. Combust. Flame **152**, 80–99 (2008)
Michel, J.-B., Colin, O., Angelberger, C., Veynanteb, D.: Using the tabulated diffusion flamelet model ADF-PCM to simulate a lifted methane-air jet flame. Combust. Flame **156**, 1318–1331 (2009)
Michel, J.-B., Colin, O., Angelberger, C.: On the formulation of species reaction rates in the context of multi-species CFD codes using complex chemistry tabulation techniques. Combust. Flame **157**, 701–714 (2010)
Miller, W.G., Alberty, R.A.: Kinetics of the reversible Michaelis–Menten mechanism and the applicability of the Steady-state Approximation. J. Am. Chem. Soc. **80**, 5146–5151 (1958)
Mirgolbabaei, H., Echekki, T.: A novel principal component analysis-based acceleration scheme for LES–ODT: An *a priori* study. Combust. Flame **160**, 898–908 (2013)
Mirgolbabaei, H., Echekki, T.: Nonlinear reduction of combustion composition space with kernel principal component analysis. Combust. Flame **161**, 118–126 (2014)
Mirgolbabaei, H., Echekki, T., Smaoui, N.: A nonlinear principal component analysis approach for turbulent combustion composition space. Int. J. Hydrogen Energy **39**, 4622–4633 (2014)
Mitsos, A., Oxberry, G.M., Barton, P.I., Green, W.H.: Optimal automatic reaction and species elimination in kinetic mechanisms. Combust. Flame **155**, 118–132 (2008)
Montgomery, C.J., Yang, C., Parkinson, A.R., Chen, J.-Y.: Selecting the optimum quasi-steady-state species for reduced chemical kinetic mechanisms using a genetic algorithm. Combust. Flame **144**, 37–52 (2006)
Mora-Ramirez, M.A., Velasco, R.M.: Reduction of CB05 mechanism according to the CSP method. Atmos. Environ. **45**, 235–243 (2011)
Mosbach, S., Aldawood, A.M., Kraft, M.: Real-time evaluation of a detailed chemistry HCCI engine model using a tabulation technique. Combust. Sci. Technol. **180**, 1263–1277 (2008)
Nafe, J., Maas, U.: A general algorithm for improving ILDMs. Combust. Theory Model. **6**, 697–709 (2002)
Nafe, J., Maas, U.: Hierarchical generation of ILDMs of higher hydrocarbons. Combust. Flame **135**, 17–26 (2003)
Nagy, T., Turányi, T.: Reduction of very large reaction mechanisms using methods based on simulation error minimization. Combust. Flame **156**, 417–428 (2009)
Naik, C.V., Puduppakkam, K.V., Modak, A., Wang, C., Meeks, E.: Validated F-T fuel surrogate model for simulation of jet-engine combustion. Proc. ASME Turbo Expo **2**, 1301–1308 (2010)
Najafi-Yazdi, A., Cuenot, B., Mongeau, L.: Systematic definition of progress variables and Intrinsically Low-Dimensional. Flamelet Generated Manifolds for chemistry tabulation. Combust. Flame **159**, 1197–1204 (2012)
Németh, A., Vidóczy, T., Héberger, K., Kúti, Z., Wágner, J.: MECHGEN: Computer aided generation and reduction of reaction mechanisms. J. Chem. Inf. Comput. Sci. **42**, 208–214 (2002)
Neophytou, M.K., Goussis, D.A., van Loon, M., Mastorakos, E.: Reduced chemical mechanisms for atmospheric pollution using computational singular perturbation analysis. Atmos. Environ. **38**, 3661–3673 (2004)
Niemann, H., Schmidt, D., Maas, U.: An efficient storage scheme for reduced chemical kinetics based on orthogonal polynomials. J. Eng. Math. **31**, 131–142 (1997)
Niemeyer, K.E., Sung, C.J., Raju, M.P.: Skeletal mechanism generation for surrogate fuels using directed relation graph with error propagation and sensitivity analysis. Combust. Flame **157**, 1760–1770 (2010)
Niemeyer, K.E., Sung, C.J.: On the importance of graph search algorithms for DRGEP-based mechanism reduction methods. Combust. Flame **158**, 1439–1443 (2011)
Niemeyer, K.E., Sung, C.J.: Mechanism reduction for multicomponent surrogates: a case study using toluene reference fuels. Combust. Flame **161**, 2752–2764 (2014)
Nilsson, D., Løvås, T., Amneus, P., Mauss, F.: Reduction of complex fuel chemistry for simulation of combustion in an HCCI engine. VDI-Berichte **1492**, 511–516 (1999)

Niu, Y.-S., Vervisch, L., Tao, P.D.: An optimization-based approach to detailed chemistry tabulation: automated progress variable definition. Combust. Flame **160**, 776–785 (2013)
Ocone, R., Astarita, G.: Lumping nonlinear kinetics in porous catalysts: diffusion-reaction lumping strategy. AIChE J. **39**, 288–293 (1993)
Okino, M.S., Mavrovouniotis, M.L.: Simplification of mathematical models of chemical reaction systems. Chem. Rev. **98**, 391–408 (1998)
Oluwole, O.O., Bhattacharjee, B., Tolsma, J.E., Barton, P.I., Green, W.H.: Rigorous valid ranges for optimally reduced kinetic models. Combust. Flame **146**, 348–365 (2006)
Oluwole, O.O., Shi, Y., Wong, H.W., Green, W.H.: An exact-steady-state adaptive chemistry method for combustion simulations: combining the efficiency of reduced models and the accuracy of the full model. Combust. Flame **159**, 2352–2362 (2012)
Paczko, G., Lefdal, P.M., Peters, N.: Reduced reaction schemes for methane, methanol and propane flames. Proc. Combust. Inst. **21**, 739–748 (1986)
Pantea, C., Gupta, A., Rawlings, J.B., Craciun, G.: The QSSA in chemical kinetics: as taught and as practiced. In: Jonoska, N., Saito, M. (eds.) Discrete and Topological Models in Molecular Biology, pp. 419–442. Springer, Berlin (2014)
Parente, A., Sutherland, J.C., Tognotti, L., Smith, P.J.: Identification of low-dimensional manifolds in turbulent flames. Proc. Combust. Inst. **32**, 1579–1586 (2009)
Parente, A., Sutherland, J.C., Dally, B.B., Tognotti, L., Smith, P.J.: Investigation of the MILD combustion regime via principal component analysis. Proc. Combust. Inst. **33**, 3333–3341 (2011)
Pepiot, P., Pitsch, H.: Systematic reduction of large chemical mechanisms. In: 4th Joint Meeting of the U.S. Sections of the Combustion Institute, Philadelphia (2005)
Pepiot-Desjardins, P., Pitsch, H.: An efficient error-propagation-based reduction method for large chemical kinetic mechanisms. Combust. Flame **154**, 67–81 (2008)
Pera, C., Colin, O., Jay, S.: Development of a FPI detailed chemistry tabulation methodology for internal combustion engines. Oil Gas Sci. Technol. Rev. IFP **64**, 243–258 (2009)
Perini, F., Brakora, L.J., Reitz, D.R., Cantore, G.: Development of reduced and optimized reaction mechanisms based on genetic algorithms and element flux analysis. Combust. Flame **159**, 103–119 (2012)
Peters, N.: Numerical and asymptotic analysis of systematically reduced reaction schemes for hydrocarbon flames. Lect. Notes Phys. **241**, 90–109 (1985)
Peters, N., Kee, R.J.: The computation of stretched laminar methane-air diffusion flames using a reduced four-step mechanism. Combust. Flame **68**, 17–29 (1987)
Peters, N., Rogg, B. (eds.): Reduced Kinetic Mechanisms for Applications in Combustion Systems. Springer, Berlin (1993)
Peters, N., Williams, F.A.: The asymptotic structure of stoichiometric methane-air flames. Combust. Flame **68**, 185–207 (1987)
Petzold, L., Zhu, W.: Model reduction for chemical kinetics: an optimization approach. AIChE J. **45**, 869–886 (1999)
Polifke, W., Geng, W., Döbbeling, K.: Optimization of rate coefficients for simplified reaction mechanisms with genetic algorithms. Combust. Flame **113**, 119–135 (1998)
Poon, H., Ng, H., Gan, S., Pang, K., Schramm, J.: Evaluation and development of chemical kinetic mechanism reduction scheme for biodiesel and Diesel fuel surrogates. SAE Int. J. Fuels Lubr. **6**, 729–744 (2013)
Pope, S.B.: Computationally efficient implementation of combustion chemistry using in situ adaptive tabulation. Combust. Theory Model. **1**, 41–63 (1997)
Pope, S.B.: Small scales, many species and the manifold challenges of turbulent combustion. Proc. Combust. Inst. **34**, 1–31 (2013)
Pope, S.B., Ren, Z.: Efficient implementation of chemistry in computational combustion. Flow Turbulence Combust. **82**, 437–453 (2009)
Prasad, G.N., Agnew, J.B., Sridhar, T.: Continuous reaction mixture for coal liquefaction. Theory. AIChE J. **32**, 1277–1287 (1986)

Radulescu, O., Gorban, A.N., Zinovyev, A., Lilienbaum, A.: Robust simplifications of multiscale biochemical networks. BMC Syst. Biol. **2**, 86 (2008)

Ramaroson, R., Pirre, M., Cariolle, D.: A box model for online computations of diurnal-variations in a 1-d model—potential for application in multidimensional cases. Ann. Geophys. Atmos. Hydrospheres Space Sci. **10**, 416–428 (1992)

Ranzi, E., Faravelli, T., Gaffuri, P., Sogaro, A.: Low-temperature combustion: automatic generation of primary oxidation reactions and lumping procedures. Combust. Flame **102**, 179–192 (1995)

Ranzi, E., Faravelli, T., Gaffuri, P., Sogaro, A., D'Anna, A., Ciajolo, A.: A wide-range modeling study of *iso*-octane oxidation. Combust. Flame **108**, 24–42 (1997)

Ranzi, E., Dente, M., Goldaniga, A., Bozzano, G., Faravelli, T.: Lumping procedures in detailed kinetic modeling of gasification, pyrolysis, partial oxidation and combustion of hydrocarbon mixtures. Prog. Energy Combust. Sci. **27**, 99–139 (2001)

Ranzi, E., Frassoldati, A., Granata, S., Faravelli, T.: Wide-range kinetic modeling study of the pyrolysis, partial oxidation, and combustion of heavy *n*-alkanes. Ind. Eng. Chem. Res. **44**, 5170–5183 (2005)

Ren, Z., Pope, S.B.: Species reconstruction using pre-image curves. Proc. Combust. Inst. **30**, 1293–1300 (2005)

Ren, Z., Pope, S.B.: The geometry of reaction trajectories and attracting manifolds in composition space. Combust. Theory Model. **10**, 361–388 (2006a)

Ren, Z., Pope, S.B.: The use of slow manifolds in reactive flows. Combust. Flame **147**, 243–261 (2006b)

Ren, Z., Pope, S.B.: Reduced description of complex dynamics in reactive systems. J. Phys. Chem. A **111**, 8464–8474 (2007a)

Ren, Z., Pope, S.B.: Transport-chemistry coupling in the reduced description of reactive flows. Combust. Theory Model. **11**, 715–739 (2007b)

Ren, Z., Pope, S.B., Vladimirsky, A., Guckenheimer, J.M.: The invariant constrained equilibrium edge preimage curve method for the dimension reduction of chemical kinetics. J. Chem. Phys. **124**, 114111 (2006)

Ren, Z., Pope, S.B., Vladimirsky, A., Guckenheimer, J.M., John, M.: Application of the ICE-PIC method for the dimension reduction of chemical kinetics coupled with transport. Proc. Combust. Inst. **31**, 473–481 (2007)

Ren, Z., Liu, Y., Lu, T., Lu, L., Oluwole, O.O., Goldin, G.M.: The use of dynamic adaptive chemistry and tabulation in reactive flow simulations. Combust. Flame **161**, 127–137 (2014a)

Ren, Z., Xu, C., Lu, T., Singer, M.A.: Dynamic adaptive chemistry with operator splitting schemes for reactive flow simulations. J. Comput. Phys. **263**, 19–36 (2014b)

Reonhardt, V., Winckler, M., Lebiedz, D.: Approximation of slow attracting manifolds in chemical kinetics by trajectory-based optimization approaches. J. Phys. Chem. A **112**, 1712–1718 (2008)

Rhodes, C., Morari, M., Wiggins, S.: Identification of low order manifolds: validating the algorithm of Maas and Pope. Chaos **9**, 108–123 (1999)

Rice, O.K.: Conditions for a steady state in chemical kinetics. J. Phys. Chem. **64**, 1851–1857 (1960)

Riedel, U., Schmidt, D., Maas, U., Warnatz, J.: Laminar flame calculations based on automatically simplified chemical kinetics. In: Proceedings of Eutherm. Seminar #35, Compact Fired Heating Systems, Leuven, Belgium (1994)

Rigopoulos, S.: The rate-controlled constrained equilibrium (RCCE) method for reducing chemical kinetics in systems with time-scale separation. Int. J. Multiscale Comput. Eng. **5**, 11–18 (2007)

Rigopoulos, S., Løvås, T.: A LOI-RCCE methodology for reducing chemical kinetics, with application to laminar premixed flames. Proc. Combust. Inst. **32**, 569–576 (2009)

Ross, J.: Determination of complex reaction mechanisms. Analysis of chemical, biological and genetic networks. J. Phys. Chem. A **112**, 2134–2143 (2008)

Ross, J., Vlad, M.O.: Nonlinear kinetics and new approaches to complex reaction mechanisms. Ann. Rev. Phys. Chem. **50**, 51–78 (1999)
Roussel, M.R., Fraser, S.J.: Geometry of the steady-state approximation: perturbation and accelerated convergence methods. J. Chem. Phys. **93**, 1072–1081 (1990)
Roussel, M.R., Fraser, S.J.: Accurate steady-state approximation: implications for kinetics experiments and mechanism. J. Chem. Phys. **94**, 7106–7113 (1991a)
Roussel, M.R., Fraser, S.J.: On the geometry of transient relaxation. J. Chem. Phys. **94**, 7106–7113 (1991b)
Roussel, M.R., Fraser, S.J.: Invariant manifold methods for metabolic model reduction. Chaos **11**, 196–206 (2001)
Roussel, M.R., Tang, T.: The functional equation truncation method for approximating slow invariant manifolds: a rapid method for computing intrinsic low-dimensional manifolds. J. Chem. Phys. **125**, 214103 (2006)
Russi, T., Packard, A., Feeley, R., Frenklach, M.: Sensitivity analysis of uncertainty in model prediction. J. Phys. Chem. A **112**, 2579–2588 (2008)
Russi, T., Packard, A., Frenklach, M.: Uncertainty quantification: making predictions of complex reaction systems reliable. Chem. Phys. Lett. **499**, 1–8 (2010)
Sandu, A., Verwer, J.G., Blom, J.G., Spee, E.J., Carmichael, G.R., Potra, F.A.: Benchmarking stiff ODE solvers for atmospheric chemistry problems II: Rosenbrock solvers. Atmos. Environ. **31**, 3459–3472 (1997a)
Sandu, A., Verwer, J.G., Van Loon, M., Carmichael, G.R., Potra, F.A., Dabdub, D., Seinfeld, J.H.: Benchmarking stiff ODE solvers for atmospheric chemistry problems I. implicit vs. explicit. Atmos. Environ. **31**, 3151–3166 (1997b)
Sankaran, R., Hawkes, E.R., Chen, J.H., Lu, T., Law, C.K.: Structure of a spatially developing turbulent lean methane–air Bunsen flame. Proc. Combust. Inst. **31**, 1291–1298 (2007)
Saunders, S.M., Pascoe, S., Johnson, A.P., Pilling, M.J., Jenkin, M.E.: Development and preliminary test results of an expert system for the automatic generation of tropospheric VOC degradation mechanisms. Atmos. Environ. **37**, 1723–1735 (2003)
Savage, P.E.: Pyrolysis of a binary mixture of complex hydrocarbons—reaction modeling. Chem. Eng. Sci. **45**, 859–873 (1990)
Saxena, V., Pope, S.B.: PDF simulations of turbulent combustion incorporating detailed chemistry. Combust. Flame **117**, 340–350 (1999)
Sayasov, Y.S., Vasil'eva, A.B.: Обоснование и условия применимости метода квазистационарных концентраций Семенова–Боденштейна. Ж. Физ. Хим. **29**, 802–810 (1955)
Schuchardt, K., Oluwole, O., Pitz, W., Rahn, L.A., Green, W.H., Leahy, D., Pancerella, C., Sjöberg, M., Dec, J.: Development of the RIOT web service and information technologies to enable mechanism reduction for HCCI simulations. J. Phys. Conf. Ser. **16**, 107–112 (2005)
Schwer, D.A., Lu, P., Green, W.H.: An adaptive chemistry approach to modeling complex kinetics in reacting flows. Combust. Flame **133**, 451–465 (2003)
Segel, L.A.: On the validity of the steady-state assumption of enzyme kinetics. Bull. Math. Biol. **50**, 579–593 (1988)
Segel, L.A., Slemrod, M.: The quasi-steady-state assumption: a case study in perturbation. SIAM Rev. **31**, 446–477 (1989)
Semenoff, N.: On the kinetics of complex reactions. J. Chem. Phys. **7**, 683–699 (1939)
Semenov, N.N.: Кинетика сложных гомогенных реакции. Ж. Физ. Хим. **17**, 187–214 (1943)
Seshadri, K., Lu, T.F., Herbinet, O., Humer, S.B., Niemann, U., Pitz, W.J., Seiser, R., Law, C.K.: Experimental and kinetic modeling study of extinction and ignition of methyl decanoate in laminar non-premixed flows. Proc. Combust. Inst. **32**, 1067–1074 (2009)
Shanks, D.: Non-linear transformations of divergent and slowly convergent sequences and an example from hydrodynamics. Phys. Rev. **76**, 876–876 (1949)
Sheen, D., Wang, H.: Combustion kinetic modeling using multispecies time histories in shock-tube oxidation of heptane. Combust. Flame **158**, 645–656 (2011a)

Sheen, D.A., Wang, H.: The method of uncertainty quantification and minimization using polynomial chaos expansions. Combust. Flame **158**, 2358–2374 (2011b)
Sheen, D.A., You, X., Wang, H., Løvås, T.: Spectral uncertainty quantification, propagation and optimization of a detailed kinetic model for ethylene combustion. Proc. Combust. Inst. **32**, 535–542 (2009)
Sheen, D.A., Rosado-Reyes, C.M., Tsang, W.: Kinetics of H atom attack on unsaturated hydrocarbons using spectral uncertainty propagation and minimization techniques. Proc. Combust. Inst. **34**, 527–536 (2013)
Shenvi, N., Geremia, J., Rabitz, H.: Efficient chemical kinetic modeling through neural network maps. J. Chem. Phys. **120**, 9942–9951 (2004)
Shi, Y., Ge, H.W., Brakora, J.L., Reitz, R.D.: Automatic chemistry mechanism reduction of hydrocarbon fuels for HCCI engines based on DRGEP and PCA methods with error control. Energy Fuels **24**, 1646–1654 (2010a)
Shi, Y., Liang, L., Ge, H.W., Reitz, R.D.: Acceleration of the chemistry solver for modeling DI engine combustion using dynamic adaptive chemistry (DAC) schemes. Combust. Theory Model. **14**, 69–89 (2010b)
Shorter, J.A., Ip, P.C., Rabitz, H.A.: An efficient chemical kinetics solver using high dimensional model representation. J. Phys. Chem. A **103**, 7192–7198 (1999)
Sikalo, N., Hasemann, O., Schulz, C., Kempf, A., Wlokas, I.: A genetic algorithm-based method for the automatic reduction of reaction mechanisms. Int J Chem. Kinet. **46**, 41–59 (2014)
Singer, M.A., Pope, S.B.: Exploiting ISAT to solve the reaction-diffusion equation. Combust. Theory Model **8**, 361–383 (2004)
Singer, M.A., Pope, S.B., Najm, H.N.: Operator-splitting with ISAT to model reacting flow with detailed chemistry. Combust. Theory Model. **10**, 199–217 (2006)
Singh, S., Powers, J.M., Paolucci, S.: On slow manifolds of chemically reactive systems. J. Chem. Phys. **117**, 1482–1496 (2002)
Skodje, R.T., Davis, M.J.: Geometrical simplification of complex kinetic systems. J. Phys. Chem. A **105**, 10356–10365 (2001)
Snow, R.M.: A chemical kinetics computer program for homogeneous and free-radical systems of reactions. J. Phys. Chem. **70**, 2780–2786 (1966)
Soyhan, H., Mauss, F., Sorusbay, C.: Chemical kinetic modeling of combustion in internal combustion engines using reduced chemistry. Combust. Sci. Technol. **174**, 73–91 (2002)
Sportisse, B., Djouad, R.: Reduction of chemical kinetics in air pollution modelling. J. Comp. Phys. **164**, 354–376 (2000)
Sportisse, B., Djouad, R.: Use of proper orthogonal decompositions for the reduction of atmospheric chemistry. J. Geophys. Res. Atmos. **112**(D06303) (2007)
Stagni, A., Cuoci, A., Frassoldati, A., Faravelli, T., Ranzi, E.: Lumping and reduction of detailed kinetic schemes: an effective coupling. Ind. Eng. Chem. Res. **53**, 9004–9016 (2014)
Stockmayer, W.H.: The steady-state approximation in polymerization kinetics. J. Chem. Phys. **12**, 143–144 (1944)
Strang, G.: On construction and comparison of difference schemes. SIAM J. Numer. Anal. **5**, 506–517 (1968)
Straube, R., Flockerzi, D., Müller, S.C., Hauser, M.J.B.: Reduction of chemical reaction networks using quasi-integrals. J. Phys. Chem. A **109**, 441–450 (2005)
Ströhle, J., Myhrvold, T.: Reduction of a detailed reaction mechanism for hydrogen combustion under gas turbine conditions. Combust. Flame **144**, 545–557 (2006)
Sun, W.T., Chen, Z., Gou, X.L., Ju, Y.G.: A path flux analysis method for the reduction of detailed chemical kinetic mechanisms. Combust. Flame **157**, 1298–1307 (2010)
Sundaram, K.M., Froment, G.F.: Accuracy of pseudo-steady-state approximation for radicals in thermal-cracking. Int. J. Chem. Kinet. **10**(11), 1189–1193 (1978)
Sunnaker, M., Schmidt, H., Jirstrand, M., Cedersund, G.: Zooming of states and parameters using a lumping approach including back-translation. BMC Syst. Biol. **4**, 28 (2010)

Sunnaker, M., Cedersund, G., Jirstrand, M.: A method for zooming of nonlinear models of biochemical systems. BMC Syst. Biol. **5**, 140 (2011)

Surovtsova, I., Simus, N., Lorenz, T., König, A., Sahle, S., Kumme, U.: Accessible methods for the dynamic time-scale decomposition of biochemical systems. Bioinformatics **25**, 2816–2823 (2009)

Sutherland, J.C., Parente, A.: Combustion modeling using principal component analysis. Proc. Combust. Inst. **32**, 1563–1570 (2009)

Taing, S., Masri, A.R., Pope, S.B.: *pdf* calculations of turbulent nonpremixed flames of H_2/CO_2 using reduced chemical mechanisms. Combust. Flame **95**, 133–150 (1993)

Tang, Q., Pope, S.B.: Implementation of combustion chemistry by in situ adaptive tabulation of rate-controlled constrained equilibrium manifolds. Proc. Combust. Inst. **29**, 1411–1417 (2002)

Tang, Q., Pope, S.B.: A more accurate projection in the rate-controlled constrained-equilibrium method for dimension reduction of combustion chemistry. Combust. Theory Model. **8**, 255–279 (2004)

Tang, Q., Xu, J., Pope, S.B.: Probability density function calculations of local extinction and no production in piloted-jet turbulent methane/air flames. Proc. Combust. Inst. **28**, 133–139 (2000)

Taylor, S.R., Doyle III, F.J., Petzold, L.R.: Oscillator model reduction preserving the phase response: application to the circadian clock. Biophys. J. **95**, 1658–1673 (2008)

Tihonov, A.N.: Системы дифференциальных уравнений, содержащие малые параметры при производных. Мат. Сборник **31**, 575–586 (1952)

Tomlin, A.S., Pilling, M.J., Turányi, T., Merkin, J.H., Brindley, J.: Mechanism reduction for the oscillatory oxidation of hydrogen: sensitivity and quasi-steady-state analyses. Combust. Flame **91**, 107–130 (1992)

Tomlin, A.S., Li, G.Y., Rabitz, H., Tóth, J.: A general-analysis of approximate nonlinear lumping in chemical-kinetics 2. Constrained lumping. J. Chem. Phys. **101**, 1188–1201 (1994)

Tomlin, A.S., Turányi, T., Pilling, M.J.: Mathematical tools for the construction, investigation and reduction of combustion mechanisms. In: Pilling, M.J., Hancock, G. (eds.) Low-temperature Combustion and Autoignition. Comprehensive Chemical Kinetics, vol. 35, pp. 293–437. Elsevier, Amsterdam (1997)

Tomlin, A.S., Whitehouse, L., Lowe, R., Pilling, M.J.: Low-dimensional manifolds in tropospheric chemical systems. Faraday Discuss. **120**, 125–146 (2001)

Tonse, S.R., Moriarty, N.W., Brown, N.J., Frenklach, M.: PRISM: Piece-wise reusable implementation of solution mapping. An economical strategy for chemical kinetics. Israel J. Chem. **39**, 97–106 (1999)

Tonse, S.R., Moriarty, N.W., Frenklach, M., Brown, N.J.: Computational economy improvements in PRISM. Int. J. Chem. Kinet. **35**, 438–452 (2003)

Tosatto, L., Bennett, B.A.V., Smooke, M.D.: A transport-flux-based directed relation graph method for the spatially inhomogeneous instantaneous reduction of chemical kinetic mechanisms. Combust. Flame **158**, 820–835 (2011)

Tosatto, L., Bennett, B.A.V., Smooke, M.D.: Comparison of different DRG-based methods for the skeletal reduction of JP-8 surrogate mechanisms. Combust. Flame **160**, 1572–1582 (2013)

Toth, J., Li, G.Y., Rabitz, H., Tomlin, A.S.: Effect of lumping and expanding on kinetic differential equations. SIAM J. Appl. Math. **57**(6), 1531–1556 (1997)

Treviño, C.: Ignition phenomena in H_2/O_2 mixtures. Prog. Astronaut. Aeronautics **131**, 19–43 (1991)

Treviño, C., Liñan, A.: Numerical and asymptotic analysis of ignition processes. In: Buckmaster, J., Jackson, T.L., Kumar, A. (eds.) Combustion in High-Speed Flows, pp. 477–490. Kluwer Academic, Dordrecht (1994)

Treviño, C., Mendez, F.: Asymptotic analysis of the ignition of hydrogen by a hot plate in a boundary layer flow. Combust. Sci. Technol. **78**, 197–216 (1991)

Treviño, C., Mendez, F.: Reduced kinetic mechanism for methane ignition. Proc. Combust. Inst. **24**, 121–127 (1992)

Treviño, C., Solorio, F.: Asymptotic analysis of high temperature ignition of $CO/H_2/O_2$ mixtures. Combust. Flame **86**, 285–295 (1991)
Turányi, T.: KINAL - A program package for kinetic-analysis of reaction-mechanisms. Comput. Chem. **14**, 253–254 (1990a)
Turányi, T.: Reduction of large reaction mechanisms. New J. Chem. **14**, 795–803 (1990b)
Turányi, T.: Sensitivity analysis of complex kinetic systems. Tools and applications. J. Math. Chem. **5**, 203–248 (1990c)
Turányi, T.: Parametrization of reaction mechanisms using orthonormal polynomials. Comput. Chem. **18**, 45–54 (1994)
Turányi, T.: Application of repro-modelling for the reduction of combustion mechanisms. Proc. Combust. Inst. **25**, 948–955 (1995)
Turányi, T., Tóth, J.: Comments to an article of Frank-Kamenetskii on the quasi-steady-state approximation. Acta Chim. Hung. Models Chem. **129**(6), 903–907 (1992)
Turányi, T., Bérces, T., Vajda, S.: Reaction rate analysis of complex kinetic systems. Int. J. Chem. Kinet. **21**, 83–99 (1989)
Turányi, T., Györgyi, L., Field, R.J.: Analysis and simplification of the GTF model of the Belousov-Zhabotinsky reaction. J. Phys. Chem. **97**, 1931–1941 (1993a)
Turányi, T., Tomlin, A.S., Pilling, M.J.: On the error of the quasi-steady-state approximation. J. Phys. Chem. **97**, 163–172 (1993b)
Turco, R.P., Whitten, R.C.: Comparison of several computational techniques for solving some common aeronomic problems. J. Geophys. Res. **79**, 3179–3185 (1974)
Tzafriri, A.R., Edelman, E.R.: The total quasi-steady-state approximation is valid for reversible enzyme kinetics. J. Theor. Biol. **226**, 303–313 (2004)
Tzafriri, A.R., Edelman, E.R.: On the validity of the quasi-steady state approximation of bimolecular reactions in solution. J. Theor. Biol. **233**, 343–350 (2005)
Ugarte, S., Gao, Y., Metghalchi, H.: Application of the maximum entropy principle in the analysis of a non-equilibrium chemically reacting mixture. Int. J. Thermodyn. **8**, 43–53 (2005)
Vajda, S., Turányi, T.: Principal component analysis for reducing the Edelson-Field-Noyes model of the Belousov-Zhabotinsky reaction. J. Phys. Chem. **90**, 1664–1670 (1986)
Vajda, S., Valkó, P., Turányi, T.: Principal component analysis of kinetic models. Int. J. Chem. Kinet. **17**, 55–81 (1985)
Valorani, M., Creta, F., Goussis, D.A., Najm, H.N., Lee, J.C.: Chemical kinetics mechanism simplification via CSP. In: Bathe, K.J. (ed.) Computational Fluid and Solid Mechanics, pp. 900–904. Elsevier, Amsterdam (2005)
Valorani, M., Creta, F., Goussis, D., Lee, J., Najm, H.: An automatic procedure for the simplification of chemical kinetic mechanisms based on CSP. Combust. Flame **146**, 29–51 (2006)
Van Oijen, J.A., de Goey, L.P.H.: Modelling of premixed laminar flames using Flamelet Generated Manifolds. Combust. Sci. Technol. **161**, 113–137 (2000)
Van Oijen, J.A., de Goey, L.P.H.: Modelling of premixed counterflow flames using the flamelet-generated manifold method. Combust. Theory Model. **6**, 463–478 (2002)
Van Oijen, J.A., Lammers, F.A., de Goey, L.P.H.: Modeling of complex premixed burner systems by using flamelet-generated manifolds. Combust. Flame **127**, 2124–2134 (2001)
Verhoeven, L.M., Ramaekers, W.J.S., van Oijen, J.A., de Goey, L.P.H.: Modeling non-premixed laminar co-flow flames using flamelet-generated manifolds. Combust. Flame **159**, 230–241 (2012)
Vervisch, P.E., Colin, O., Michel, J.-B., Darabiha, N.: NO relaxation approach (NORA) to predict thermal NO in combustion chambers. Combust. Flame **158**, 1480–1490 (2011)
Vol'pert, A.I.: Дифференциальные уравнения на графах. Мат. Сборник **88**, 578–588 (1972)
Vol'pert, A.I., Hudjaev, S.I.: Analysis in Classes of Discontinuous Functions and Equations of Mathematical Physics. Martinus Nijhoff, Dordrecht (1985)
Vora, N., Daoutidis, P.: Nonlinear model reduction of chemical reaction systems. AIChE J. **47**, 2320–2332 (2001)

Wang, Q.-D.: Skeletal mechanism generation for high-temperature combustion of $H_2/CO/C_1-C_4$ hydrocarbons. Energy Fuels **27**, 4021–4030 (2013)
Wang, L.G., Fox, R.O.: Application of in situ adaptive tabulation to CFD simulation of nanoparticle formation by reactive precipitation. Chem. Eng. Sci. **58**, 4387–4401 (2003)
Wang, H., Frenklach, M.: Detailed reduction of reaction mechanisms for combustion modeling. Combust. Flame **87**, 365–370 (1991)
Wang, W., Rogg, B.: Premixed ethylene/air and ethane/air flames: reduced mechanisms based on inner iteration. In: Peters, N., Rogg, B. (eds.) Reduced Kinetic Mechanisms for Applications in Combustion Systems. Lecture Notes in Physics Monographs, vol. 15, pp. 82–107. Springer, New York (1993)
Wang, S.W., Georgopoulos, P.G., Li, G., Rabitz, H.: Computationally efficient atmospheric chemical kinetic modeling by means of high dimensional model representation (HDMR). Lect. Note Comput. Sci. **2179**, 326–333 (2001)
Wang, S.W., Balakrishnan, S., Georgopoulos, P.: Fast equivalent operational model of tropospheric alkane photochemistry. AIChE J. **51**, 1297–1303 (2005)
Wang, H., Yao, M., Reitz, R.D.: Development of a reduced primary reference fuel mechanism for internal combustion engine combustion simulations. Energy Fuels **27**, 7843–7853 (2013)
Warnatz, J.: Resolution of gas phase and surface combustion chemistry into elementary reactions. Proc. Combust. Inst. **24**, 553–579 (1992)
Warth, V., Battin-Leclerc, F., Fournet, R., Glaude, P.A., Côme, G.M., Scacchi, G.: Computer based generation of reaction mechanisms for gas-phase oxidation. Comput. Chem. **24**, 541–560 (2000)
Watson, L.A., Shallcross, D.E., Utembe, S.R., Jenkin, M.E.: A Common Representative Intermediates (CRI) mechanism for VOC degradation. Part 2: Gas phase mechanism reduction. Atmos. Environ. **42**, 7196–7204 (2008)
Weekman Jr., V.W.: Lumps, models, and kinetics in practice. AIChE Monogr. Ser. **11**, 3–29 (1979)
Wei, J., Kuo, J.C.W.: A lumping analysis in monomolecular reaction systems. Ind. Eng. Chem. Fundam. **8**, 114–123 (1969)
Whitehouse, L.E., Tomlin, A.S., Pilling, M.J.: Systematic reduction of complex tropospheric chemical mechanisms using sensitivity and time-scale analyses. Atmos. Chem. Phys. Discuss. **4**, 3721–3783 (2004a)
Whitehouse, L.E., Tomlin, A.S., Pilling, M.J.: Systematic reduction of complex tropospheric chemical mechanisms. Part I: sensitivity and time-scale analyses. Atmos. Chem. Phys. **4**, 2025–2056 (2004b)
Whitehouse, L.E., Tomlin, A.S., Pilling, M.J.: Systematic reduction of complex tropospheric chemical mechanisms.Part II: Lumping using a time-scale based approach. Atmos. Chem. Phys. **4**, 2057–2081 (2004c)
Whitten, G.Z., Hogo, H., Killus, J.P.: The Carbon Bond Mechanism: a condensed kinetic mechanism for photochemical smog analysis techniques to a photochemical ozone model. Environ. Sci. Technol. **14**, 690–700 (1980)
Wu, Z., Qiao, X., Huang, Z.: A criterion based on computational singular perturbation for the construction of a reduced mechanism for dimethyl ether oxidation. J. Serb. Chem. Soc. **78**, 1177–1188 (2013)
Xia, A.G., Michelangeli, D.V., Makar, P.A.: Mechanism reduction for the formation of secondary organic aerosol for integration into a 3-dimensional regional air quality model: alpha-pinene oxidation system. Atmos. Chem. Phys. **9**, 4341–4362 (2009)
Xie, N., Battaglia, F., Fox, R.O.: Simulations of multiphase reactive flows in fluidized beds using in situ adaptive tabulation. Combust. Theory Model. **8**, 195–209 (2004)
Xu, J., Pope, S.B.: PDF calculations of turbulent nonpremixed flames with local extinction. Combust. Flame **123**, 281–307 (2000)
Xu, M., Fan, Y., Yuan, J.: Simplification of the mechanims of NO_x formation in a CH_4/air combustion system. Int. J. Energy Res. **23**, 1267–1276 (1999)

Xuan, Y., Blanquart, G.: A flamelet-based a priori analysis on the chemistry tabulation of polycyclic aromatic hydrocarbons in non-premixed flames. Combust. Flame **161**, 1516–1525 (2014)

Yang, B., Pope, S.B.: Treating chemistry in combustion with detailed mechanisms -In situ adaptive tabulation in principal directions—premixed combustion. Combust. Flame **112**, 85–112 (1998)

Yang, H., Ren, Z., Lu, T., Goldin, G.M.: Dynamic adaptive chemistry for turbulent flame simulations. Combust. Theory Model. **17**, 167–183 (2013)

Yannacopoulos, A.N., Tomlin, A.S., Brindley, J., Merkin, J.H., Pilling, M.J.: The use of algebraic sets in the approximation of inertial manifolds and lumping in chemical kinetic systems. Physica D **83**, 421–449 (1995)

Yannacopoulos, A.N., Tomlin, A.S., Brindley, J., Merkin, J.H., Pilling, M.J.: The error of the quasi steady-state approximation in spatially distributed systems. Chem. Phys. Lett. **248**, 63–70 (1996a)

Yannacopoulos, A.N., Tomlin, A.S., Brindley, J., Merkin, J.H., Pilling, M.J.: Error propagation in approximations to reaction-diffusion-advection equations. Phys. Lett. A **223**, 82–90 (1996b)

Yarwood, G., Rao, S., Yocke, M., Whitten, G.: Updates to the Carbon Bond chemical mechanism: CB05. Final Report to the US EPA, RT-0400675 (2005)

Yoo, C.S., Lu, T.F., Chen, J.H., Law, C.K.: Direct numerical simulations of ignition of a lean *n*-heptane/air mixture with temperature inhomogeneities at constant volume: parametric study. Combust. Flame **158**, 1727–1741 (2011)

Yoo, C.S., Luo, Z., Lu, T.F., Kim, H., Chen, J.H.: DNS study of the ignition of a lean iso-octane/air mixture under HCCI and SACI conditions. Proc. Combust. Inst. **34**, 2985–2993 (2012)

You, X.Q., Russi, T., Packard, A., Frenklach, M.: Optimization of combustion kinetic models on a feasible set. Proc. Combust. Inst. **33**, 509–516 (2011)

You, X.Q., Packard, A., Frenklach, M.: Process informatics tools for predictive modeling: hydrogen combustion. Int. J. Chem. Kinet. **44**, 101–116 (2012)

Zambon, A.C., Chelliah, H.K.: Explicit reduced reaction models for ignition, flame propagation, and extinction of $C_2H_4/CH_4/H_2$ and air systems. Combust. Flame **150**, 71–91 (2007)

Zhang, S., Androulakis, I.P., Ierapetritou, M.G.: A hybrid kinetic mechanism reduction scheme based on the on-the-fly reduction and quasi-steady-state approximation. Chem. Eng. Sci. **93**, 150–162 (2013)

Zhang, S., Broadbelt, L.J., Androulakis, I.P., Ierapetritou, M.G.: Reactive flow simulation based on the integration of automated mechanism generation and on-the-fly reduction. Energy Fuels **28**, 4801–4811 (2014)

Zhao, W., Chen, D., Hu, S.: Differential fraction-based kinetic model for simulating hydrodesulfurization process of petroleum fraction. Comput. Chem. **26**, 141–148 (2002)

Zheng, X.L., Lu, T.F., Law, C.K.: Experimental counterflow ignition temperatures and reaction mechanisms of 1,3-butadiene. Proc. Combust. Inst. **31**, 367–375 (2007)

Zhou, Z.J., Lü, Y., Wang, Z.H., Xu, Y.W., Zhou, J.H., Cen, K.F.: Systematic method of applying ANN for chemical kinetics reduction in turbulent premixed combustion modeling. Chin. Sci. Bull. **58**, 486–492 (2013)

Zsély, I.G., Turányi, T.: Investigation and reduction of two methane combustion mechanisms. Arch. Combust. **21**, 173–177 (2001)

Zsély, I.G., Turányi, T.: The influence of thermal coupling and diffusion on the importance of reactions: the case study of hydrogen-air combustion. PCCP **5**, 3622–3631 (2003)

Zsély, I.G., Zádor, J., Turányi, T.: On the similarity of the sensitivity functions of methane combustion models. Combust. Theory Model. **9**, 721–738 (2005)

Zsély, I.G., Nagy, T., Simmie, J.M., Curran, H.J.: Reduction of a detailed kinetic model for the ignition of methane/propane mixtures at gas turbine conditions using simulation error minimization methods. Combust. Flame **158**, 1469–1479 (2011)